ISSN 2663-9084 (Print)
ISSN 2663-9092 (Online)

Ukrainian Neurosurgical Journal

Том 31, №3, 2025

Is a scholarly Open Access journal
Founded in April 1995. Quarterly.
State Registration Certificate KV No 23771-13611PR dated 14 February 2019

The journal is on the List of Scientific Professional Editions of Ukraine, where results of thesis research for earning academic degrees of doctor and candidate of sciences and PhD may be published (Order of the Ministry of Education and Science of Ukraine No. 1721 dated 10 December 2024)
The journal is included in the Scopus scientometric database.

Journal publishes peer-reviewed works.

Founders

Romodanov Neurosurgery Institute

Ukrainian Association of Neurosurgeons

National Academy of Medical Sciences of Ukraine

Publisher

Romodanov Neurosurgery Institute

Contact

32 Platona Mayborody st., Kyiv, 04050, Ukraine

tel. +380 44 483-91-98

fax +380 44 489-35-61

E-mail: unj.office@gmail.com

http://theunj.org

The journal went to press 05 September 2025

Format 60 × 841/8. Offset Paper No.1

Order No. 25-20

Circulation 300 copies

Polygraphic services

FOP Golosuy IE

Certificate AA No. 9221702

86 Kyrylivska st., Kyiv, 04080, Ukraine

Tel. +380 44 239-19-85

The master layout of the journal was approved and recommended for publication and distribution via the Internet at the joint meeting of the Editorial Board of the Ukrainian Neurosurgical Journal and the Academic Council of Romodanov Neurosurgery Institute (Meeting Minutes N. 10 dated 27 June 2025)

Content

Review article

Ukrainian Neurosurgical Journal. 2025;31(3):3-13
doi: 10.25305/unj.325812

A personalized approach to the treatment of traumatic spinal injuries: rationale, basic concept, and potential methods of implementation

Oleksii S. Nekhlopochyn

Spine Surgery Department, Romodanov Neurosurgery Institute, Kyiv, Ukraine

Received: 30 March 2025
Accepted: 09 May 2025

Address for correspondence*: Oleksii S. Nekhlopochyn, Spine Surgery Department, Romodanov Neurosurgery Institute, 32 Platona Maiborody st., Kyiv, 04050, Ukraine, e-mail: AlexeyNS@gmail.com*

Traumatic spinal injuries (TSIs) are a leading cause of disability and represent a significant socio-economic burden. Despite advancements in diagnostic and surgical techniques, treatment outcomes remain inconsistent. Standardized protocols often fail to account for individual patient characteristics, which can reduce the effectiveness of interventions and increase the risk of complications. This highlights the growing relevance of adopting individualized approaches in the treatment of TSIs.

Objective: To comprehensively analyze the economic, legal, clinical, and deontological aspects of implementing individualized approaches to the treatment of TSIs.

Materials and methods: An analytical literature review was conducted in accordance with the PRISMA protocol. Sources were selected from international scientific databases over the past 10 years using relevant MeSH terms.

Results: The literature review revealed that, despite technological advances, treatment outcomes in TSIs do not always improve proportionally with increased healthcare spending, illustrating the phenomenon of diminishing returns. The use of the QALY metric in several countries enables the evaluation of the cost-effectiveness of medical interventions; however, it has ethical limitations and is not yet implemented in Ukraine. The domestic Health Technology Assessment (HTA) system, introduced in 2020, does not currently include mandatory protocols for managing TSIs due to clinical heterogeneity, resource constraints, and legal risks. Standardized, diagnosis-driven protocols focused on the "average patient" often disregard individual variability, potentially leading to both overtreatment and undertreatment. Simplified injury classification systems enhance standardization but may reduce clinical decision-making accuracy in atypical cases. Furthermore, limited public understanding of evidence-based medicine contributes to ethical and communicative challenges. These findings underscore the importance of individualized approaches in TSI management.

Conclusions: Individualization of TSI treatment represents a logical extension of evidence-based medicine and promotes optimization of outcomes. It allows for flexible, patient-specific therapeutic strategies, improves the efficiency of healthcare resource utilization, and reduces complication rates. The ongoing development of analytical tools offers promising prospects for constructing personalized algorithms for managing highly heterogeneous patient populations.

Keywords: *traumatic spinal injuries; personalized approach; diagnosis-oriented strategy; clinical and economic effectiveness; prospects for healthcare development*

Introduction

Traumatic spinal injuries (TSIs) represent one of the most pressing issues in modern traumatology and neurosurgery. Each year, a significant number of cases involving damage to the osteoligamentous structures of the spine are recorded globally. These injuries are commonly associated with road traffic accidents, falls from heights, industrial and sports injuries, among other causes [1]. The proportion of osteoporotic fractures in elderly patients within the structure of TSIs is increasing, which is attributed to the general aging of the population, lifestyle changes, dietary preferences, and the growing prevalence of osteoporosis [2]. According to the Global Burden of Disease estimates (Institute for Health Metrics and Evaluation, University of Washington, Seattle, USA), the global incidence of TSIs in 2021 was approximately 7.50 million (95% confidence interval [CI]: 5.83–9.74 million), while the prevalence—defined as the presence of clinically significant consequences of previously sustained TSIs—reached 5.37 million cases (95% CI: 4.70–6.20 million) [3]. TSIs are often accompanied by acute symptoms such as severe

pain, marked limitation of mobility, and may require emergency medical care, including surgical intervention [4]. Their consequences often manifest in the long term. Neurological deficits, frequently observed due to spinal cord or nerve root injury, can result in persistent disability and significantly impaired quality of life [5]. This, in turn, limits daily activity, work capacity, and self-care abilities, and may lead to social isolation. Long-term consequences of spinal injuries impose a substantial socioeconomic burden on healthcare systems due to the need for prolonged treatment, rehabilitation, social reintegration, and continuous support. Additionally, they increase expenditures related to disability and reduce overall population productivity [6]. In 2021, the estimated number of patients suffering from the effects of traumatic cervical spinal cord injury was approximately 7.42 million (95% CI: 6.74–8.35 million), with an annual incidence of around 0.31 million (95% CI: 0.22–0.46 million). Thoracolumbar injuries are even more prevalent, with an estimated 7.98 million (95% CI: 7.15–9.16 million) individuals presenting with persistent symptoms and approximately 0.27 million (95% CI: 0.18–0.39 million) new cases annually [3]. These figures highlight the urgent need for a comprehensive approach to injury prevention, rehabilitation of patients with TSIs, and optimization of surgical treatment strategies aimed at achieving adequate spinal stabilization, restoration of neurological function, and reduction of rehabilitation duration.

In recent decades, significant progress has been made in the diagnostic techniques for TSIs [7]. Modern technologies such as multislice computed tomography [8,9], magnetic resonance imaging [10, 11], and high-resolution ultrasonography [12, 13] provide detailed visualization of damaged structures and allow evaluation of surrounding tissues. These tools enhance diagnostic precision, enabling assessment of spinal segment stability, spinal cord compression, and soft tissue injury severity.

Furthermore, the implementation of advanced anesthesiology practices—such as multimodal anesthesia and regional analgesia techniques—has significantly reduced perioperative complications and improved surgical tolerability, even in patients with severe comorbidities [14, 15]. Advances in surgical methods, particularly minimally invasive techniques, endoscopic approaches, robotic systems, and real-time navigation, have markedly improved surgical accuracy, reduced operative time, and shortened the recovery period [16, 17].

The expanding range of available treatment options and a growing emphasis not only on clinical effectiveness but also on the economic feasibility of each method are key trends shaping contemporary healthcare. Nevertheless, numerous issues accompanying these developments remain debatable and/or insufficiently explored.

The aim of this review is to comprehensively evaluate the prospects of implementing an individualized approach to the treatment of traumatic spinal injuries—one of the most socially significant categories of musculoskeletal disorders. The review explores economic, legal, medical, and deontological aspects associated with integrating individualization strategies into the existing diagnostically oriented paradigm.

Materials and methods

This analytical review was conducted following the PRISMA protocol (Preferred Reporting Items for Systematic Reviews and Meta-Analyses), which ensured transparency, systematicity, and objectivity throughout the search and selection process. The literature search was carried out using international scientometric databases including PubMed, Scopus, Web of Science, and Google Scholar. The key inclusion criteria were: relevance to individualized approaches in the treatment of spinal trauma, the presence of economic, legal, medical, or deontological aspects, and a publication date within the last 10 years. The main keywords (MeSH terms) used during the search included: "Spinal Injuries", "Spinal Fractures", "Precision Medicine", "Individualized Medicine", "Treatment Outcome", "Cost-Benefit Analysis", "Health Economics", "Clinical Effectiveness", "Ethics, Medical", "Jurisprudence", "Diagnostic Techniques and Procedures", "Evidence-Based Medicine".

A stepwise screening process was applied, initially based on titles and abstracts, followed by full-text evaluation. In addition, reference lists of the selected articles were reviewed to identify further relevant sources. The final analytical review included original research articles, systematic reviews, clinical guidelines, and methodological materials that met the aforementioned criteria.

The results of the analysis were structured according to the thematic sections of the review.

Results

The Economic threshold of excellence

Despite significant advances, the outcomes of TSI remain equivocal [18]. In certain cases, the introduction of novel technologies and treatment methods results in only marginal improvements in long-term clinical outcomes, whereas the associated healthcare costs continue to rise steadily. This leads to the attainment of a certain threshold, beyond which further technological advancements yield diminishing clinical benefits while requiring increasingly substantial financial and resource investments [19]. This phenomenon, known as diminishing returns, indicates that the effectiveness of treatment does not increase indefinitely with the sophistication and expense of technology. On the contrary, additional investments in high-end solutions may offer only minimal clinical advantages, which often do not justify the resources and efforts expended [20–22]. In spinal surgery, this phenomenon is already clearly observable. While modern approaches help reduce intraoperative risks and shorten postoperative recovery periods, their impact on long-term outcomes—such as functional recovery, disability reduction, or improvements in patient quality of life—diminishes with each successive technological enhancement [19]. This

This article contains some figures that are displayed in color online but in black and white in the print edition.

raises not only medical but also economic concerns regarding the rationale for employing highly complex and expensive technologies in cases where more accessible methods may yield comparable results. As such, it is essential to reconsider priorities and emphasize strategies that ensure an optimal balance between cost and clinical benefit. One promising solution is the implementation of a personalized approach, enabling targeted use of advanced technologies where they provide the greatest benefit. Furthermore, developing predictive methodologies to assess in advance the effectiveness of costly interventions for individual patients may help improve decision-making efficiency [23].

A practical manifestation of efforts to regulate the effect of diminishing returns is the application of the Quality-Adjusted Life Year (QALY) metric in several countries. QALY incorporates two primary components: the number of additional years a patient may gain from treatment and the projected quality of those years, expressed on a scale from 0 to 1—where 1 represents perfect health and 0 equates to a health state comparable to death [24]. The core purpose of QALY is to quantitatively evaluate the potential benefit of a given medical intervention or therapy. For example, if a treatment adds one year of life in perfect health, it results in a gain of 1.0 QALY; if it prolongs life by four years in a condition rated at 0.5, the total benefit would amount to 2.0 QALYs.

Utilization of the QALY metric supports evidence-based decision-making under limited healthcare budgets, particularly when assessing the appropriateness of expensive technologies, pharmaceuticals, or surgical procedures [25]. In countries with well-developed healthcare systems, there are established thresholds for the cost per QALY. For instance, in the United Kingdom, the National Institute for Health and Care Excellence (NICE) has set the threshold at £30,000 per 1.0 QALY [26, 27]. If the cost of treatment exceeds a certain threshold, it may be deemed economically unjustifiable, even when it offers clear clinical benefits. The use of QALY is associated with several ethical and methodological challenges. For instance, patients with chronic illnesses or disabilities typically have a lower baseline health status assessment, which inevitably results in lower QALY estimates, effectively introducing a discriminatory factor. This raises concerns about the fairness of applying QALY in resource allocation decisions, especially in cases involving the preservation of life in patients with initially low quality of life. Furthermore, the QALY methodology can lead to situations where expensive interventions with marginal QALY gains are rejected in favor of more cost-effective measures that produce greater impact at the population level [28]. This creates significant challenges in decision-making for the treatment of orphan or severe diseases, where the cost per 1.0 QALY may be extraordinarily high due to the rarity or complexity of the condition [29].

Even in the most developed countries, QALY has limited applicability in the context of injuries in general, and TSI in particular. This is due to inherent conflicts involving both medical and legal considerations, primarily rooted in the need to balance limited healthcare resources with the patient's right to receive necessary medical care [30, 31].

In Ukraine, the QALY criterion has not yet been adopted. However, in 2020, the country officially introduced the Health Technology Assessment (HTA) mechanism—a systematic process for evaluating the clinical effectiveness, safety, economic feasibility, and social impact of medical interventions. The assessment is conducted by the State Expert Center of the Ministry of Health of Ukraine, as regulated by Resolution No. 1300 of December 23, 2020, "On the Approval of the procedure for the state assessment of health technologies" [32]. Nevertheless, neither in Ukraine nor globally have mandatory algorithms or protocols been developed for providing medical care to patients with TSIs, existing guidelines remain merely recommendatory in nature [33, 34].

Problems of standards and protocols

Mandatory recommendations for the treatment of specific diseases, especially those as resource-intensive as TSI, appear particularly promising for institutions that fund healthcare services—such as insurance companies or governmental health authorities. This approach could promote a more rational allocation of financial and medical resources, facilitate monitoring of their utilization, prevent potential overspending, and ensure effective planning. A commonly cited argument in favor of implementing such guidelines is the improvement of care quality and treatment outcomes through reduced variability in clinical decision-making [4].

However, mandatory treatment protocols for TSI are currently lacking due to several key factors. Firstly, these injuries represent an extremely heterogeneous group of clinical conditions, including varying degrees of spinal instability, neurological deficits, soft tissue injuries, and concomitant trauma. Capturing all such variables within a single, universally applicable protocol is inherently challenging [35]. Secondly, despite the traditional diagnosis-driven approach in modern medicine, there is a gradual shift toward individualized treatment strategies, wherein decisions are tailored to patient-specific factors such as age, bone quality, overall health status, and trauma characteristics. Universal mandatory protocols risk limiting the flexibility required in complex or atypical cases. Moreover, ethical and legal concerns are also relevant [36].

Pronounced and inevitable disparities in resource availability across regions within the same healthcare system complicate the development of standardized protocols. These include significant differences in staff qualifications, access to advanced technologies, and institutional capacity. For instance, high-cost, high-resolution diagnostic equipment that may be available in major referral centers is often inaccessible in peripheral facilities, rendering certain mandatory recommendations unfeasible in practice [37].

Mandatory protocols carry the risk of shifting liability onto individual healthcare providers in situations where strict adherence to such guidelines results in complications or suboptimal outcomes [38]. In practice, the legal implications of this vary. Physicians may be accused of failing to address individual patient needs, even when strictly following the guidelines, particularly

in cases where the intervention proves ineffective or leads to adverse effects, and the harmed party can demonstrate that such outcomes were foreseeable. This places healthcare professionals in a dilemma: whether to adhere rigidly to protocols or to deviate in favor of personalized care—potentially violating regulations [39].

At the level of protocol developers, responsibility may fall on the institutions or experts involved in drafting the guidelines, especially if the recommendations fail to consider rare or atypical clinical scenarios. Outdated or flawed protocols may carry reputational risks.

At the health system level, governmental or regulatory authorities that mandate such protocols may face criticism for insufficient due diligence, particularly if the guidelines fail to reflect local conditions or are inadequately adapted to clinical realities [40]. In such cases, the greatest burden of negative consequences tends to fall on the implementation tier—namely, the individual clinician providing direct care. This asymmetry of liability, as demonstrated by global practice, is often a key reason why the medical community resists over-standardization, especially when decision-makers are not subject to clearly defined legal repercussions for adverse outcomes [41–43].

Diagnosis-oriented and individualized strategy

When considering the concept of individualization in the context of the overall evolution of medicine, and TSI in particular, it is important to note that its gradual implementation reflects a shift from universal, standardized treatment protocols toward more flexible, targeted approaches that account for individual patient characteristics [44]. Historically, medicine has evolved from general empirical methods to evidence-based, diagnosis-oriented strategies, and subsequently to personalized solutions [45]. In the field of vertebrology, especially in the management of TSI, individualization comes to the forefront, as anatomical, physiological, and psychosocial differences between patients can significantly affect the choice of optimal treatment tactics [46].

The traditional diagnosis-oriented strategy in the surgical treatment of TSI is based on unified classification principles derived from widely accepted systems such as the AO Spine classification, and the TLICS (Thoracolumbar Injury Classification and Severity Score) and SLIC (Subaxial Cervical Spine Injury Classification) scales for thoracolumbar and subaxial cervical injuries, respectively. This approach involves standardized protocols for diagnosis, timing, surgical technique, and the extent of intervention [47–49]. Based on the assessment of anatomical localization, injury characteristics, degree of instability, and presence of neurological deficits, the diagnosis-oriented strategy enables surgeons to select optimal implants and fixation methods according to a formally defined injury type. This unification, shaped by years of clinical experience, provides a convenient framework for decision-making in typical cases, facilitates outcome prediction, and promotes adherence to widely accepted standards of care [50]. However, this approach targets the "average" patient and does not always adequately account for anatomical, physiological, and psychosocial differences that may substantially influence treatment outcomes. Consequently, in some cases, this may lead to insufficient or excessive surgical intervention, thereby reducing the quality of results and increasing the risk of complications [4]. A mechanism that can partially mitigate these negative effects is the pre-defined variability and adaptability of protocols. Nevertheless, both TSI treatment recommendations and most clinical guidelines lack clearly delineated boundaries for acceptable deviations from the recommended strategy. In cases involving pronounced patient-specific characteristics or injuries that deviate significantly from the "average", it becomes difficult to determine precisely where acceptable protocol adaptation ends and protocol violation begins—creating additional uncertainty and risks in clinical decision-making [51].

However, the diagnosis-oriented strategy, which aims to precisely define the nosological form of a disease and relies on systematized clinical and diagnostic criteria, has significantly simplified and standardized the selection of optimal treatment tactics, while simultaneously increasing the predictability of outcomes in typical clinical scenarios. The use of evidence-based medicine principles has made it possible to scientifically substantiate this approach and achieve broad recognition [52]. Through the systematic evaluation of clinical research data and the application of statistical methods, evidence-based medicine has provided the necessary methodological foundation to compare the efficacy and safety of different treatment algorithms, thereby supporting the validity of a diagnosis-oriented approach not only at the level of expert opinion but also through objective and reproducible results. Overall, a diagnosis-oriented strategy supplemented by an evidence base enables physicians to make informed decisions, better understand disease pathogenesis, tailor treatment to individual patient characteristics, and improve the quality of medical care. The accumulation and systematization of numerous research findings, which form the foundation of evidence-based medicine, underscore the relevance of the so-called "average patient" problem [53]. This issue arises from the fact that the results obtained from studying large groups of individuals reflect averaged indicators of treatment efficacy and safety, thus masking individual differences among study participants. Because clinical trials and statistical analyses are primarily focused on the "mean" value within a sample, real patients—with their unique combinations of genetic traits, comorbidities, age, lifestyle, and treatment responses—may fall outside the scope of the "typical" scenario [54]. Such variability may lead to a significant dispersion of treatment outcomes even when the same therapeutic method is applied [55]. Beyond the medical aspect, the "average patient" problem has considerable economic implications. Within a single classification category that prescribes uniform therapy (whether pharmacological or surgical), a subset of patients will inevitably receive overtreatment (including diagnostics, rehabilitation, recommended disability durations, etc.), while for another subset, the same method will be insufficiently aggressive or effective. As a result, the total cost of treatment may increase, the efficiency of healthcare resource utilization may decline, and the socio-economic burden on both

patients and the healthcare system as a whole may rise [56,57].

The described phenomenon can be illustrated using spinal trauma as an example. Let us assume a cohort of patients with AO Spine type A4 thoracolumbar injuries is selected for analysis. These patients have confirmed posterior ligamentous complex injuries without significant neurological deficits or severe spinal canal compression by bone fragments (5 points according to the TLICS scale). For most such cases, the optimal treatment strategy is transpedicular stabilization. However, within this cohort, patients may differ significantly in terms of sex, age, body mass index, lifestyle, anatomical level of the injury, degree of vertebral body fragmentation, bone mineral density, presence of comorbidities, and other factors. All of these parameters are dynamically interrelated and collectively determine an individual's conditional "severity" of disease, which, however, is not considered in the AO Spine classification system. If we plot this conditional severity of disease along the X-axis within a single classification category, and the number of patients along the Y-axis, we obtain a Gaussian curve, representing a normal distribution. This follows from the Central Limit Theorem, which states that if a variable is formed as a sum of many independent or weakly dependent random factors, the resulting distribution tends toward normality [58]. The peak of this curve corresponds to the "average patient" for whom transpedicular stabilization presents the optimal balance of risks and benefits (***Fig. 1A***). Patients within the central range of the distribution receive the most appropriate level of care, offering the best benefit–risk ratio.

However, in real-world clinical practice, individual patient characteristics often diverge significantly from the conditional "average." As we move away from the center of the Gaussian curve in either direction, we encounter scenarios that are not fully accounted for by standard protocols. Patients in the "right tail" of the distribution may find that the universal protocol is insufficiently effective or surgically aggressive, leading to underestimation of disease severity and, consequently, inadequate treatment. An example would be the use of short-segment fixation for TSI at the thoracolumbar junction, which often results in construct failure and pseudarthrosis [59]. Conversely, patients in the "left tail" may receive overtreatment. For instance, successful conservative management of type A4 fractures has been documented in specific patient populations. Clearly, performing surgery when it could be avoided not only increases the risk of complications but is also economically unjustified [60]. It is logical that, further along the abscissa axis to the right, another cohort of A4 fracture patients—those whose disease severity is explicitly accounted for in clinical protocols, such as those with neurological deficits—requires a different therapeutic approach, namely decompression combined with stabilization.

Two strategies can be employed to reduce episodes of overtreatment in patients with TSI. The first involves "shifting " the entire distribution curve toward less aggressive interventions. This approach entails revising standardized protocols to adopt more conservative or minimally invasive procedures as the default. Such a shift reduces surgical complications and the economic burden of unnecessary operations [61]. However, this carries the risk of undertreatment for patients whose conditions significantly exceed the "average" severity (right "tail " of the curve), resulting in increased likelihood of reoperations, exacerbations, construct failures, and prolonged rehabilitation (***Fig. 1B***). As a result, this group is more likely to experience repeated interventions, exacerbations, inability to stabilise, fragmentation of structures, and a prolonged rehabilitation period. In addition, the existence of a statistically established "average patient" complicates the idea of "shifting" the curve, since the entire logic of standardised protocols is most often built around this averaged model [62]. The "center" of the distribution is not merely an abstract point on a curve but the outcome of large-scale data analysis that underpins existing classifications, clinical guidelines, and treatment algorithms. Any shift would necessitate redefining the criteria that determine what constitutes a "typical" case and "standard" therapy [63].

The second approach involves "narrowing" the curve by applying stricter inclusion criteria and additional patient stratification. In this case, individuals whose specific characteristics (e.g., risk factors or presence of multifactorial comorbidities) do not align with the "typical" representative of the target category are excluded from the general cohort. This results in a more homogeneous group for which a standardized protocol is genuinely effective. At the same time, this approach reduces the risk of unjustifiably aggressive therapy in "mild" cases, since patients with extremely unfavorable or highly favorable clinical profiles are excluded from the standard protocol and either referred to specialized centers or offered alternative treatment regimens. However, such stringent filtering narrows the scope of the protocol, complicates patient routing, and may lead to the exclusion of individuals who formally meet the criteria but in reality require a different level of care. Furthermore, reliable verification of clinical status demands more comprehensive diagnostics, which increases both time and resource expenditures [64].

Thus, "shifting" the curve toward less invasive methods reduces the number of cases in which patients are exposed to unnecessarily aggressive interventions, but increases the risk of insufficient consideration of individual factors in severely ill patients. Conversely, "narrowing" the curve enhances the precision and effectiveness of standard protocols for a narrowly defined subgroup, but significantly increases the risk of excluding patients who could have benefited from the protocol, while also complicating diagnostic and stratification processes.

Therefore, a standard protocol designed for the "average patient" indeed delivers the most effective outcomes for the majority of the population. Nevertheless, as the diversity of clinical conditions increases, the efficacy of such a protocol predictably diminishes—especially at the "margins" of the distribution. The very methodology underlying the development of clinical practice guidelines implies that achieving 100% treatment effectiveness for all patients is fundamentally impossible, regardless of the expertise of healthcare professionals, the quality of medical infrastructure, or the resources invested in the diagnostic and therapeutic process. Such a "universal" approach inevitably leaves a

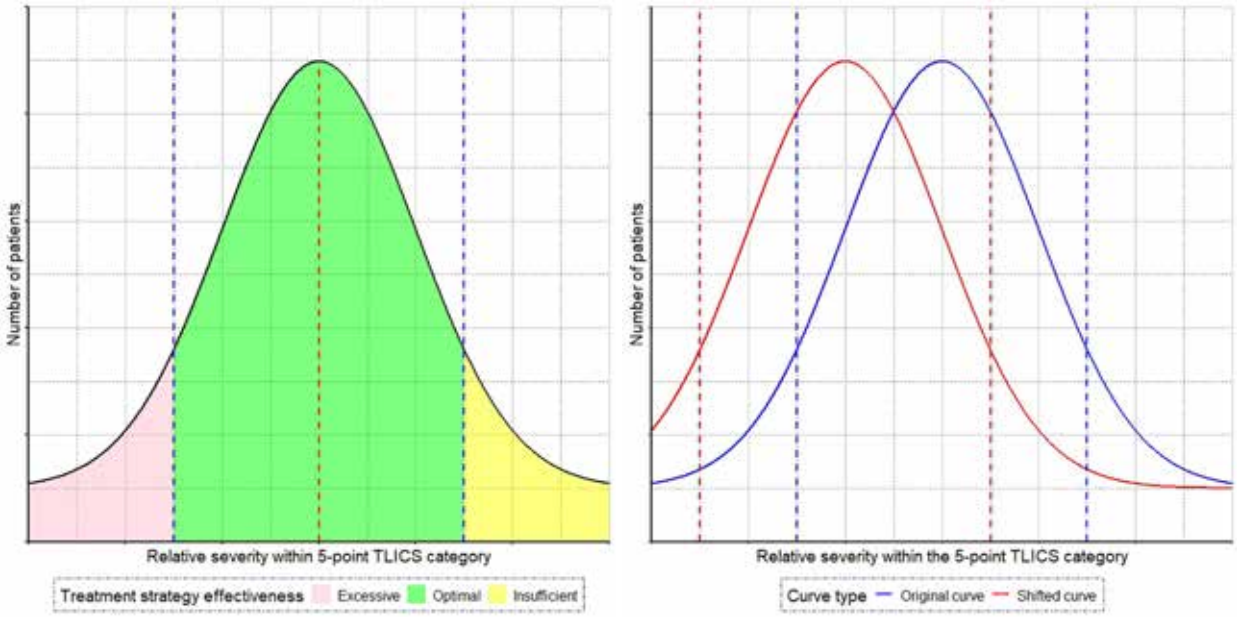

Fig. 1. Visual representation of the "average patient" problem

subset of patients with suboptimal treatment outcomes, as their individual characteristics fall outside the capabilities of an averaged clinical algorithm [65].

The Problem of classifications

Despite advances in diagnostic methods that provide ample opportunities for detailed characterization and assessment of injury severity, recent decades have seen a trend toward simplification of spinal trauma classification systems in vertebrology. This tendency contradicts the logic of the aforementioned arguments. The accumulation of data on the biomechanics and morphology of traumatic injuries through imaging technologies throughout the 20th century led to the evolution of TSI grading schemes. Most researchers aimed to enhance detail and precision in describing the anatomical and biomechanical features of injuries to facilitate optimal treatment strategies. Examples of such classification systems include those proposed by F. Magerl et al. for the thoracolumbar spine (1994) and by B. L. Allen et al. for the subaxial cervical spine (1982) [66,67]. Some authors developed classification categories not based on empirically documented and described injury types, but rather on hypothetical ones predicted by presumed mechanisms of trauma [68]. A pivotal historical shift in the conceptualization of TSI classification occurred with the attempt to unify all existing systems of musculoskeletal injury classification, initiated by the Association for the Study of Internal Fixation/Orthopaedic Trauma Association (AO/OTA). This initiative culminated in the development and global implementation of the AO/OTA Fracture and Dislocation Classification, a system based on a unified structural principle [69]. Within this framework, each anatomical region is assigned a code—"51" for the cervical spine, "52" for the thoracic spine, "53" for the lumbar spine, and "54" for the sacrum. Each region encompasses three primary injury types: Type A (injuries involving only bony structures), Type B (combined injuries of bone and ligamentous structures), and Type C (predominantly ligamentous injuries, possibly with bony involvement and displacement). Each type is further subdivided into subtypes (usually numbered from 1 to 3, or more), reflecting increasing severity. In addition, TSI classifications incorporate modifiers assessing neurological deficits, involvement of facet joints, and other pathological processes, allowing for more precise injury characterization [70]. The widely adopted AO Spine Subaxial Cervical Spine Classification System and the AO Spine Thoracolumbar Spine Classification System are in fact segments of this global classification framework [47, 71].

One of the primary reasons for modifying the concept of classifying traumatic injuries was the pursuit of greater reproducibility and standardization. It is well established that complex, multi-level schemes often led to low inter-rater agreement—different specialists, using the same classification system, could arrive at different diagnoses and propose divergent treatment strategies. In contrast, simplified systems based on a few key factors (such as stability, neurological status, and the condition of the ligamentous and bony structures) offer improved reproducibility and predictability of outcomes [72, 73].

In the context of evidence-based medicine, simplified classifications are also more appropriate. Firstly, they allow for the formation of large homogeneous patient samples and facilitate the objective evaluation of the effectiveness of specific treatment approaches. Secondly, the results of multicenter studies and meta-analyses that rely on such standardized classifications are easier to compare across various institutions and regions, thereby ensuring a higher level of evidentiary strength. The simplicity and standardization of criteria enable the development of clinical guidelines that can subsequently serve as the foundation for protocols and manuals aligned with evidence-based principles [74].

It is assumed that excessive detail complicates rapid decision-making and often fails to offer significant advantages in treatment selection, particularly when a swift and standardized approach is required [75]. Therefore, the current trend in TSI grading is oriented toward a tactics-driven approach, with a notable shift in emphasis toward practicality over precision [76].

Nonetheless, in the broader context of evidence-based medicine and scientific research, simplified assessment systems have limitations, as they may obscure critical parameters that influence treatment outcomes [77]. For example, in a previously analyzed cohort of patients with B2 spinal trauma (type A4 vertebral body injuries) and a TLICS score of 5, one can evaluate the efficacy of a specific treatment modality, such as transpedicular fixation, using a set of defined criteria. However, comparing the effectiveness of different approaches based solely on these parameters is challenging, and selecting the optimal treatment for an individual patient becomes even more difficult [54]. Thus, while a simplified scoring system or classification (albeit convenient for rapid diagnostics and statistical analysis) does not provide a comprehensive answer to the question of which treatment method would be most effective for a given patient [78].

Optimizing treatment within the framework of evidence-based medicine requires that standardized protocols—although useful in generalized form—be complemented by personalized criteria. This would establish a more reliable foundation for comparing various methods (e.g., transpedicular fixation, combined surgical intervention, or conservative management) and facilitate the selection of an approach most beneficial to the patient [79].

Deontological challenges

The issue of the "average patient" remains a key factor influencing the unconditional acceptance of results from high-evidence-level studies [80]. Although this issue has accompanied evidence-based medicine throughout its historical development, it remains insufficiently recognized both among medical professionals and the general public, leading to not only medical but also deontological challenges [81, 82]. Modern patients often possess broad yet superficial knowledge about available treatment options. With the advancement of the internet and digital technologies, information on medical procedures has become readily accessible to a wide audience. Patients can quickly find details about various diseases, diagnostic methods, and treatments, thereby expanding their general awareness [83]. However, not all available information is of high quality or scientifically validated [83]. Many sources provide incomplete, outdated, erroneous, or deliberately distorted data, which results in a superficial understanding of complex medical concepts [84]. Furthermore, even when high-quality information is available, patients often face difficulties interpreting it due to a lack of specialized knowledge. This almost invariably leads to misinterpretation of medical recommendations or suboptimal treatment choices when such a choice is permitted. A further challenge in today's society is the active promotion of certain medical methods and pharmaceutical products through marketing campaigns and social media, which distorts public perceptions of their effectiveness and safety. Patients may be influenced by misleading reviews and promotional promises, further complicating informed decision-making about their care [85,86]. Moreover, the popularity of evidence-based medicine as a trend, and the perception of its standards as absolute dogma, often leads to situations where deviations from established protocols are viewed by patients or their relatives as signs of professional incompetence, rather than as attempts to adapt treatment to individual patient characteristics and the capabilities of the healthcare facility [87]. Similar situations arise during expert evaluations of medical staff actions, where certain flexibility in clinical approaches may be perceived as a lack of professionalism or an absence of a clear treatment strategy for a given nosological unit, despite the clinical rationale behind such decisions [88].

Discussion

The concept of individualization is embedded within the very foundation of evidence-based medicine. One of its pioneers, Archie Cochrane, emphasized that evidence is only useful insofar as it can guide the treatment of individual patients [89,90]. His work highlighted the need to differentiate between approaches aimed at populations as a whole and those designed for individual medical care. The former, according to Cochrane, should serve primarily as the basis for developing general recommendations or clinical protocols [91]. As a potential solution, he proposed the use of subgroup analysis in clinical research to determine how treatments affect different patient categories [92].

The exponential growth in computational power over recent decades, the development of new statistical analysis techniques, and the adoption of previously known but computationally intensive methods—such as Bayesian approaches—have enabled a fundamentally new level of patient-specific treatment adaptation. This transition marks a shift from the physician's subjective judgment in a given clinical situation to mathematically and statistically grounded decision-making [93, 94].

A review of the literature has identified several methodologies most commonly applied in the context of personalized treatment strategies:

- regression analysis methods – used for modeling and predicting relationships between variables. This category includes linear regression, logistic regression, multilevel (hierarchical) regression, and Poisson regression [95, 96];
- survival analysis methods – focused on time-to-event data, including Kaplan–Meier curves, Cox proportional hazards models, and competing risks models [97, 98];
- machine learning and artificial intelligence methods – employed to process large datasets and uncover complex nonlinear patterns. Key techniques include decision trees, random forests, gradient boosting, neural networks, and deep learning algorithms [99, 100];
- bayesian methods – based on Bayes' theorem for updating probabilities as new data becomes available.

Examples include Bayesian networks, naïve Bayes classifiers, and Markov chain Monte Carlo (MCMC) simulations [101, 102];

- cluster analysis methods – used to group patients based on similar characteristics without prior labeling. Common approaches include K-means clustering, hierarchical clustering, and DBSCAN (Density-Based Spatial Clustering of Applications with Noise) [103, 104];
- feature selection methods – assist in identifying the most informative variables for model building, thereby reducing data dimensionality and preventing overfitting. These include stepwise regression, LASSO and Ridge regression, and feature importance–based techniques [105].

While this list is by no means exhaustive, it demonstrates the wide and diverse range of data analysis methods available for identifying the most informative predictors and their interactions. The appropriate selection and application of such methods allow for the development of effective, individualized treatment plans.

The findings presented in this review highlight specific aspects of the rationale for developing individualized approaches to treating a heterogeneous condition such as TSI. It is emphasized that protocols and standards based on the principles of evidence-based medicine should not be seen as rigid doctrines but rather as frameworks that define the general direction of therapy, within which individualized treatment plans are to be developed. The relevance of such an approach is underscored by the growing body of research demonstrating the effectiveness of advanced models—particularly those using neural networks—not only for diagnostic purposes but also for optimizing therapeutic decision-making. Individualization provides clear advantages not only in medical terms but also in economic contexts, by contributing to reduced treatment costs and more efficient use of healthcare resources—thus addressing one of the pressing challenges of modern healthcare systems.

Conclusions

An individualized approach to the treatment of TSI represents a significant advancement in contemporary medical practice. The preconditions discussed highlight the necessity of shifting from standardized therapeutic methods toward more flexible and tailored strategies that account for the unique characteristics of each patient. Personalizing TSI treatment not only enhances the efficacy and safety of both surgical and conservative interventions but also contributes to the development of a more resilient and cost-effective healthcare system. Ongoing advancements in technology and data analysis methods support the refinement of these approaches, enabling more precise and patient-centered care. The relevance of research in this field is driven by the growing societal demand for effective and economically sound individualized medical solutions.

Disclosure

Conflict of interest

The author declares no conflict of interest.

Funding

This research received no external funding.

References

1. Diseases GBD, Injuries C. Global burden of 369 diseases and injuries in 204 countries and territories, 1990-2019: a systematic analysis for the Global Burden of Disease Study 2019. Lancet (London, England). 2020;396(10258):1204-1222. doi: 10.1016/S0140-6736(20)30925-9
2. Williams AL, Al-Busaidi A, Sparrow PJ, Adams JE, Whitehouse RW. Under-reporting of osteoporotic vertebral fractures on computed tomography. Eur J Radiol. 2009;69(1):179-183. doi: 10.1016/j.ejrad.2007.08.028
3. Global Burden of Disease Collaborative Network. Global Burden of Disease Study 2021 (GBD 2021) Results. Seattle, United States: Institute for Health Metrics and Evaluation (IHME); 2022. https://vizhub.healthdata.org/gbd-results/
4. Sandean D. Management of acute spinal cord injury: A summary of the evidence pertaining to the acute management, operative and non-operative management. World J Orthop. 2020;11(12):573-583. doi: 10.5312/wjo.v11.i12.573
5. Peterson MD, Meade MA, Lin P, Kamdar N, Rodriguez G, Krause JS, et al. Psychological morbidity following spinal cord injury and among those without spinal cord injury: the impact of chronic centralized and neuropathic pain. Spinal Cord. 2022;60(2):163-169. doi: 10.1038/s41393-021-00731-4
6. Limthongkul W, Singhatanadgige W, Vaccaro AR, Albert TJ, Radcliff K. Health-related quality of life and cost after cervical spine trauma. Seminars in Spine Surgery. 2014;26(1):30-37. doi: 10.1053/j.semss.2013.07.008
7. Fiani B, Noblett C, Nanney J, Doan T, Pennington E, Jarrah R, et al. Diffusion tensor imaging of the spinal cord status post trauma. Surg Neurol Int. 2020;11:276. doi: 10.25259/SNI_495_2020
8. Fatehi D, Dayani MA, Rostamzadeh A. Role of CT scan in theranostic and management of traumatic spinal cord injury. Saudi J Biol Sci. 2018;25(4):739-746. doi: 10.1016/j.sjbs.2016.08.004
9. Ordonez CA, Parra MW, Holguin A, Garcia C, Guzman-Rodriguez M, Padilla N, et al. Whole-body computed tomography is safe, effective and efficient in the severely injured hemodynamically unstable trauma patient. Colomb Med (Cali). 2020;51(4):e4054362. doi: 10.25100/cm.v51i4.4362
10. Seif M, Curt A, Thompson AJ, Grabher P, Weiskopf N, Freund P. Quantitative MRI of rostral spinal cord and brain regions is predictive of functional recovery in acute spinal cord injury. Neuroimage Clin. 2018;20:556-563. doi: 10.1016/j.nicl.2018.08.026
11. Aly MM, Al-Shoaibi AM, Aljuzair AH, Issa TZ, Vaccaro AR. A Proposal for a Standardized Imaging Algorithm to Improve the Accuracy and Reliability for the Diagnosis of Thoracolumbar Posterior Ligamentous Complex Injury in Computed Tomography and Magnetic Resonance Imaging. Global Spine J. 2023;13(3):873-896. doi: 10.1177/21925682221129220
12. Chuang CH, Huang CY, Ho SW, Chen CC. Rapid Detecting Brachial Plexus Injury by Point-of-Care Ultrasonography. J Med Ultrasound. 2022;30(4):303-305. doi: 10.4103/jmu.jmu_185_21
13. Vk V, Bhoi S, Aggarwal P, Murmu LR, Agrawal D, Kumar A, et al. Diagnostic utility of point of care ultrasound in identifying cervical spine injury in emergency settings. Australas J Ultrasound Med. 2021;24(4):208-216. doi: 10.1002/ajum.12274
14. Taylor C, Metcalf A, Morales A, Lam J, Wilson R, Baribeault T. Multimodal Analgesia and Opioid-Free Anesthesia in Spinal Surgery: A Literature Review. J Perianesth Nurs. 2023;38(6):938-942. doi: 10.1016/j.jopan.2023.04.003
15. Yang S, Xiao W, Wu H, Liu Y, Feng S, Lu J, et al. Management Based on Multimodal Brain Monitoring May Improve Functional Connectivity and Post-operative Neurocognition in Elderly Patients Undergoing Spinal Surgery. Front Aging Neurosci. 2021;13:705287. doi: 10.3389/fnagi.2021.705287
16. Avrumova F, Lebl DR. Augmented reality for minimally invasive spinal surgery. Front Surg. 2022;9:1086988. doi: 10.3389/fsurg.2022.1086988
17. Walker CT, Xu DS, Godzik J, Turner JD, Uribe JS, Smith

WD. Minimally invasive surgery for thoracolumbar spinal trauma. Ann Transl Med. 2018;6(6):102. doi: 10.21037/atm.2018.02.10
18. Ding W, Hu S, Wang P, Kang H, Peng R, Dong Y, et al. Spinal Cord Injury: The Global Incidence, Prevalence, and Disability From the Global Burden of Disease Study 2019. Spine (Phila Pa 1976). 2022;47(21):1532-1540. doi: 10.1097/BRS.0000000000004417
19. Morone G, Pirrera A, Iannone A, Giansanti D. Development and Use of Assistive Technologies in Spinal Cord Injury: A Narrative Review of Reviews on the Evolution, Opportunities, and Bottlenecks of Their Integration in the Health Domain. Healthcare (Basel). 2023 Jun 4;11(11):1646. doi: 10.3390/healthcare11111646
20. Sammon JD, Abdollah F, Klett DE, Pucheril D, Sood A, Trinh QD, et al. The diminishing returns of robotic diffusion: complications after robot-assisted radical prostatectomy. BJU Int. 2016;117(2):211-212. doi: 10.1111/bju.13111
21. Passias PG, Bortz C, Horn SR, Segreto FA, Stekas N, Ge DH, et al. Diminishing Clinical Returns of Multilevel Minimally Invasive Lumbar Interbody Fusion. Spine (Phila Pa 1976). 2019;44(20):E1181-E1187. doi: 10.1097/BRS.0000000000003110
22. Gold MR, Siegel JE, Russell LB, Weinstein MC, editors. Cost-Effectiveness in Health and Medicine. New York: Oxford Academic; 1996. doi: 10.1093/oso/9780195108248.001.0001
23. Dietz N, Sharma M, Alhourani A, Ugiliweneza B, Wang D, Nuno MA, et al. Variability in the utility of predictive models in predicting patient-reported outcomes following spine surgery for degenerative conditions: a systematic review. Neurosurg Focus. 2018;45(5):E10. doi: 10.3171/2018.8.FOCUS18331
24. Toure M, Kouakou CRC, Poder TG. Dimensions Used in Instruments for QALY Calculation: A Systematic Review. Int J Environ Res Public Health. 2021;18(9). doi: 10.3390/ijerph18094428
25. Lotfi R, Haqiqat E, Sadra Rajabi M, Hematyar A. Robust and resilience budget allocation for projects with a risk-averse approach: A case study in healthcare projects. Computers and Industrial Engineering. 2023 Feb;176:108948. doi: 10.1016/j.cie.2022.108948
26. Siverskog J, Henriksson M. On the role of cost-effectiveness thresholds in healthcare priority setting. Int J Technol Assess Health Care. 2021;37:e23. doi: 10.1017/S0266462321000015
27. Iino H, Hashiguchi M, Hori S. Estimating the range of incremental cost-effectiveness thresholds for healthcare based on willingness to pay and GDP per capita: A systematic review. PLoS One. 2022;17(4):e0266934. doi: 10.1371/journal.pone.0266934
28. Petrou S. Methodological challenges surrounding QALY estimation for paediatric economic evaluation. Cost Eff Resour Alloc. 2022;20(1):10. doi: 10.1186/s12962-022-00345-4
29. Towse A, Garau M. Appraising ultra-orphan drugs: is cost-per-QALY appropriate? A review of the evidence. Consulting Report. 2018 Mar 1(001978). https://www.ohe.org/wp-content/uploads/2018/03/468-Appraising-ultra-orphan-drugs.pdf
30. Use of QALYs: advantages and concerns. PharmacoEconomics & Outcomes News. 2018;806(1):2-2. doi: 10.1007/s40274-018-5045-5.
31. Pollard D, Fuller G, Goodacre S, van Rein EAJ, Waalwijk JF, van Heijl M. An economic evaluation of triage tools for patients with suspected severe injuries in England. BMC Emerg Med. 2022;22(1):4. doi: 10.1186/s12873-021-00557-6
32. Кабінет Міністрів України. Постанова від 23 грудня 2020 р. № 1300 "Про затвердження Порядку проведення державної оцінки медичних технологій". Київ: Кабінет Міністрів України; 2020. https://zakon.rada.gov.ua/laws/show/1300-2020-%D0%BF#Text Cabinet of Ministers of Ukraine. Resolution of December 23, 2020 No. 1300 "On Approval of the Procedure for Conducting State Assessment of Medical Technologies." Kyiv: Cabinet of Ministers of Ukraine; 2020. https://zakon.rada.gov.ua/laws/show/1300-2020-%D0%BF#Text.
33. Greenberg JK, Burks SS, Dibble CF, Javeed S, Gupta VP, Yahanda AT, et al. An updated management algorithm for incorporating minimally invasive techniques to treat thoracolumbar trauma. J Neurosurg Spine. 2022;36(4):558-567. doi: 10.3171/2021.7.SPINE21790
34. Portelli Tremont JN, Cook N, Murray LH, Udekwu PO, Motameni AT. Acute Traumatic Spinal Cord Injury: Implementation of a Multidisciplinary Care Pathway. J Trauma Nurs. 2022;29(4):218-224. doi: 10.1097/JTN.0000000000000664
35. O'Toole JE, Kaiser MG, Anderson PA, Arnold PM, Chi JH, Dailey AT, et al. Congress of Neurological Surgeons Systematic Review and Evidence-Based Guidelines on the Evaluation and Treatment of Patients with Thoracolumbar Spine Trauma: Executive Summary. Neurosurgery. 2019;84(1):2-6. doi: 10.1093/neuros/nyy394
36. Bolcato M, Fassina G, Rodriguez D, Russo M, Aprile A. The contribution of legal medicine in clinical risk management. BMC Health Serv Res. 2019;19(1):85. doi: 10.1186/s12913-018-3846-7
37. Agha L, Frandsen B, Rebitzer JB. Fragmented division of labor and healthcare costs: Evidence from moves across regions. Journal of Public Economics. 2019;169:144-159. doi: 10.1016/j.jpubeco.2018.11.001.
38. Kellner DB, Urman RD, Greenberg P, Brovman EY. Analysis of adverse outcomes in the post-anesthesia care unit based on anesthesia liability data. J Clin Anesth. 2018;50:48-56. doi: 10.1016/j.jclinane.2018.06.038
39. Corte-Real A, Caetano C, Alves S, Pereira AD, Rocha S, Nuno Vieira D. Patient Safety in Dental Practice: Lessons to Learn About the Risks and Limits of Professional Liability. Int Dent J. 2021;71(5):378-383. doi: 10.1016/j.identj.2020.12.014
40. Akmal A, Podgorodnichenko N, Foote J, Greatbanks R, Stokes T, Gauld R. Why is Quality Improvement so Challenging? A Viable Systems Model Perspective to Understand the Frustrations of Healthcare Quality Improvement Managers. Health Policy. 2021;125(5):658-664. doi: 10.1016/j.healthpol.2021.03.015
41. Arntsen B, Torjesen DO, Karlsen TI. Asymmetry in inter-municipal cooperation in health services - How does it affect service quality and autonomy? Soc Sci Med. 2021;273:113744. doi: 10.1016/j.socscimed.2021.113744
42. Sittig DF, Belmont E, Singh H. Improving the safety of health information technology requires shared responsibility: It is time we all step up. Healthc (Amst). 2018;6(1):7-12. doi: 10.1016/j.hjdsi.2017.06.004
43. Vilchyk TB, Krainyk HS, Shandula OO. Legal enforcement and development directions of health law in Ukraine. Wiad Lek. 2019;72(4):692-696. doi: 10.36740/wlek201904136
44. Guest JD, Kelly-Hedrick M, Williamson T, Park C, Ali DM, Sivaganesan A, et al. Development of a Systems Medicine Approach to Spinal Cord Injury. J Neurotrauma. 2023;40(17-18):1849-1877. doi: 10.1089/neu.2023.0024
45. Gameiro GR, Sinkunas V, Liguori GR, Auler-Junior JOC. Precision Medicine: Changing the way we think about healthcare. Clinics (Sao Paulo, Brazil). 2018;73:e723. doi: 10.6061/clinics/2017/e723
46. Tian C, Lv Y, Li S, Wang DD, Bai Y, Zhou F, et al. Factors related to improved American Spinal Injury Association grade of acute traumatic spinal cord injury. World J Clin Cases. 2020;8(20):4807-4815. doi: 10.12998/wjcc.v8.i20.4807
47. Vaccaro AR, Oner C, Kepler CK, Dvorak M, Schnake K, Bellabarba C, et al. AOSpine thoracolumbar spine injury classification system: fracture description, neurological status, and key modifiers. Spine (Phila Pa 1976). 2013;38(23):2028-2037. doi: 10.1097/BRS.0b013e3182a8a381
48. Vaccaro AR, Lehman RA, Jr., Hurlbert RJ, Anderson PA, Harris M, Hedlund R, et al. A new classification of thoracolumbar injuries: the importance of injury morphology, the integrity of the posterior ligamentous complex, and neurologic status. Spine (Phila Pa 1976). 2005;30(20):2325-2333. doi: 10.1097/01.brs.0000182986.43345.cb
49. Canseco JA, Schroeder GD, Paziuk TM, Karamian BA, Kandziora F, Vialle EN, et al. The Subaxial Cervical AO Spine Injury Score. Global Spine J. 2022;12(6):1066-1073. doi:

10.1177/2192568220974339
50. Verheyden AP, Spiegl UJ, Ekkerlein H, Gercek E, Hauck S, Josten C, et al. Treatment of Fractures of the Thoracolumbar Spine: Recommendations of the Spine Section of the German Society for Orthopaedics and Trauma (DGOU). Global Spine J. 2018;8(2 Suppl):34S-45S. doi: 10.1177/2192568218771668
51. Nilsbakken IMW, Sollid S, Wisborg T, Jeppesen E. Assessing Trauma Management in Urban and Rural Populations in Norway: A National Register-Based Research Protocol. JMIR Res Protoc. 2022;11(6):e30656. doi: 10.2196/30656
52. Wuthisuthimethawee P, Sookmee W, Damnoi S. Non-randomized comparative study on the efficacy of a trauma protocol in the emergency department. Chinese journal of traumatology = Zhonghua chuang shang za zhi. 2019;22(4):207-211. doi: 10.1016/j.cjtee.2019.04.003
53. Jureidini J, McHenry LB. The illusion of evidence based medicine. BMJ (Clinical research ed). 2022;376:o702. doi: 10.1136/bmj.o702
54. Sadeghi-Bazargani H, Tabrizi JS, Azami-Aghdash S. Barriers to evidence-based medicine: a systematic review. J Eval Clin Pract. 2014;20(6):793-802. doi: 10.1111/jep.12222
55. Every-Palmer S, Howick J. How evidence-based medicine is failing due to biased trials and selective publication. J Eval Clin Pract. 2014;20(6):908-914. doi: 10.1111/jep.12147
56. Ioannidis JP. Why Most Clinical Research Is Not Useful. PLoS Med. 2016;13(6):e1002049. doi: 10.1371/journal.pmed.1002049
57. Greenhalgh T, Howick J, Maskrey N, Evidence Based Medicine Renaissance G. Evidence based medicine: a movement in crisis? BMJ (Clinical research ed). 2014;348:g3725. doi: 10.1136/bmj.g3725
58. Kwak SG, Kim JH. Central limit theorem: the cornerstone of modern statistics. Korean J Anesthesiol. 2017;70(2):144-156. doi: 10.4097/kjae.2017.70.2.144
59. Alimohammadi E, Bagheri SR, Joseph B, Sharifi H, Shokri B, Khodadadi L. Analysis of factors associated with the failure of treatment in thoracolumbar burst fractures treated with short-segment posterior spinal fixation. Journal of orthopaedic surgery and research. 2023;18(1):690. doi: 10.1186/s13018-023-04190-w
60. Soultanis K, Thano A, Soucacos PN. "Outcome of thoracolumbar compression fractures following non-operative treatment". Injury. 2021;52(12):3685-3690. doi: 10.1016/j.injury.2021.05.019
61. Bruckner J, Hashmi S, Williams SK, Ludwig S. Minimally invasive surgery for the management of thoracolumbar burst fractures. Seminars in Spine Surgery. 2021;33(1):100848. doi: 10.1016/j.semss.2021.100848.
62. Cowley A, Nelson M, Hall C, Goodwin S, Kumar DS, Moore F. Recommendation for changes to the guidelines of trauma patients with potential spinal injury within a regional UK ambulance trust. Br Paramed J. 2022;7(3):59-67. doi: 10.29045/14784726.2022.12.7.3.59
63. Alfaro-Mico J, Ramirez-Villaescusa J, Martinez-Lozano MD, Sanchez-Honrubia RM, Ruiz-Picazo D. Emergency stabilisation by single-stage posterior transpedicular approach for treatment of unstable lumbar spine fracture with neurological injury. Trauma case reports. 2020;27:100300. doi: 10.1016/j.tcr.2020.100300
64. Rogers JR, Pavisic J, Ta CN, Liu C, Soroush A, Kuen Cheung Y, et al. Leveraging electronic health record data for clinical trial planning by assessing eligibility criteria's impact on patient count and safety. J Biomed Inform. 2022;127:104032. doi: 10.1016/j.jbi.2022.104032
65. Nouhi M, Hadian M, Olyaeemanesh A. The clinical and economic consequences of practice style variations in common surgical interventions: A protocol for systematic review. Medicine (Baltimore). 2018;97(42):e12439. doi: 10.1097/MD.0000000000012439
66. Allen BL, Jr., Ferguson RL, Lehmann TR, O'Brien RP. A mechanistic classification of closed, indirect fractures and dislocations of the lower cervical spine. Spine (Phila Pa 1976). 1982;7(1):1-27. doi: 10.1097/00007632-198200710-00001
67. Magerl F, Aebi M, Gertzbein SD, Harms J, Nazarian S. A comprehensive classification of thoracic and lumbar injuries. Eur Spine J. 1994;3(4):184-201. doi: 10.1007/BF02221591
68. Nekhlopochyn OS, Cheshuk YV. Traumatic injuries of the thoracolumbar junction. Classification by Friedrich P. Magerl et al. Trauma. 2022;23(3):4-22. doi: 10.22141/1608-1706.3.23.2022.895.
69. Marsh JL, Slongo TF, Agel J, Broderick JS, Creevey W, DeCoster TA, et al. Fracture and dislocation classification compendium - 2007: Orthopaedic Trauma Association classification, database and outcomes committee. J Orthop Trauma. 2007;21(10 Suppl):S1-133. doi: 10.1097/00005131-200711101-00001
70. Divi SN, Schroeder GD, Oner FC, Kandziora F, Schnake KJ, Dvorak MF, et al. AOSpine-Spine Trauma Classification System: The Value of Modifiers: A Narrative Review With Commentary on Evolving Descriptive Principles. Global Spine J. 2019;9(1 Suppl):77S-88S. doi: 10.1177/2192568219827260
71. Vaccaro AR, Koerner JD, Radcliff KE, Oner FC, Reinhold M, Schnake KJ, et al. AOSpine subaxial cervical spine injury classification system. Eur Spine J. 2016;25(7):2173-2184. doi: 10.1007/s00586-015-3831-3
72. Azimi P, Mohammadi HR, Azhari S, Alizadeh P, Montazeri A. The AOSpine thoracolumbar spine injury classification system: A reliability and agreement study. Asian journal of neurosurgery. 2015;10(4):282-285. doi: 10.4103/1793-5482.162703
73. Lopes FAR, Ferreira A, Santos R, Macaneiro CH. Intraobserver and interobserver reproducibility of the old and new classifications of toracolombar fractures. Rev Bras Ortop. 2018;53(5):521-526. doi: 10.1016/j.rboe.2018.07.015
74. Sriganesh K, Shanthanna H, Busse JW. A brief overview of systematic reviews and meta-analyses. Indian journal of anaesthesia. 2016;60(9):689-694. doi: 10.4103/0019-5049.190628
75. Vaccaro AR, Schroeder GD, Kepler CK, Cumhur Oner F, Vialle LR, Kandziora F, et al. The surgical algorithm for the AOSpine thoracolumbar spine injury classification system. Eur Spine J. 2016;25(4):1087-1094. doi: 10.1007/s00586-015-3982-2
76. Pishnamaz M, Balosu S, Curfs I, Uhing D, Laubach M, Herren C, et al. Reliability and Agreement of Different Spine Fracture Classification Systems: An Independent Intraobserver and Interobserver Study. World Neurosurg. 2018;115:e695-e702. doi: 10.1016/j.wneu.2018.04.138
77. Berkman ND, Lohr KN, Ansari MT, Balk EM, Kane R, McDonagh M, et al. Grading the strength of a body of evidence when assessing health care interventions: an EPC update. J Clin Epidemiol. 2015;68(11):1312-1324. doi: 10.1016/j.jclinepi.2014.11.023
78. Kent DM, Steyerberg E, van Klaveren D. Personalized evidence based medicine: predictive approaches to heterogeneous treatment effects. BMJ (Clinical research ed). 2018;363:k4245. doi: 10.1136/bmj.k4245
79. Gugiu PC. Hierarchy of evidence and appraisal of limitations (HEAL) grading system. Eval Program Plann. 2015;48:149-159. doi: 10.1016/j.evalprogplan.2014.08.003
80. Ioannidis JPA. Hijacked evidence-based medicine: stay the course and throw the pirates overboard. J Clin Epidemiol. 2017;84:11-13. doi: 10.1016/j.jclinepi.2017.02.001
81. Keane M, Berg C. Evidence-based medicine: A predictably flawed paradigm. Trends in Anaesthesia and Critical Care. 2016;9:49-52. doi: 10.1016/j.tacc.2016.07.002
82. Tebala GD. The Emperor's New Clothes: a Critical Appraisal of Evidence-based Medicine. Int J Med Sci. 2018;15(12):1397-1405. doi: 10.7150/ijms.25869
83. Roland D. Social Media, Health Policy, and Knowledge Translation. J Am Coll Radiol. 2018;15(1 Pt B):149-152. doi: 10.1016/j.jacr.2017.09.009
84. Jeyaraman M, Ramasubramanian S, Kumar S, Jeyaraman N, Selvaraj P, Nallakumarasamy A, et al. Multifaceted Role of Social Media in Healthcare: Opportunities, Challenges, and the Need for Quality Control. Cureus. 2023;15(5):e39111. doi: 10.7759/cureus.39111
85. Dijkstra S, Kok G, Ledford JG, Sandalova E, Stevelink R. Possibilities and Pitfalls of Social Media for Translational Medicine. Front Med (Lausanne). 2018;5:345. doi: 10.3389/fmed.2018.00345

86. Jacobs R, Prabhu AV, Monaco EA, Tonetti D, Agarwal N. Patient perception of gamma knife stereotactic radiosurgery through twitter and instagram. Interdisciplinary Neurosurgery. 2018;13:138-140. doi: 10.1016/j.inat.2018.05.005
87. Forgie EME, Lai H, Cao B, Stroulia E, Greenshaw AJ, Goez H. Social Media and the Transformation of the Physician-Patient Relationship: Viewpoint. J Med Internet Res. 2021;23(12):e25230. doi: 10.2196/25230
88. Boushehri E, Soltani Arabshahi K, Monajemi A. Clinical reasoning assessment through medical expertise theories: past, present and future directions. Med J Islam Repub Iran. 2015;29:222
89. Shah HM, Chung KC. Archie Cochrane and his vision for evidence-based medicine. Plast Reconstr Surg. 2009;124(3):982-988. doi: 10.1097/PRS.0b013e3181b03928
90. Cochrane A. Effectiveness and Efficiency: Random Reflections on Health Services. London: Nuffield Provincial Hospitals Trust; 1972. https://www.nuffieldtrust.org.uk/research/effectiveness-and-efficiency-random-reflections-on-health-services
91. Gerris J. The legacy of Archibald Cochrane: from authority based towards evidence based medicine. Facts Views Vis Obgyn. 2011;3(4):233-237
92. Askheim C, Sandset T, Engebretsen E. Who cares? The lost legacy of Archie Cochrane. Med Humanit. 2017;43(1):41-46. doi: 10.1136/medhum-2016-011037
93. Arjas E, Gasbarra D. Adaptive treatment allocation and selection in multi-arm clinical trials: a Bayesian perspective. BMC Med Res Methodol. 2022;22(1):50. doi: 10.1186/s12874-022-01526-8
94. Williamson SF, Jacko P, Villar SS, Jaki T. A Bayesian adaptive design for clinical trials in rare diseases. Comput Stat Data Anal. 2017;113:136-153. doi: 10.1016/j.csda.2016.09.006
95. Edlitz Y, Segal E. Prediction of type 2 diabetes mellitus onset using logistic regression-based scorecards. Elife. 2022;11. doi: 10.7554/eLife.71862
96. Fukunishi H, Nishiyama M, Luo Y, Kubo M, Kobayashi Y. Alzheimer-type dementia prediction by sparse logistic regression using claim data. Comput Methods Programs Biomed. 2020;196:105582. doi: 10.1016/j.cmpb.2020.105582
97. van Walraven C, McAlister FA. Competing risk bias was common in Kaplan-Meier risk estimates published in prominent medical journals. J Clin Epidemiol. 2016;69:170-173 e178. doi: 10.1016/j.jclinepi.2015.07.006
98. Hu C, Cao J, Zeng L, Luo Y, Fan H. Prognostic factors for squamous cervical carcinoma identified by competing-risks analysis: A study based on the SEER database. Medicine (Baltimore). 2022;101(39):e30901. doi: 10.1097/MD.0000000000030901
99. Khan O, Badhiwala JH, Grasso G, Fehlings MG. Use of Machine Learning and Artificial Intelligence to Drive Personalized Medicine Approaches for Spine Care. World Neurosurg. 2020;140:512-518. doi: 10.1016/j.wneu.2020.04.022
100. Inoue T, Ichikawa D, Ueno T, Cheong M, Inoue T, Whetstone WD, et al. XGBoost, a Machine Learning Method, Predicts Neurological Recovery in Patients with Cervical Spinal Cord Injury. Neurotrauma Rep. 2020;1(1):8-16. doi: 10.1089/neur.2020.0009
101. Langarizadeh M, Moghbeli F. Applying Naive Bayesian Networks to Disease Prediction: a Systematic Review. Acta informatica medica : AIM : journal of the Society for Medical Informatics of Bosnia & Herzegovina : casopis Drustva za medicinsku informatiku BiH. 2016;24(5):364-369. doi: 10.5455/aim.2016.24.364-369
102. Vemulapalli V, Qu J, Garren JM, Rodrigues LO, Kiebish MA, Sarangarajan R, et al. Non-obvious correlations to disease management unraveled by Bayesian artificial intelligence analyses of CMS data. Artif Intell Med. 2016;74:1-8. doi: 10.1016/j.artmed.2016.11.001
103. Khanmohammadi S, Adibeig N, Shanehbandy S. An improved overlapping k-means clustering method for medical applications. Expert Systems with Applications. 2017;67:12-18. doi: 10.1016/j.eswa.2016.09.025
104. Zhu H, He H, Xu J, Fang Q, Wang W. Medical Image Segmentation Using Fruit Fly Optimization and Density Peaks Clustering. Comput Math Methods Med. 2018;2018:3052852. doi: 10.1155/2018/3052852
105. Kocbek P, Fijacko N, Soguero-Ruiz C, Mikalsen KO, Maver U, Povalej Brzan P, et al. Maximizing Interpretability and Cost-Effectiveness of Surgical Site Infection (SSI) Predictive Models Using Feature-Specific Regularized Logistic Regression on Preoperative Temporal Data. Comput Math Methods Med. 2019;2019:2059851. doi: 10.1155/2019/2059851

Review article

Ukrainian Neurosurgical Journal. 2025;31(3):14-21
doi: 10.25305/unj.328419

Neurosurgical anatomy of the insula and Sylvian fissure: Literature review and personal experience. The third report. Anatomy of sylvian fissure, sylvian cistern, gyri and fissures of the insula

Valentyn M. Kliuchka [1], Artem V. Rozumenko [1], Volodymyr D. Rozumenko [1], Oleksandr M. Lisianyi [1], Tetyana A. Malysheva [2], Volodymyr Y. Shutka [3], Andrii V. Dashchakovskyi [1]

[1] Department of Innovative Neurosurgical Technologies, Romodanov Neurosurgery Institute, Kyiv, Ukraine
[2] Department of Neuropathomorphology, Romodanov Neurosurgery Institute, Kyiv, Ukraine
[3] Department of Traumatology, Orthopedics and Neurosurgery, Bukovinian State Medical University, Chernivtsy, Ukraine

Received: 29 April 2025
Accepted: 26 May 2025

Address for correspondence*: Valentyn M. Kliuchka, Department of Innovative Neurosurgical Technologies, Romodanov Neurosurgery Institute, 32 Platona Maiborody st., Kyiv, 04050, Ukraine, email:kimeria80@gmail.com*

Despite being a region where numerous pathological processes may develop, the insula remains one of the least studied anatomical structures of the human brain. The clinical course of insular glioma is accompanied by a severe morbidity, caused by the proximity of the central core, important projection and associative pathways, main arteries and large venous collectors. For a long time, surgery of patients with insular gliomas, which would involve the total volume tumor removal while ensuring high quality of post-surgery life, was considered impossible.

Understanding the surgical anatomy of the insula is key to successful transsylvian-transinsular, transopercular approaches to insular gliomas and their radical removal.

The article provides a detailed surgical anatomy of the sylvian fissure, the operculum and the insula.

Key words: *insular gliomas; sylvian fissure; sylvian cistern; operculum; surgical anatomy of the insula*

Introduction

Insular gliomas (IGs) are the most common internal tumors that can arise in this region, accounting for up to 25% of all low-grade gliomas and 10% of all high-grade gliomas [1, 2]. IGs are typically associated with pronounced neurological symptoms, including pharmacoresistant epilepsy, motor and sensory aphasia, and motor deficits [2]. These tumors are aggressive and destructive due to their invasive growth patterns and progressive involvement of deep subcortical structures, as well as critical associative and projection pathways.

Recently, the anatomy and functional significance of the insular region have been thoroughly studied and described, allowing for a reconsideration and refinement of surgical strategies and resection techniques for IGs [3].

The insula is a hidden lobe of the cerebral hemispheres that becomes visible only after dissection of the Sylvian fissure (SF) and retraction of the opercula [4, 5]. The opercula, projection and association white matter tracts, and subcortical nuclei surrounding the insula are functionally significant, particularly in the dominant hemisphere. Additional limitations to the surgical access of IGs are associated with the complex branching patterns of the venous system within the Sylvian fissure, as well as with the individual topography of the middle cerebral artery (MCA) and the course of its branches deep within the lateral sulcus [6, 7]. All these factors make the surgical management of IGs an extremely challenging task, even in the era of advanced diagnostic and intraoperative technologies.

Surgical anatomy of the Sylvian fissure

The insula (according to anatomical nomenclature A14.1.09.149 [8, 9]) is a triangular protrusion of cerebral tissue located in the depth of the SF. It is bounded by the circular sulcus of the insula. The surface of the insula is divided by sulci into short and long gyri. The portions of the frontal, parietal, and temporal lobes that cover the insula are referred to as the operculum. The Sylvian fissure of the brain is a deep groove on the lateral convex surface of the brain, extending from the crest of the sphenoid bone to the supramarginal gyrus. It separates the lateral cerebral surface into the frontal and parietal lobes above, and the temporal lobe below.

The SF is conventionally divided into anterior and posterior segments (***Fig. 1***). The anterior segment begins at the anterior clinoid process, extends laterally and posteriorly along the lesser wing of the sphenoid bone (sphenoidal segment), and ends at the level of

the pars opercularis of the frontal lobe. In the frontal operculum, the Sylvian fissure gives rise to the anterior horizontal and anterior ascending rami [10]. The anterior horizontal ramus divides the frontal operculum into the pars orbitalis and pars triangularis. The anterior ascending ramus separates the pars triangularis from the pars opercularis. The junction point of the anterior segment of the SF, the anterior horizontal and ascending rami, and the beginning of the posterior segment is termed the "Sylvian point". This is the widest part of the SF and serves as a landmark for initiating SF dissection. From the "Sylvian point", the apex of the insula is located 12.6 mm inferiorly [5]. The posterior segment of the SF extends from the "Sylvian point" to the parietal lobe, where it is surrounded by the supramarginal gyrus. In its posterior portion, the SF reaches a depth of 25 mm from the superior edge of the supramarginal gyrus [5]. Within the opercula of the posterior SF there are several functionally significant brain regions: the cortical area in the inferior portion of the third frontal gyrus of the left hemisphere (Broca's area), the premotor and facial motor zones in the frontal operculum, the primary sensory area of the face in the parietal operculum, the transverse temporal gyri (gyri temporales transversi, Heschl's gyri) involved in auditory processing, and Wernicke's area in the temporal operculum.

Based on meticulous intraoperative observations of the SF and its cistern, M.G. Yasargil described four anatomical variations of the SF [12]. The first type is characterized by a straight and wide SF, the second type by a straight and narrow SF, while the third and fourth types are distinguished by the invagination of the frontal and temporal lobes into the SF, respectively [12]. A widely used practical classification of the SF among radiologists was proposed by H.M. Ngando et al., who, taking into account data from spiral computed tomography, slightly modified M.G. Yasargil's classification (***Fig. 2***) [13].

The Sylvian fissure contains a large subarachnoid space — the Sylvian fissure cistern (A14.1.01.209), which extends from the carotid cistern at its medial and deepest point to the outer SF membrane at the posterolateral end [11]. The deepest wall of the SF cistern lies in the sphenoidal segment near the anterior clinoid process. At this location, the SF cistern and the carotid cistern are separated by the proximal SF membrane, which is penetrated by the M_1 - segment of the MCA. Above the insular surface, the Sylvian cistern contains three partitions that divide the subarachnoid space into four levels [11]. The deepest level includes the medial Sylvian membrane, which is anchored to the deepest part of the frontoparietal operculum and the insular surface, and also contains the M_2 - segment of the MCA. The M2 branches continue as M3 branches, penetrating the medial Sylvian membrane. The M_3- segment of the MCA, en route to the surface of the Sylvian fissure, passes through another membrane — the intermediate Sylvian membrane. Lateral to this intermediate membrane lies the outer Sylvian membrane, on which the superficial Sylvian veins are located. Branches of the M_3 - segment penetrate the outer Sylvian membrane and continue as the M_4 - segment of the MCA (cortical branches). The superficial Sylvian veins and M4 branches traverse the outer Sylvian membrane, which is the most superficial layer, and are covered by the common arachnoid membrane. The outer arachnoid membrane encloses all cortical vessels and has a denser and more robust structure. Thus, the SF contains the M_1 - M_3 segments of the MCA with their perforating and cortical (M_4) branches, as well as the superficial and deep veins (***Fig. 3***) [12].

The SF cistern is unique due to its specific and variable microanatomy of the arachnoid membrane, particularly at different depths [2,14]. This necessitates the use of diverse technical approaches at each stage of SF dissection. A. Tayebi Meybodi et al. have provided a detailed description of the arachnoid membrane's anatomy within the SF and identified six potential types of arachnoid adhesions (septations) between arteries (A), veins (V), and brain tissue (B): (1) A–A, (2) A–B, (3) A–V, (4) B–V, (5) B–B, and (6) V–V [14]. The authors also outlined the typical configurations of these interrelationships in various compartments of SF (superficial opercular, deep opercular, and cisternal), aimed at optimizing surgical maneuvers during sulcus dissection (see ***Fig. 3***) [15].

Surgical anatomy of the opercula of the insula

The lobus limbicus consists of structures that form a complex located centrally within the hemispherium cerebri. This complex is considered to include the medial regions of the frontal, parietal, and temporal lobes, as well as the insula, which lies deep within the fossa lateralis cerebri.

The portion of the cerebral cortex that covers the insula laterally forms the operculum or pars opercularis, and it is composed of adjacent regions of the frontal, temporal, and parietal lobes.

In our view, the anatomical subdivision of the opercular compartments proposed by U. Türe et al. (1999) — into fronto-orbital, fronto-parietal, and temporal — is appropriate and practical.

It is commonly accepted that the gyri and sulci of the insular cortex continue into the corresponding gyri and sulci of the opercular compartments, with the CSI serving as the boundary between them [16]. In their seminal work on the surgical anatomy of the insula, U. Türe et al. (1999) emphasize that the gyri and sulci of the insula do not always form a continuous extension of the opercular structures. However, they note that in most cases, there is a configuration suggestive of such continuity. Continuations of the gyri and sulci have been identified between the anterior insular region and the frontal lobe, as well as between the posterior insular region and the parietal and temporal lobes [16].

Fronto-orbital operculum

The posterior orbital gyrus, the posterior segment of the lateral orbital gyrus, and the orbital portion of the inferior frontal gyrus form the suprainsular operculum, which covers the anterior surface of the insula. The anterior limiting CSI marks the boundary

This article contains some figures that are displayed in color online but in black and white in the print edition.

between the fronto-orbital operculum and the insula. The posteromedial orbital region is located at the medial end of the transverse orbital sulcus and consists of the posterior segment of the medial orbital gyrus and the medial portion of the posterior orbital gyrus. This region continues seamlessly into the transverse short insular gyrus. The posterolateral orbital region, located at the lateral end of the transverse orbital sulcus, comprises the lateral segment of the posterior orbital gyrus and the posterior segment of the lateral orbital gyrus. There is no clearly defined boundary between the lateral orbital gyrus and the orbital part of the inferior frontal gyrus. Two suborbital gyri (superior and inferior), located in the medial portion of the fronto-orbital operculum, overlie the anterior surface of the insula. These gyri are continuous with the accessory insular gyrus and the anterior surface of the anterior short insular gyrus [16].

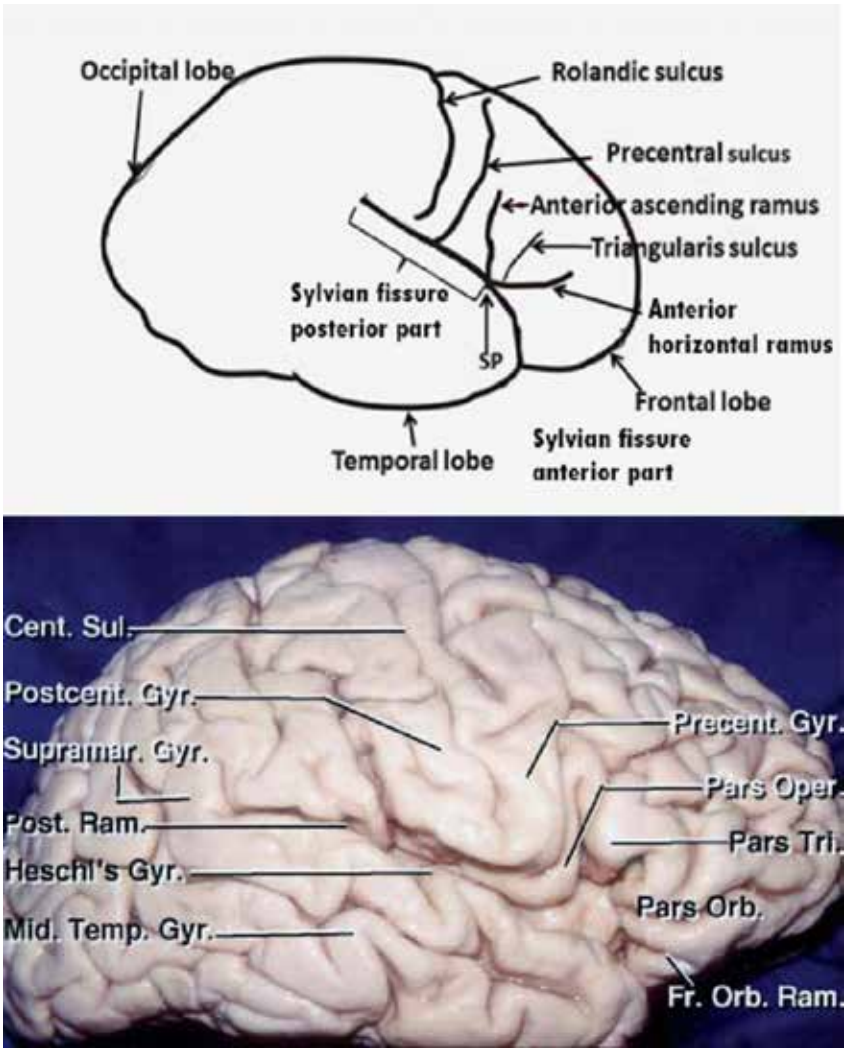

Fig. 1. Topographic anatomy of the SF [5]

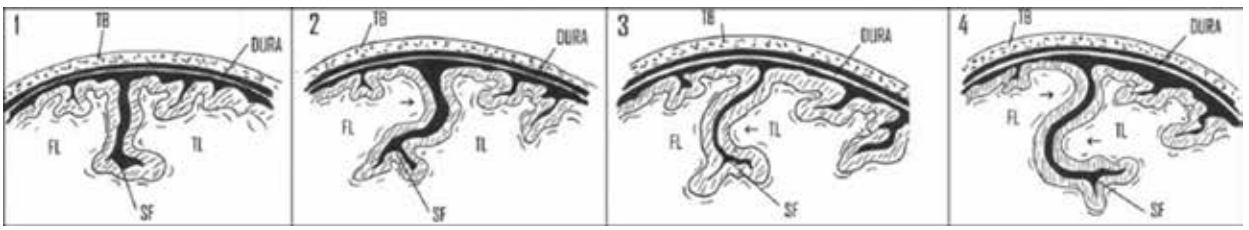

Fig. 2. Types of the SF: Type I SF – straight and wide or narrow fissure; Type II – wide fissure with invagination of the frontal or temporal lobe; Type III – invagination of the frontal or temporal lobe with a narrow SF; Type IV – invagination of both frontal and temporal lobes into the fissure. TB – temporal bone; SF – Sylvian fissure; FL – frontal lobe; TL – temporal lobe; arrow – invagination of the frontal or temporal lobe [13]

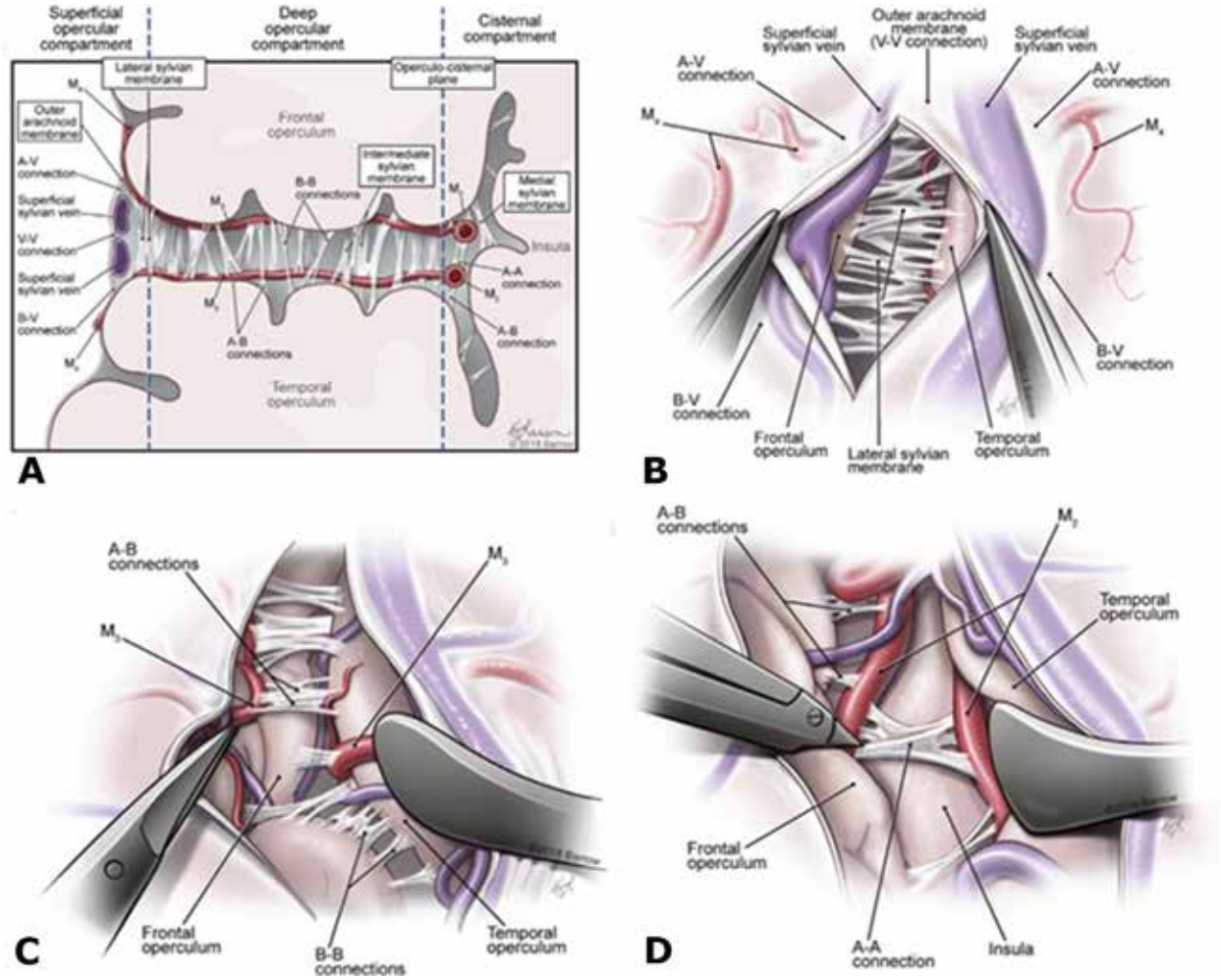

Fig. 3. A – Visualization of the superficial opercular, deep opercular, and cisternal compartments of the SF; B – Dissection of the outer arachnoid membrane provides access to the superficial opercular compartment. The paired superficial Sylvian veins are shown with a dissection plane created between them (V–V membranes opened). An alternative dissection of the outer arachnoid membrane on the temporal side of the superficial Sylvian vein (B–V membranes) may be selected depending on the patient's individual anatomy. The outer membrane of the SF is shown at the depth of the superficial opercular compartment, serving as the boundary between the superficial and deep opercular compartments; C – The deep opercular compartment with M3 branches running along their respective opercula. The main arachnoid membranes in this compartment are represented by A–C (between the M3 branches and the opposite operculum) and C–C membranes between opposite/adjacent opercula; D – Exposure of the cisternal compartment with M2 branches. A–A membranes between M2 branches are predominant among arachnoid adhesions in this compartment. Dissection of the A–C membranes between the M2 branches and their corresponding opercula may be required to expand the dissection toward the circular sulcus of the insula (CSI) [15]

Fronto-parietal operculum

The triangular and opercular parts of the inferior frontal gyrus, along with the inferior segments of the precentral and postcentral gyri and the superior portion of the supramarginal gyrus, form the fronto-parietal operculum, which overlies the superior surface of the insula. The posterior portion of this operculum also includes the temporal operculum, with the two regions separated by the "retroinsular sulcus" located in the deep posterior segment of the SF.

The superior CSI demarcates the boundary between the fronto-parietal operculum and the insula. The triangular part lies between the horizontal and ascending rami of the SF. The horizontal ramus of the SF is a continuation of the superior CSI, while the ascending ramus continues the anterior CSI. The intersection of these sulci is identified as the "anterior insular point". The medial aspect of the triangular part is referred to as the "subtriangular gyrus", which covers the anterior short insular gyrus and transitions into it. The orbital and subopercular gyri encircle the anterior short insular gyrus anteriorly and posteriorly, respectively. The opercular part of the inferior frontal gyrus lies between the ascending ramus of the SF and the inferior precentral sulcus, overlapping with Broca's area (Brodmann area 44). The medial surface of this part is called the subopercular gyrus, which covers the short insular sulcus, the middle short insular gyrus, and the posterior portion of the anterior short insular gyrus. The subprecentral gyrus is located medially to the

opercular part and the inferior precentral gyrus, covering the middle short insular gyrus and the precentral insular sulcus [16].

In 82% of hemispheres, the inferior end of the Rolandic (central) sulcus does not reach the SF. The subcentral gyrus occupies the medial region of both the inferior precentral and postcentral gyri and is delimited by the anterior, posterior, or subcentral sulci. This gyrus overlies the central insular sulcus [16].

The inferior postcentral gyrus and the superior part of the supramarginal gyrus constitute the remaining portion of the fronto-parietal operculum. The anterior, middle, and posterior transverse parietal gyri are located on the medial side of the operculum. The anterior transverse parietal gyrus covers the postcentral insular sulcus as well as the superior part of both the anterior and posterior long insular gyri, which are adjacent to Heschl's anterior gyrus of the temporal operculum. The junction between the anterior transverse parietal gyrus and Heschl's anterior gyrus is identified as the "posterior insular point". The middle transverse parietal gyrus overlies the transverse temporal sulcus of the temporal operculum. The posterior transverse parietal gyrus and the temporal planum overlap and form the medial wall of the supramarginal gyrus [17].

Temporal operculum

The superior temporal gyrus, together with the temporal pole and the inferior portion of the supramarginal gyrus, forms the temporal operculum, which covers the inferior surface of the insula and the anterior perforated substance. The polar plane, anterior and posterior Heschl's gyri, as well as the temporal plane, constitute the medial surface of the temporal operculum (see ***Fig. 3***). The lateral olfactory stria courses lateral to the limen insulae, projects medially towards the surface of the hippocampal uncus, and continues medially into the semilunar gyrus, and more laterally into the gyrus ambiens [18]. The entorhinal sulcus separates the uncus of the hippocampus from the temporal operculum and the anterior perforated substance [19].

The first lateral branch of the main trunk of the SF is referred to as the "temporal notch," which separates the piriform cortex from the temporal pole. The polar plane covers the margin and inferior surface of the insula and borders the inferior CSI, covering two-thirds of its length. The gyri of the polar plane are known as the "Schwalbe gyri" [20]. The anterior Heschl's gyrus is adjacent to the posterior part of the inferior CSI. The transverse temporal sulcus separates the anterior and posterior Heschl's gyri. The temporal plane forms the posterior part of the internal surface of the temporal operculum [17] (***Fig. 4***).

Surgical anatomy of the insular surface

The insular cortex forms the medial wall of the Sylvian cistern. The insula is shaped like a pyramid with a triangular base and a small apex (***Fig. 5, A–D***). Its base is oriented medially toward the deep subcortical structures of the cerebral hemisphere. One of the base angles is directed inferiorly and corresponds to the insular pole. The apex, located posterior and lateral to the pole, represents the highest point of the lateral surface of the insular cortex. It is positioned laterally, anteriorly, and inferiorly, resulting in an eccentric orientation relative to the base. The apex points toward the exit of the Sylvian cistern but does not reach the fissure itself. During a transsylvian approach to the insula, the apex can be visualized directly through the anterior Sylvian point — the region of the lateral sulcus where the triangular part of the inferior frontal gyrus lies opposite the superior temporal gyrus. At this point, the Sylvian cistern widens and gives rise to its anterior ascending, horizontal, and posterior branches [5].

Anatomically, the insula has three distinct surfaces: anteroinferior, posteroinferior, and lateral. The anteroinferior surface is the smallest and is concealed by the fronto-orbital operculum, which consists of the posterior portion of the posterior orbital gyrus and the orbital part of the inferior frontal gyrus. On the anteroinferior surface of the insula — an area traversed by the middle cerebral artery — a transverse gyrus (Eberstaller's gyrus) can be identified. This gyrus connects the apex of the insula with the orbital part of the inferior surface of the frontal lobe. It extends to the posteromedial regions of the frontal lobe, which include the posterior segment of the medial orbital gyrus and the medial part of the posterior orbital gyrus that courses laterally toward the lateral olfactory stria [21].

Occasionally, an accessory insular gyrus may be visualized above the transverse insular gyrus, immediately posterior to the inferior portion of the anterior limiting sulcus. If this accessory gyrus is absent, the transverse gyrus extends up to the anterior limiting sulcus (see ***Fig. 5***).

The lateral surface of the insula is the largest and most anatomically complex, containing numerous sulci and gyri. Its upper portion is hidden beneath the frontoparietal operculum (composed of the triangular and opercular parts of the inferior frontal gyrus, the precentral gyrus, and the anterior basal portion of the supramarginal gyrus), while the inferior parts are covered by the superior temporal gyrus.

The lateral and posteroinferior surfaces of the insula are surrounded and separated from the frontal, parietal, and temporal opercula by the CSI [22]. This sulcus is often referred to as the "limiting sulcus" as it demarcates the insula along its periphery. Due to the pyramidal shape of the insula, the sulcus has a triangular rather than circular configuration. It consists of three segments: anterior, superior, and inferior. The anterior segment (anterior CSI) runs obliquely upward and forward into the pars orbitalis of the frontal operculum. The superior segment of the limiting sulcus (superior CSI) runs horizontally beneath the frontoparietal operculum, extending from the superior end of the anterior segment along the anterosuperior border of the insula to the posterior end of the inferior segment. The inferior segment lies beneath the temporal operculum along the inferior border of the insula. Of the three segments, the superior one is the longest, and the anterior one is the shortest (see ***Fig. 5***).

The cortex of the lateral surface of the insula is represented by three short gyri located anteriorly, and the superior portions of the anterior long and posterior sulci, situated posterior to the short gyri. The short and long sulci are separated by the central insular sulcus. The two anterior sulci divide the three short gyri, while

a single long sulcus separates the two long gyri (see ***Fig. 3***). The central insular sulcus, being the deepest among all insular sulci, runs from the limen insulae in a posterior and superior direction, reaching the superior CSI. Additionally, the central insular sulcus courses almost parallel to the central sulcus (Rolandic sulcus) of the cerebral hemispheres. N. Tanriover et al. (2004) note that the central sulcus frequently curves around the frontoparietal opercular lip and continues into the central insular sulcus [5]. Overall, the sulci and gyri of the insula form a radial pattern extending posteriorly and superiorly from the limen of the insula.

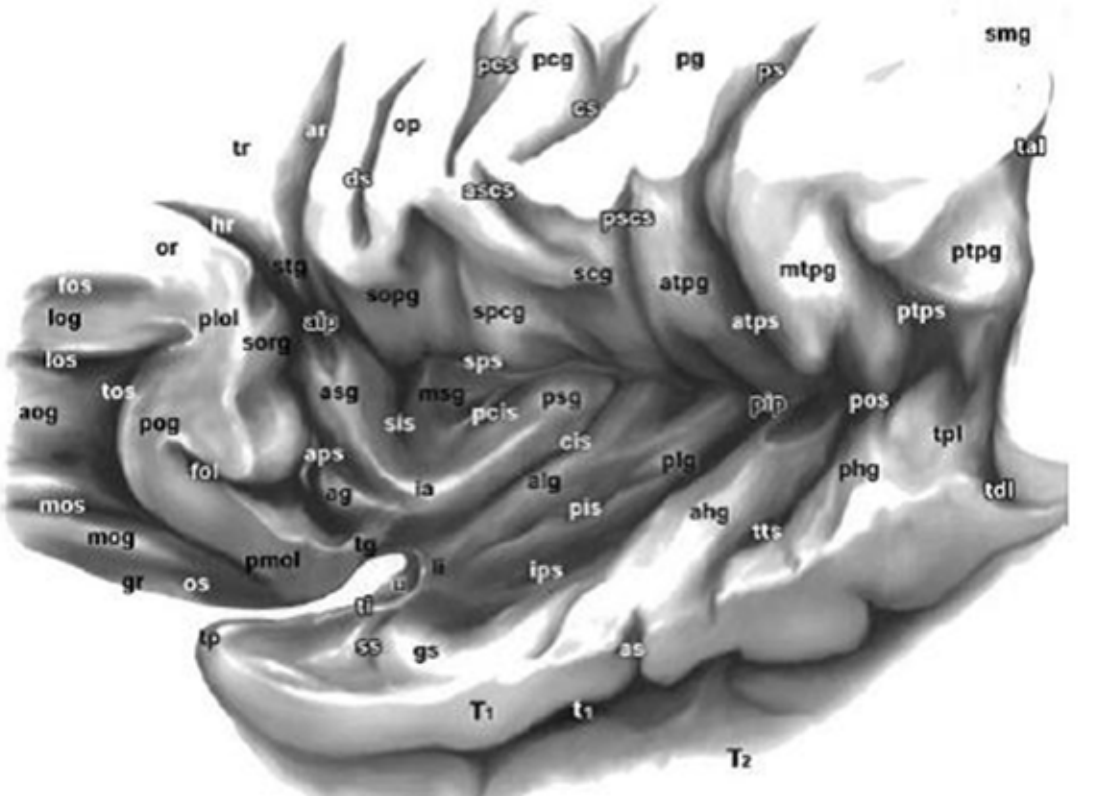

Fig. 4. Image of the left insulo-opercular region with detailed nomenclature [16]. White letters indicate sulci. Abbreviations: ag – accessory insular gyrus; ahg – anterior Heschl's gyrus; aip – anterior insular point; alg – anterior long insular gyrus; aog – anterior orbital gyrus; aps – anterior CSI; ar – ascending ramus of the Sylvian fissure; as – acoustic sulcus; ascs – anterior subcentral sulcus; asg – anterior short insular gyrus; atpg – anterior transverse parietal gyrus; atps – anterior transverse parietal sulcus; cis – central insular sulcus; cs – central sulcus of Rolando; ds – diagonal sulcus; fol – fronto-orbital lateral branch; fos – fronto-orbital sulcus; gr – gyrus rectus; gs – Schwalbe's gyrus; hr – horizontal ramus of the inferior frontal sulcus; ia – insular apex; ips – inferior CSI; li – insular limen; log – lateral orbital gyrus; los – lateral orbital sulcus; mog – medial orbital gyrus; mos – medial orbital sulcus; msg – middle short insular gyrus; mtpg – middle transverse parietal gyrus; op – opercular part; os – olfactory sulcus; pcg – precentral gyrus; pcis – precentral insular sulcus; pcs – precentral sulcus; pg – postcentral gyrus; phg – posterior Heschl's gyrus; pip – posterior insular point; pis – postcentral insular sulcus; plg – posterior long insular gyrus; plol – posterolateral orbital lobule; pmol – posteromedial orbital lobule; pog – posterior orbital gyrus; pos – postinsular sulcus; ps – postcentral sulcus; pscs – posterior subcentral sulcus; psg – posterior short insular gyrus; ptpg – posterior transverse parietal gyrus; ptps – posterior transverse parietal sulcus; scg – subcentral gyrus; sis – short insular sulcus; smg – supramarginal gyrus; sopg – subopercular gyrus; sorg – suborbital gyrus; spcg – subprecentral gyrus; sps – superior CSI; ss – Schwalbe's sulci in the polar plane; stg – subtriangular gyrus; tal – terminal ascending part of the SF; tdl – terminal descending part of the SF; tg – transverse insular gyrus; ti – temporal incisure; tos – transverse orbital sulcus; tp – temporal pole; tpl – temporal plane; tr – triangular part; tts – transverse temporal sulcus; T1 – superior temporal gyrus; T2 – middle temporal gyrus; t1 – superior temporal sulcus

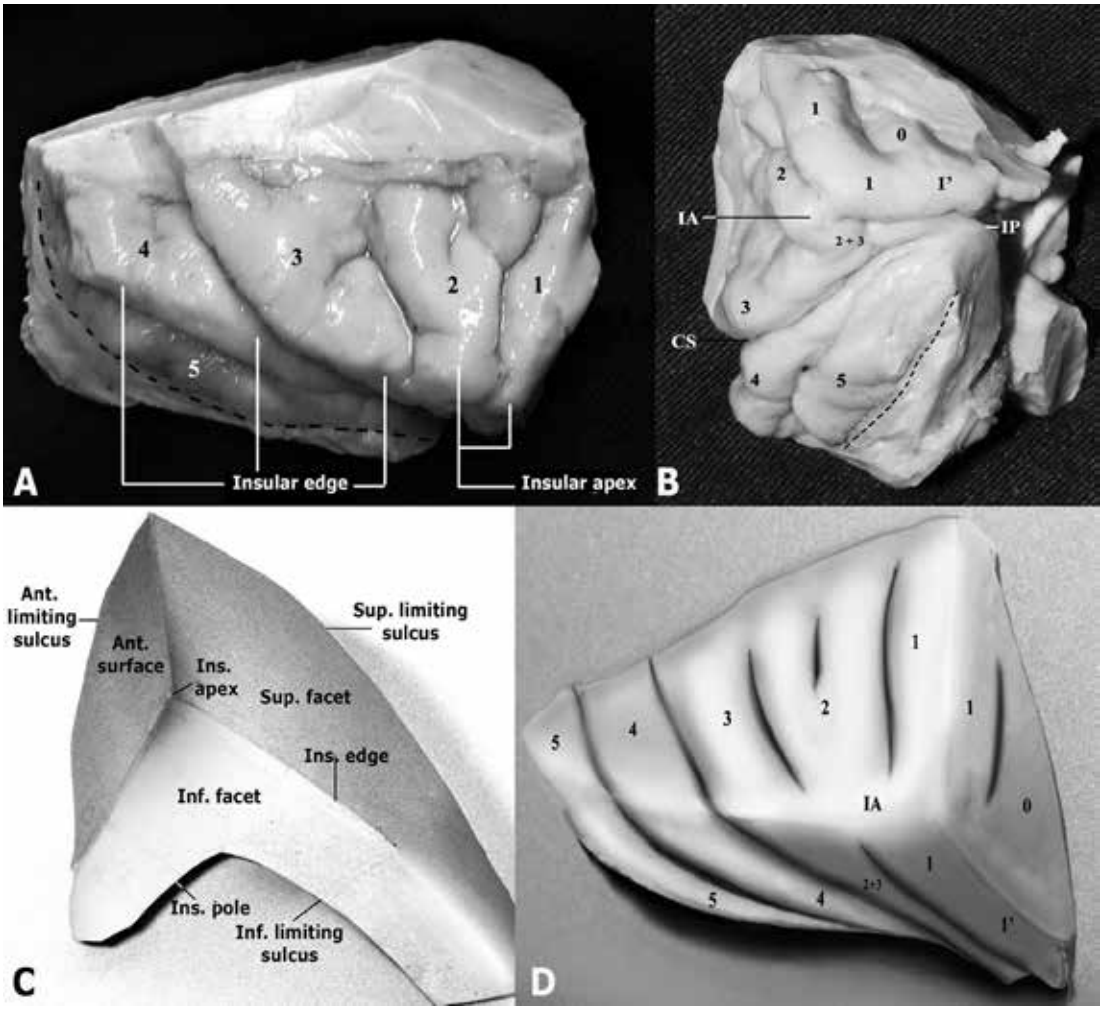

Fig. 5. Macroscopic anatomy of the insula (A, B) and schematic geometry (C, D) [24]: 0 – accessory gyrus; 1 – anterior short gyrus; 2 – middle short gyrus; 3 – posterior short gyrus; 4 – anterior long gyrus; 5 – posterior long gyrus; 6 – transverse gyrus; AI – apex of the insula; PI – pole of the insula; LI – limen insula; MI – margin of the insula; ACSI – anterior CSI; SCSI – superior CSI; ICSI – inferior CSI; red dot – anterior insular point; green dot – posterior insular point

Thus, the central insular sulcus divides the insula into a larger anterior portion, formed by the short gyri, and a smaller posterior portion, composed of the long gyri. The short gyri of the insula are separated by two sulci: the short insular sulcus separates the anterior and middle short gyri, while the precentral insular sulcus divides the middle and posterior short gyri (see ***Fig. 5***).

The long gyri are located on the posteroinferior surface of the insula, posterior to the central insular sulcus. Most commonly, they originate below the insular apex near the limen as a single gyrus, which then bifurcates posteriorly into the anterior and posterior long gyri, separated by the long insular sulcus (see ***Fig. 5***). The anterior long gyrus is typically broader.

Significant anatomical structures on the lateral surface of the insula include the pole, apex, limen, and margin of the insula. The insular pole is located at the anteroinferior edge of the insula, where the short gyri converge, forming a rounded area lateral to the limen (see ***Fig. 5***). The apex of the insula, its highest point on the lateral surface, is situated above and posterior to the pole, typically on the middle short gyrus (see ***Fig. 5***). The limen insulae is a slightly protruding arcuate ridge located at the junction of the limen of the Sylvian fissure and the operculo-insular transition. It extends from the temporal pole to the orbital surface of the frontal lobe. The long gyri of the insula terminate here [23]. The limen is composed of a thin layer of gray matter covering the uncinate fasciculus. The anterior perforated substance lies medially to the limen and serves as an important surgical landmark. The entry point of the most lateral lenticulostriate artery (LSA) is considered the lateral boundary of the anterior perforated substance. The distance from the entry point of the extreme lateral LSA into the anterior perforated substance to the medial boundary of the limen insulae averages 15.3 mm [5]. The margin of the insula represents the edge of the triangular pyramid-shaped insula, extending from its apex to the posterior insular point and protruding onto the lateral surface (see ***Fig. 5***).

Conclusions

Insular gliomas are associated with profound neurological deficits due to the proximity of functionally critical brain regions, major projection and association pathways, as well as large arterial trunks and venous collectors.

In cases of insular involvement or extension of gliomas from other lobes into the insular region, spatial anatomy undergoes significant individual pathological alterations. These changes, along with the degree of involvement or displacement of eloquent cortical areas, must be carefully considered during surgical planning.

Understanding the microsurgical anatomy of the Sylvian fissure, the Sylvian cistern, and the insular surface is a crucial prerequisite for the successful execution of transinsular and transcortical approaches to insular gliomas.

Disclosure

Conflict of interest

The authors declare no conflict of interest.

Funding

This study received no financial support.

References

1. Sanai N, Berger MS. Recent surgical management of gliomas. In: Yamanaka R, ed. Glioma: Immunotherapeutic Approaches. 1-st ed. New York: Landes Bioscience & Springer Science+Business Media; 2012. Vol.746, Ch.2, p.12-25. (Series: Advances in experimental medicine and biology). doi: 10.1007/978-1-4614-3146-6_2
2. Rey-Dios R, Cohen-Gadol AA. Technical nuances for surgery of insular gliomas: lessons learned. Neurosurg Focus. 2013 Feb;34(2):E6. doi: 10.3171/2012.12.FOCUS12342
3. Hervey-Jumper SL, Berger MS. Insular glioma surgery: an evolution of thought and practice. J Neurosurg. 2019 Jan 1;130(1):9-16. doi: 10.3171/2018.10.JNS181519
4. Rhoton AL Jr. The cerebrum. Anatomy. Neurosurgery. 2007 Jul;61(1 Suppl):37-118; discussion 118-9. doi: 10.1227/01.NEU.0000255490.88321.CE
5. Tanriover N, Rhoton AL Jr, Kawashima M, Ulm AJ, Yasuda A. Microsurgical anatomy of the insula and the sylvian fissure. J Neurosurg. 2004 May;100(5):891-922. doi: 10.3171/jns.2004.100.5.0891
6. Gogia B, Chavali LS, Lang FF, Hayman LA, Rai P, Prabhu SS, Schomer DF, Kumar VA. MRI venous architecture of insula. J Neurol Sci. 2018 Jul 15;390:156-161. doi: 10.1016/j.jns.2018.04.032
7. Türe U, Yaşargil MG, Al-Mefty O, Yaşargil DC. Arteries of the insula. J Neurosurg. 2000 Apr;92(4):676-87. doi: 10.3171/jns.2000.92.4.0676
8. Terminologia anatomica: international anatomical terminology By the Federative Committee on Anatomical Terminology (FCAT). Stuttgart: Georg Thieme Verlag; 1998. 300 p. ISBN-10: 3-13-114361-4. ISBN-13: 978-3-13-114361-7.
9. FIPAT. Terminologia Anatomica. 2nd ed. FIPAT.library.dal.ca. Federative International Programme for Anatomical Terminology, 2019.
10. Meybodi AT, Griswold D, Tabani H, Lawton MT, Mokhtari P, Payman A, Benet A. Topographic Surgical Anatomy of the Parasylvian Anterior Temporal Artery for Intracranial-Intracranial Bypass. World Neurosurg. 2016 Sep;93:67-72. doi: 10.1016/j.wneu.2016.05.050
11. Inoue K, Seker A, Osawa S, Alencastro LF, Matsushima T, Rhoton AL Jr. Microsurgical and endoscopic anatomy of the supratentorial arachnoidal membranes and cisterns. Neurosurgery. 2009 Oct;65(4):644-64; discussion 665. doi: 10.1227/01.NEU.0000351774.81674.32
12. Yasargil MG. Operative anatomy. In: Yasargil MG, ed. Microneurosurgery. Vol. I: Microsurgical Anatomy of the Basal Cisterns and Vessels of the Brain, Diagnostic Studies, General Operative Techniques and Pathological Considerations of the Intracranial Aneurysms. Stuttgart: Thieme Publishers; 1984. p. 252-290. ISBN 3131734914, 9783131734914.
13. Ngando HM, Maslehaty H, Schreiber L, Blaeser K, Scholz M, Petridis AK. Anatomical configuration of the Sylvian fissure and its influence on outcome after pterional approach for microsurgical aneurysm clipping. Surg Neurol Int. 2013 Sep 30;4:129. doi: 10.4103/2152-7806.119073
14. Lawton MT, ed. Seven Aneurysms: Tenets and Techniques for Clipping. 1-st ed. New York: Thieme; 2010. 240 p. ISBN-10: 1604060549, ISBN-13: 978-1604060546.
15. Tayebi Meybodi A, Borba Moreira L, Gandhi S, Preul MC, Lawton MT. Sylvian fissure splitting revisited: Applied arachnoidal anatomy and proposition of a live practice model. J Clin Neurosci. 2019 Mar;61:235-242. doi: 10.1016/j.jocn.2018.10.088
16. Türe U, Yaşargil DC, Al-Mefty O, Yaşargil MG. Topographic anatomy of the insular region. J Neurosurg. 1999 Apr;90(4):720-33. doi: 10.3171/jns.1999.90.4.0720
17. Kucukyuruk B, Richardson RM, Wen HT, Fernandez-Miranda JC, Rhoton AL Jr. Microsurgical anatomy of the temporal lobe and its implications on temporal lobe epilepsy surgery. Epilepsy Res Treat. 2012;2012:769825. doi: 10.1155/2012/769825
18. Riley HA. An Atlas of the Basal Ganglia, Brain Stem and Spinal Cord. New York: Hafner; 1960, p. 576, 582-583, 606, 609.
19. Wen HT, Rhoton AL Jr, de Oliveira E, Cardoso AC, Tedeschi H, Baccanelli M, Marino R Jr. Microsurgical anatomy of the temporal lobe: Part 1: mesial temporal lobe anatomy and its vascular relationships as applied to amygdalohippocampectomy. Neurosurgery. 1999 Sep;45(3):549-91; discussion 591-2. doi: 10.1097/00006123-199909000-00028
20. Fiol ME, Leppik IE, Mireles R, Maxwell R. Ictus emeticus and the insular cortex. Epilepsy Res. 1988 Mar-Apr;2(2):127-31. doi: 10.1016/0920-1211(88)90030-7
21. Ribas GC. The cerebral sulci and gyri. Neurosurg Focus. 2010 Feb;28(2):E2. doi: 10.3171/2009.11.FOCUS09245
22. Williams PL, Bannister LH, Berry MM, Collins P, Dyson M, Dussek JE, Ferguson MW. Gray's Anatomy. The anatomical basis of medicine and surgery. 38th Edition. New York: Churchill Livingstone; 1995.
23. Wolf BS, Huang YP: The insula and deep middle cerebral venous drainage system: normal anatomy and angiography. Am J Roentgenol Radium Ther Nucl Med. 1963 Sep;90:472-89.
24. Wen HT, Rhoton AL Jr, de Oliveira E, Castro LH, Figueiredo EG, Teixeira MJ. Microsurgical anatomy of the temporal lobe: part 2 – sylvian fissure region and its clinical application. Neurosurgery. 2009 Dec;65(6 Suppl):1-35; discussion 36. doi: 10.1227/01.NEU.0000336314.20759.85

Original article

Ukrainian Neurosurgical Journal. 2025;31(3):22-29
doi: 10.25305/unj.327169

Neuro-ophthalmological symptoms of compressive optic neuropathy depending on chiasmal position and pituitary adenoma extension

Kateryna S. Iegorova [1], Oleksii V. Ukrainets [2]

[1] Ophthalmology Group, Romodanov Neurosurgery Institute, Kyiv, Ukraine
[2] Endonasal Skull Base Neurosurgery Department, Romodanov Neurosurgery Institute, Kyiv, Ukraine

Received: 17 April 2025
Accepted: 09 May 2025

Address for correspondence*:*
Oleksii V. Ukrainets, Endonasal Skull Base Neurosurgery Department, Romodanov Neurosurgery Institute, 32 Platona Maiborody st., Kyiv, 04050, Ukraine, e-mail: ukrainets.md@gmail.com

Objective: to analyze the characteristics of compressive optic neuropathy depending on the anatomical position of the optic chiasm.

Materials and methods: The study was conducted at the A.P. Romodanov Institute of Neurosurgery of the National Academy of Medical Sciences of Ukraine between 2018 and 2024, within the Departments of Endonasal Skull Base Neurosurgery and Neuro-ophthalmology. We retrospectively analyzed data from a consecutive surgical series involving 212 patients (424 eyes) diagnosed with pituitary adenoma (PA) and compressive optic neuropathy manifested by decreased visual acuity and/or visual field defects. The cohort included 116 women (54.7%) and 96 men (45.3%) aged 18 to 76 years (mean age 52.3 ± 11.8 years). Based on the direction of PA growth and the anatomical position of the optic chiasm, patients were classified into three groups:

Group I – anterior growth and/or posterior chiasmal position (34 patients, 16.1%; 68 eyes); Group II – suprasellar growth and/or central chiasmal position (147 patients, 69.3%; 294 eyes); Group III – posterior growth and/or anterior chiasmal position (31 patients, 14.6%; 62 eyes).

Results: No statistically significant difference in mean age was observed among the groups ($p > 0.05$). The mean duration of visual impairment was (14.8 ± 3.9) months in Group I, (8.80 ± 0.95) months in Group II, and (9.1 ± 2.5) months in Group III ($p > 0.05$). Mean visual acuity was 0.60 ± 0.05, 0.60 ± 0.03, and 0.60 ± 0.04, respectively ($p > 0.05$). Mean cumulative loss of light sensitivity was (10.39 ± 0.80) dB, (11.2 ± 0.3) dB, and (10.25 ± 0.80) dB in Groups I, II, and III, respectively ($p > 0.05$). The mean tumor volume of PA was significantly larger in Groups I ((20.4 ± 6.7) cm^3) and III ((24.9 ± 5.9) cm^3) compared to Group II ((9.02 ± 0.59) cm^3) ($p < 0.05$).

Regarding visual field patterns: posterior chiasmal position was associated with superior temporal quadrantanopia (32.4%), central chiasmal position with temporal hemianopia and central scotoma (30.6%), anterior chiasmal position with homonymous hemianopia (35.5%).

Conclusions. In patients with pituitary macroadenomas, visual disturbances may be delayed or absent when the chiasm is located in anterior or posterior positions. This is likely due to reduced compressive impact on the opto-chiasmal complex in these anatomical configurations.

Keywords: *neurosurgery; ophthalmology; pituitary adenoma; optic chiasm; compressive optic neuropathy*

Introduction

The topographic anatomy of the optic chiasm in relation to adjacent structures is highly variable, which significantly influences the clinical course of lesions in the chiasmal-sellar region (CSR). The position of the optic chiasm relative to the sella turcica is determined by the length of the intracranial segment of the optic nerves (ON) and plays a crucial role in the manifestation of visual disturbances.

Depending on the length of the intracranial portion of the ON, several variants of chiasm positioning are distinguished: normal, prefixed, and postfixed (***Fig. 1***).

In the anterior variant, the ONs are "short," and the chiasm is displaced anteriorly toward the chiasmatic groove, positioned over the planum sphenoidale. In the central variant, the posterior edge of the chiasm lies over the dorsum sellae. In the posterior variant, the ONs are "long," and the chiasm is displaced posteriorly, partially located behind the dorsum sellae. According to the literature, the central chiasm position is observed in 70–80% of cases, anterior in 9–15%, and posterior in 11–15% [1–6].

The most common cause of primary benign intracranial tumors in the CSR leading to compression of the opto-chiasmatic complex (OCC) is a pituitary adenoma (PA) [7,8]. According to the current WHO classification, PAs are defined as PitNETs (pituitary neuroendocrine tumors arising from epithelial cells of the anterior pituitary lobe—adenohypophysis) [9]. Various authors report that PAs account for 10–25% of all intracranial mass lesions, and according to autopsy studies, the prevalence ranges from 14.4% to 16.9% [10–14].

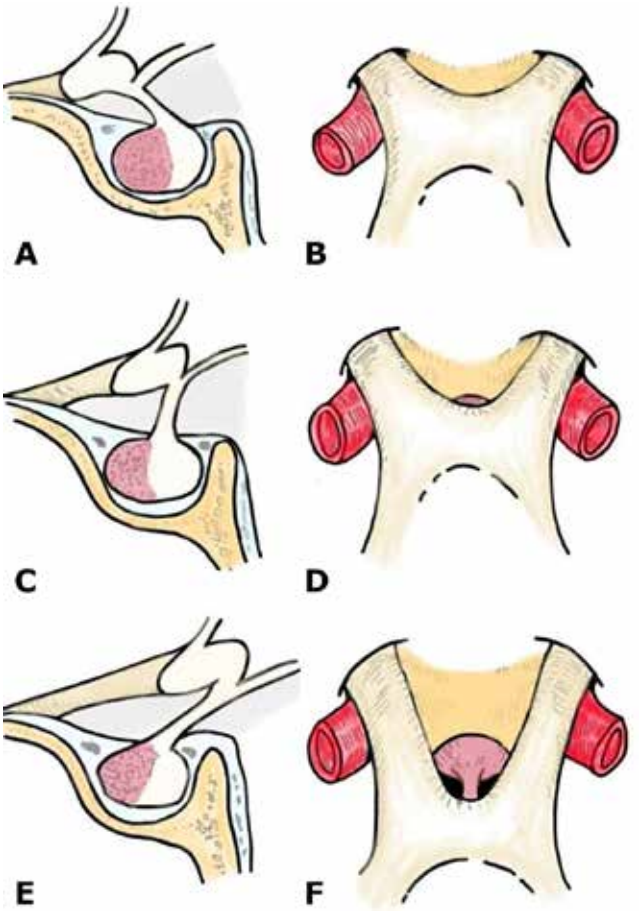

Fig. 1. Schematic illustration of the sella turcica and optic chiasm in sagittal (A, C, E) and axial (B, D, F) planes, showing anterior (A, B), central (C, D), and posterior (E, F) positioning

In hormonally active PAs, hormone hypersecretion leads to severe clinical diseases and syndromes (acromegaly, Cushing's disease, hyperprolactinemia), allowing diagnosis at the microadenoma stage (<10 mm). In contrast, hormonally inactive PAs (HIPAs) may remain clinically silent until they grow into macroadenomas (>10 mm) and cause chiasmal compression. In cases of anterior or posterior chiasmal positions, the onset of clinical symptoms may be delayed due to the unique pattern of tumor extension [15].

Preoperative assessment of chiasm positioning is crucial for neurosurgeons in surgical planning, particularly for determining the optimal timing and strategy of intervention.

However, the specific features of compressive optic neuropathy depending on chiasm position remain insufficiently explored.

Objective: to analyze the characteristics of compressive optic neuropathy in relation to different variants of optic chiasm positioning.

Materials and methods

Study participants

The study was conducted at the Romodanov Institute of Neurosurgery of the National Academy of Medical Sciences of Ukraine between 2018 and 2024, based on the Departments of Endonasal Skull Base Neurosurgery and the Neuro-ophthalmology Group. A consecutive surgical series of 212 patients (424 eyes) with pituitary adenomas (PAs) and compressive optic neuropathy associated with decreased visual acuity and/or visual field defects was analyzed. Of the patients, 116 (54.7%) were female and 96 (45.3%) were male. The age of participants ranged from 18 to 76 years, with a mean age of 52.3 ± 11.8 years.

Inclusion criteria:

- presence of visual disturbances (reduced visual acuity and/or visual field defects);
- surgical decompression of the OCC via endoscopic tumor resection (either total or subtotal resection).

Exclusion criteria:

- cases of tumor regrowth;
- evidence of intracranial hypertension or comorbid ophthalmological disorders;
- prior radiotherapy or radiosurgery;
- parasellar tumor extension;
- pituitary apoplexy.

Group characteristics

Based on the direction of PA extension and the position of the optic chiasm, the 212 patients were divided into three groups: Group I – anterior tumor growth and/or posterior chiasmal position (34 patients [16.1%], 68 eyes); Group II – suprasellar tumor growth and/or central chiasmal position (147 patients [69.3%], 294 eyes); Group III – retrosellar tumor growth and/or anterior chiasmal position (31 patients [14.6%], 62 eyes).

The variants of PA extension in relation to chiasmal positioning are illustrated in ***Fig. 2–4***.

This article contains some figures that are displayed in color online but in black and white in the print edition.

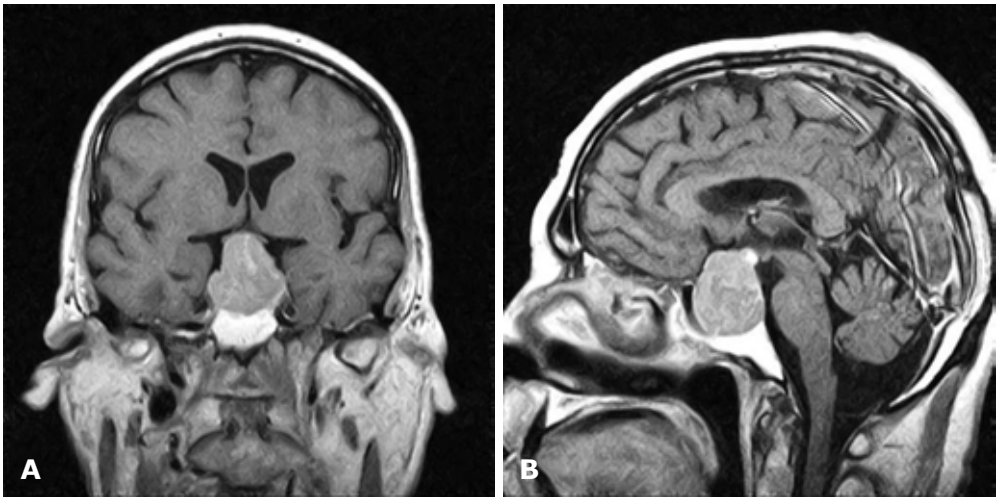

Fig. 2. Patient P., 64 years old, HIPA with suprasellar extension, central chiasmal position. Brain MRI: A – coronal projection; B – sagittal projection

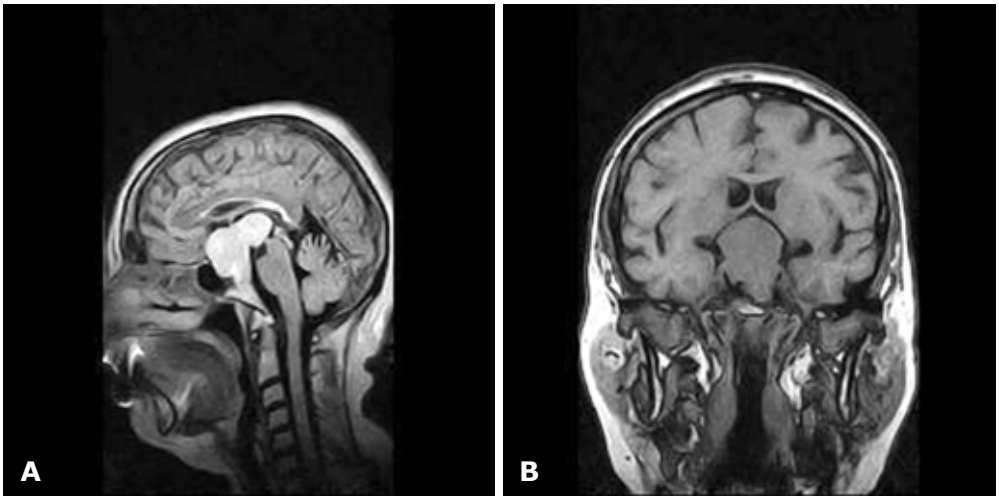

Fig. 3. Patient B., 58 years old, HIPA with retrosellar extension, anterior chiasmal position. Brain MRI: A – sagittal projection; B – coronal projection

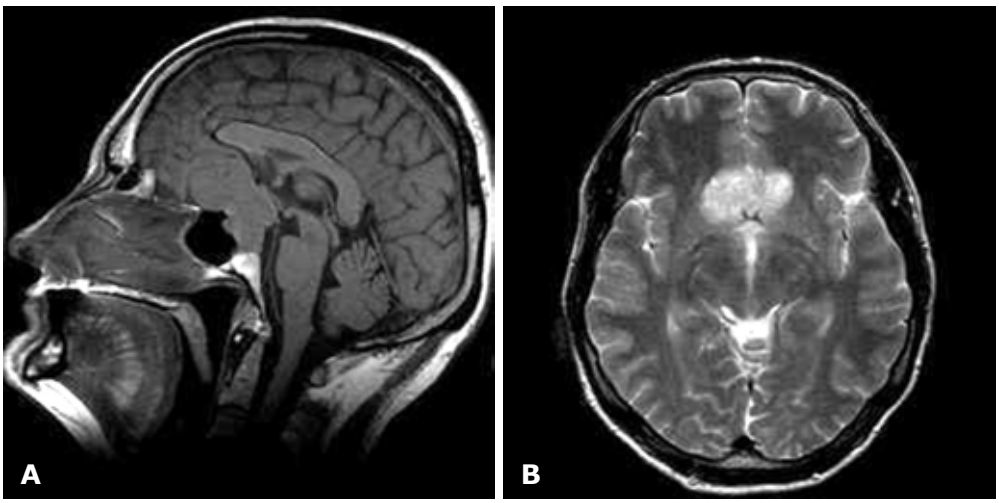

Fig. 4. Patient M., 54 years old, HIPA with antesellar extension, posterior chiasmal position. Brain MRI: A – sagittal projection; B – coronal projection

Study design

All patients underwent a comprehensive clinical-neurological and ophthalmological evaluation, complemented by neuroimaging techniques.

The ophthalmological examination included visual acuity testing with optimal correction (visometry), slit-lamp biomicroscopy, tonometry, automated static perimetry, and ophthalmoscopy. Additionally, direct and consensual pupillary light reflexes were assessed, as well as pupil width and symmetry. Visual acuity was graded as follows: 1 – normal (1.0); 2 – mild reduction (0.7–0.9); 3 – moderate (0.4–0.6); 4 – severe (0.1–0.3); 5 – profound (<0.1); 6 – blindness (0).

Automated static perimetry ("Centerfield 2", Germany) was used to determine the localization of defects and to calculate the perimetric index of mean defect (MD), reflecting cumulative light sensitivity loss. Visual field loss severity based on MD was classified as: 0 – normal visual field; 1 – mild sensitivity loss (MD –2… to –4 dB); 2 – moderate (MD –4… to –12 dB); 3 – severe (MD –12… to –20 dB); 4 – profound (MD > –20 dB).

The severity of chiasmal syndrome (CS) was assessed considering both visual acuity and visual field loss (according to MD indicator) in both eyes: mild CS: visual acuity 1.0 in both eyes, MD up to –4 dB; moderate CS: visual acuity >0.1 in both eyes, MD –4… to –12 dB; severe CS: visual acuity <0.1 in at least one eye, MD > –12 dB in at least one eye.

Chiasmal syndrome was considered symmetric when differences in visual acuity and the average total loss of photosensitivity between both eyes fell within the same stage. It was considered asymmetric if there was a one-stage difference, and markedly asymmetric if the difference was two stages or more.

Neuroimaging methods were used to determine the localization, extent, and size of the CSR, the presence of hemorrhagic or cystic components, lateralization, the relationship with adjacent structures, and the chiasmal configuration (confirmed intraoperatively).

In cases of significant PA extension, the classification by G. Yasargil was applied to analyze the tumor growth pattern. Suprasellar extension is characterized by upward growth leading to compression of the OCC; parasellar extension occurs laterally toward the cavernous sinus; infrasellar growth extends into the sphenoid sinus; antesellar and retrosellar extensions indicate growth anterior and posterior to the sella turcica, respectively. Diffuse growth is defined by multidirectional tumor extension [16].

Following the measurement of the neoplasm in three orthogonal planes, the tumor volume was estimated using the principle developed by mathematician B. Cavalieri, and calculated according to the following formula [17]:

$$\text{Volume (cm}^3\text{)} = (4/3)\,\pi \times (a/2) \times (b/2) \times (c/2)$$

where a represents the width in the coronal plane, b – the height in the coronal plane, and c – the length in the sagittal plane.

The study was conducted in accordance with the principles of bioethics and the provisions of the Declaration of Helsinki on human rights. Ethical approval was obtained from the Ethics Committee of the Romodanov Institute of Neurosurgery of the National Academy of Medical Sciences of Ukraine (Minutes No. 5 dated December 13, 2019). All patients were informed about the specifics of the diagnostic and therapeutic procedures and provided written informed consent.

Statistical analysis

The collected data were entered into Microsoft Excel and analyzed using "SPSS Statistics version 30". The results are presented as the arithmetic mean with standard deviation (M ± SD). To determine the statistical significance (p) of differences between independent groups, the Student's t-test for related samples was applied. A p-value of <0.05 was considered statistically significant. To assess the distribution of categorical variables, Pearson's chi-square (χ^2) test was used; in cases with small sample sizes, Fisher's exact test was applied.

Results

All tumors demonstrated growth directed toward the OCC, resulting in compression of the anterior visual pathway and subsequent visual disturbances (reduced visual acuity and/or visual field defects), which predominated in the clinical picture of most patients. The duration of visual symptoms ranged from 2 weeks to 6 years, with the decline in vision being progressive in nature. A total of 25 patients (11.8%) did not report any vision-related complaints; however, changes in visual acuity and/or visual field defects were detected during ophthalmological examination. Distribution by hormonal activity was as follows: HIPAs were diagnosed in 177 patients (83.5%), prolactinomas in 20 (9.5%), somatotropinomas in 13 (6.1%), and corticotropinomas in 2 (0.9%).

Visual acuity in Group I was distributed as follows: 1.0 – 22 eyes (32.4%), 0.7–0.9 – 15 eyes (22.1%), 0.4–0.6 – 12 eyes (17.6%), 0.1–0.3 – 9 eyes (13.2%) <0.1 – 10 eyes (14.7%). Visual field defects included: superior temporal quadrantanopia – 22 eyes (32.4%), partial temporal hemianopia – 10 eyes (14.7%), complete temporal hemianopia – 8 eyes (11.7%), temporal hemianopia with central scotoma – 15 eyes (22.1%), central scotoma with temporal deviation – 1 eye (1.5%), residual nasal visual field – 6 eyes (8.8%), undetectable visual field – 4 eyes (5.9%), no changes – 2 eyes (2.9%). Primary descending optic atrophy (OA) was observed in 18 patients (52.9%), including bilateral involvement in 13 patients (26 eyes) and unilateral in 5 patients (5 eyes). Based on the analysis of visual acuity and visual field parameters in both eyes, asymmetric chiasmal syndrome (CS) was found in 14 patients (41.2%), markedly asymmetric in 12 (35.3%), and symmetric in 8 (23.5%). CS severity distribution in Group I: mild – 3 patients (8.8%), moderate – 15 patients (44.1%), severe – 16 patients (47.1%).

Visual acuity in Group II (147 patients, 294 eyes) was distributed as follows: 1.0 – 81 eyes (27.5%), 0.7–0.9 – 49 eyes (16.7%), 0.4–0.6 – 70 eyes (23.8%), 0.1–0.3 – 69 eyes (23.5%), <0.1 – 25 eyes (8.5%). Visual field defects included: superior temporal quadrantanopia – 4 eyes (1.4%), partial temporal hemianopia – 45 eyes (15.3%), complete temporal hemianopia – 71 eyes (24.1%), temporal hemianopia with central scotoma – 90

eyes (30.6%), central scotoma with temporal deviation – 63 eyes (21.4%), residual nasal visual field – 15 eyes (5.1%), undetectable visual field – 1 eye (0.4%), no changes – 5 eyes (1.7%). Optic atrophy was confirmed in 105 patients (71.4%), with bilateral involvement in 72 patients (144 eyes) and unilateral in 33 (33 eyes). Symmetric CS was observed in 63 patients (42.9%), compared to asymmetric in 39 (26.5%) and markedly asymmetric in 45 (30.6%). CS severity distribution: mild – 7 patients (4.8%), moderate – 66 patients (44.9%), severe – 74 patients (50.3%).

Visual acuity in Group III (31 patients, 62 eyes) was distributed as follows: 1.0 – 17 eyes (27.4%), 0.7–0.9 – 17 eyes (27.4%), 0.4–0.6 – 10 eyes (16.1%), 0.1–0.3 – 13 eyes (21.0%), <0.1 – 5 eyes (8.1%). Visual field defects were as follows: homonymous hemianopia – 22 eyes (35.5%), partial temporal hemianopia – 5 eyes (8.1%), complete temporal hemianopia – 3 eyes (4.8%),temporal hemianopia with central scotoma – 12 eyes (19.4%), central scotoma with temporal deviation – 18 eyes (29.0%), residual visual field in the nasal half – 1 eye (1.6%), no changes – 1 eye (1.6%). OA was diagnosed in 19 patients (61.3%): bilateral in 13 patients (26 eyes) and unilateral in 6 patients (6 eyes). Symmetric chiasmal syndrome (CS) was predominant in 14 patients (45.2%), followed by asymmetric in 9 patients (29.0%) and markedly asymmetric in 8 patients (25.8%). CS severity in Group III was as follows: mild – 2 patients (6.5%), moderate – 15 patients (48.4%), severe – 14 patients (45.1%).

The clinical characteristics of the study groups are summarized in ***Table 1.***

According to the analysis, no statistically significant differences were found between the study groups in terms of mean age ($p > 0.05$), mean duration of visual disturbances, mean visual acuity, or average group-level light sensitivity loss (see ***Table 1***). The distribution of CS types varied across groups: in Group I, the asymmetric type was predominant (41.2%), whereas in Groups II and III, the symmetric type was more frequent (42.9% and 45.2%, respectively). Comparison of the groups revealed that moderate CS occurred most commonly in Group III (48.4%), while severe CS was more frequently observed in Groups I and II (47.1% and 50.3%, respectively). The highest incidence of OA was recorded in Group II (71.4%), compared to 52.9% in Group I and 61.3% in Group III.

The mean volume of the PA was significantly greater in Groups I (20.4 ± 6.7 cm³) and III (24.9 ± 5.9 cm³) compared to Group II (9.02 ± 0.59 cm³; $p < 0.05$).

Discussion

We analyzed the characteristics of compressive optic neuropathy (CON) depending on the position of the optic chiasm in a large cohort of patients with PAs. This aspect has not been adequately explored in the literature, as existing data on chiasmal positioning are primarily derived from autopsy studies. Only isolated clinical cases of homonymous hemianopia associated with CSR tumors, as well as reports involving anterior and posterior chiasmal positions, have been described in the literature [18–20].

It is well established that hormonally active PAs are typically diagnosed at the microadenoma stage (<10 mm) due to the manifestation of severe clinical syndromes induced by hormone hypersecretion, such as acromegaly, Cushing's disease, and hyperprolactinemia. At this stage, their small size precludes chiasmal compression. In contrast, HIPAs often remain clinically silent for an extended period and cause compression of the optic chiasm only after reaching sizes >10 mm [15]. The lack of hormonal activity complicates early detection at small tumor sizes. In our study, HIPAs were identified in 83.5% of patients, which is consistent with the findings of Gnanalingham et al. (2005) [21].

In cases of antesellar extension and/or posterior chiasmal position, CS was characterized by an asymmetric pattern (41.2%), a severe course (47.1%), with a predominance of superior temporal quadrantanopia (32.4%) and OA (52.9%). In cases of suprasellar extension and/or central chiasmal position, CS manifested symmetrically (42.9%), with a severe course (50.3%), commonly presenting with temporal hemianopia with central scotoma (30.6%) and OA (71.4%). In cases of retrosellar extension and/or anterior chiasmal position, CS was associated with a symmetric pattern (45.2%), a moderate course (48.4%), and predominance of homonymous hemianopia (35.5%)

Table 1. Clinical characteristics of the study groups with compressive optic neuropathy depending on the direction of pituitary adenoma extension and chiasmal position

Parameter	Group I, n=34	Group II, n=147	Group III, n=31	P value
Mean age, years (M±SD)*	48,4±13,4	52,8±11,4	54,2±11,2	$P_{1-2}>0,05$ $P^{1-3}>0,05$ $P_{2-3}>0,05$
Duration of visual disturbances, months, (M ± m)*	14,8±3,9	8,8±0,95	9,1±2,5	$P_{1-2}>0,05$ $P^{1-3}>0,05$ $P_{2-3}>0,05$
Visual acuity (M ± m)*	0,6±0,05	0,6±0,03	0,6±0,04	$P_{1-2}>0,05$ $P^{1-3}>0,05$ $P_{2-3}>0,05$
MD, dB (M ± m)*	10,39±0,80	11,2±0,3	10,25±0,80	$P_{1-2}>0,05$ $P^{1-3}>0,05$ $P_{2-3}>0,05$
PA volume, cm³, (M ± m)*	20,4±6,7	9,02±0,59	24,9±5,9	$P_{1-2}<0,05$ $P^{1-3}>0,05$ $P_{2-3}<0,05$

Note: * Based on Student's t-test.

and OA (61.3%). No statistically significant differences were found between groups in terms of mean age, mean visual acuity, or MD values ($p > 0.05$).

Bitemporal heteronymous hemianopia is considered the classical visual field defect resulting from involvement of decussating optic nerve fibers. However, the specific visual field defect pattern depends on the topographic relationship between the optic chiasm and the tumor (***Figs. 5–7***). In posterior chiasmal positions, superior temporal quadrantanopia predominated (32.4%). In central positions, the typical temporal hemianopia with central scotoma was most common (30.6%). In anterior positions, homonymous hemianopia prevailed (35.5%).

The occurrence of homonymous hemianopia in PAs is atypical and results from compression of the posterior chiasm and/or optic tracts, clinically mimicking visual deficits typically seen in retrochiasmal lesions.

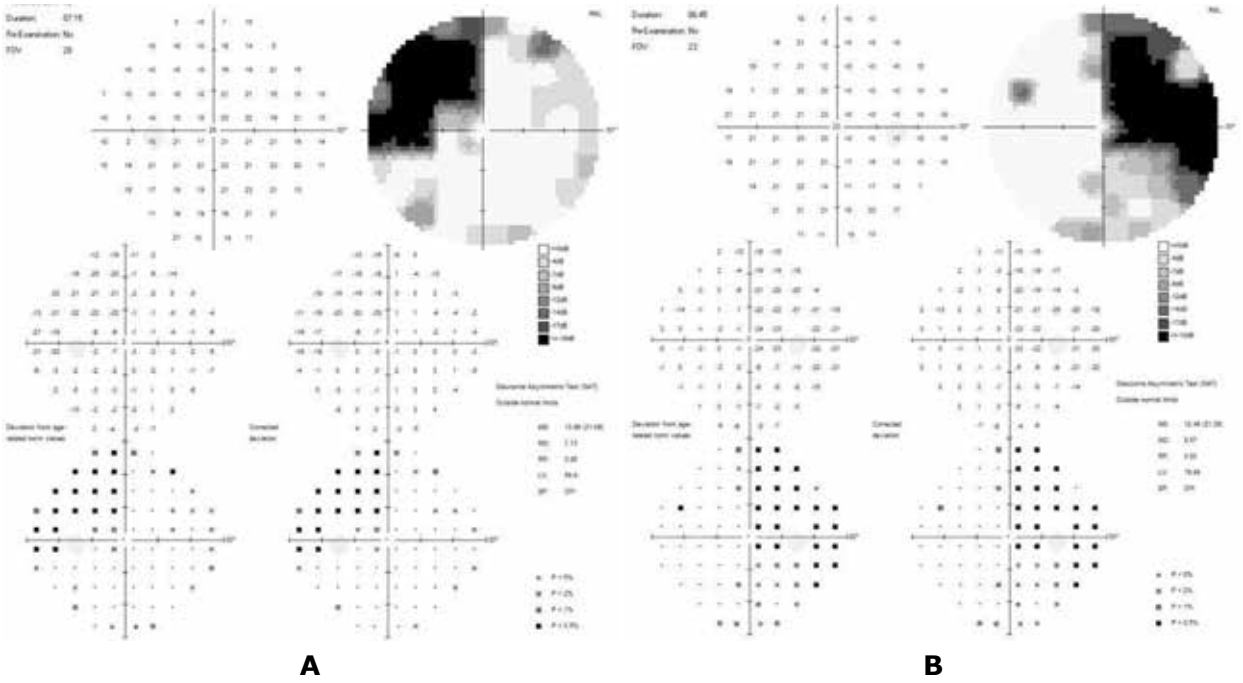

A B

Fig. 5. Automated static perimetry. Superior quadrantic bitemporal hemianopia

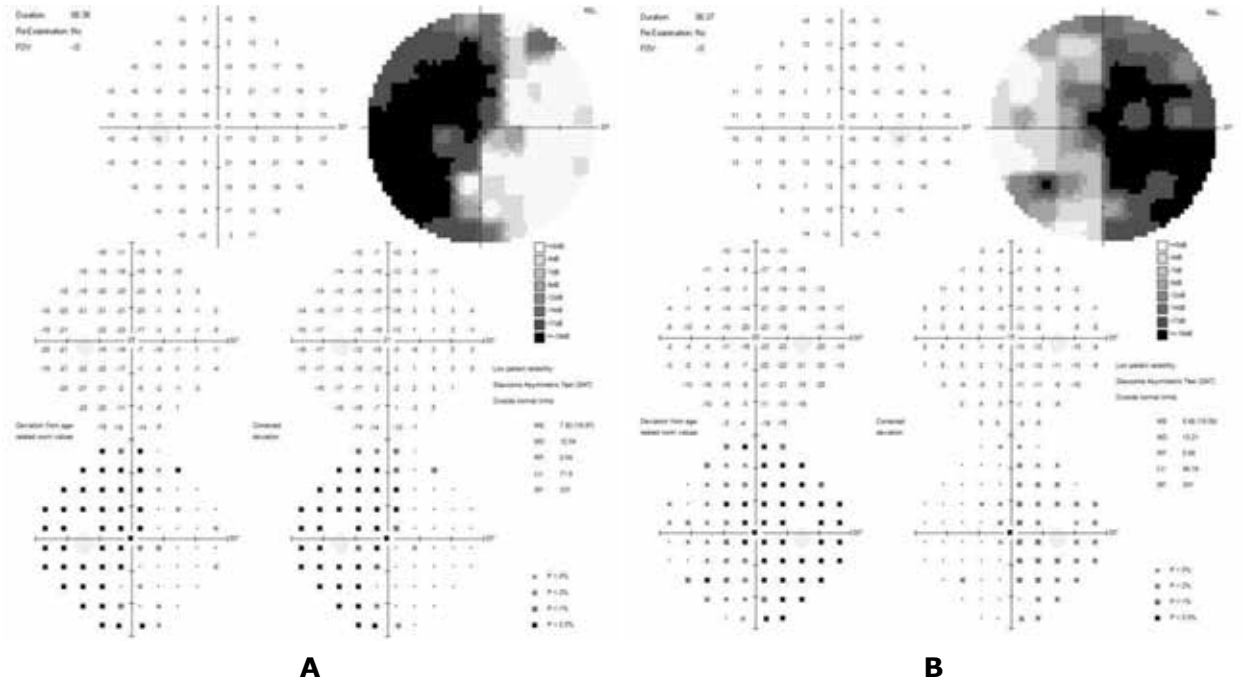

A B

Fig. 6. Automated static perimetry. Bitemporal hemianopia with central scotoma

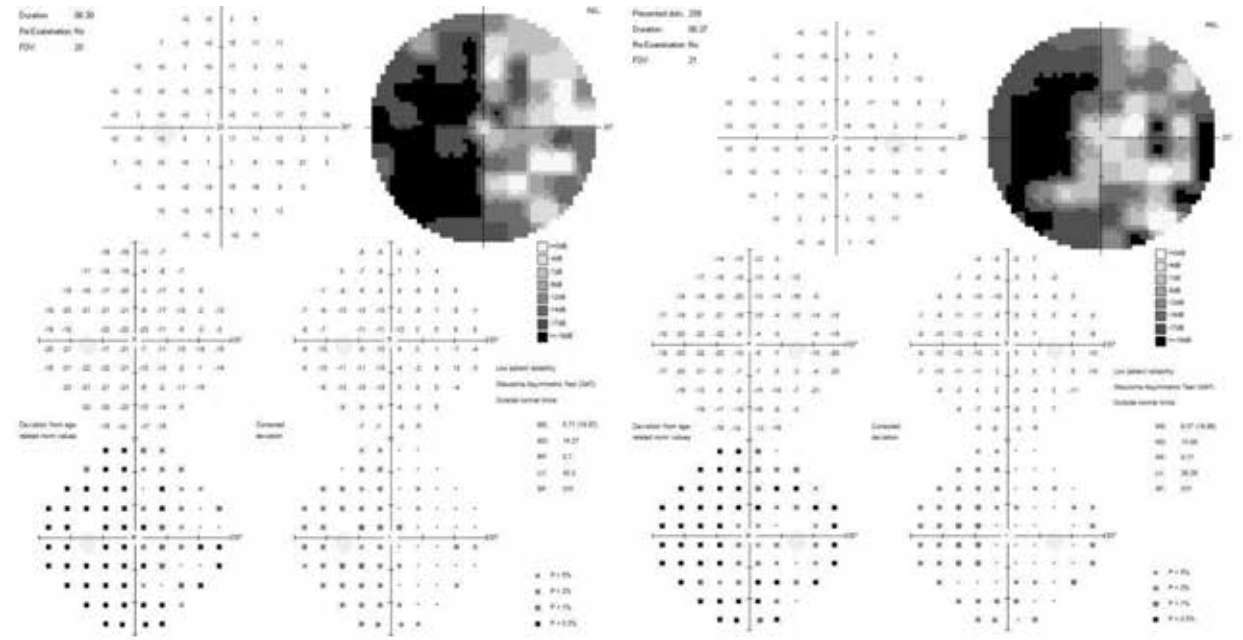

A B

Fig. 7. Automated static perimetry: Left-sided homonymous hemianopia

Based on the results of the study, a shorter duration of visual disturbances was observed in patients with a centrally positioned optic chiasm, although the difference did not reach statistical significance ($p > 0.05$). At the same time, the mean volume of PAs was significantly larger in cases with anterior and posterior chiasmal positions compared to the central position ($p < 0.05$). These findings indicate that tumors may grow to giant sizes without causing ophthalmological symptoms during the macroadenoma stage (10–40 mm), which may be explained by the presence of free space for PA in anterior and posterior chiasmal positions, unlike the central chiasmal location.

Conclusions

In patients with pituitary macroadenoma, the onset of visual impairment may be delayed or entirely absent in cases of anterior or posterior chiasmal positions, due to reduced compressive effects on the opto-chiasmatic complex.

Disclosure

Conflict of interest

The authors declare no conflicts of interest.

Ethical standards

All procedures performed in this study involving human participants were in accordance with the ethical standards of the institutional and national research committees, the 1964 Helsinki Declaration and its later amendments, or comparable ethical standards.

Informed Consent

Informed consent was obtained from all individual participants included in the study.

Funding

This study received no external funding or sponsorship.

References

1. Rhoton AL Jr. The sellar region. Neurosurgery. 2002 Oct;51(4 Suppl):S335-74. doi: 10.1097/00006123-200210001-00009
2. Griessenauer CJ, Raborn J, Mortazavi MM, Tubbs RS, Cohen-Gadol AA. Relationship between the pituitary stalk angle in prefixed, normal, and postfixed optic chiasmata: an anatomic study with microsurgical application. Acta Neurochir (Wien). 2014 Jan;156(1):147-51. doi: 10.1007/s00701-013-1944-1
3. Schiefer U, Isbert M, Mikolaschek E, Mildenberger I, Krapp E, Schiller J, Thanos S, Hart W. Distribution of scotoma pattern related to chiasmal lesions with special reference to anterior junction syndrome. Graefes Arch Clin Exp Ophthalmol. 2004 Jun;242(6):468-77. doi: 10.1007/s00417-004-0863-5
4. Miller NR, Newman NJ, Biousse V, Kerrison JB. Walsh & Hoyt's Clinical Neuro-Ophthalmology, sixth ed. Lippincott Williams & Wilkins, Philadelphia; 2005. 320 p.
5. Renn WH, Rhoton AL Jr. Microsurgical anatomy of the sellar region. J Neurosurg. 1975 Sep;43(3):288-98. doi: 10.3171/jns.1975.43.3.0288
6. Bergland RM, Ray BS, Torack RM. Anatomical variations in the pituitary gland and adjacent structures in 225 human autopsy cases. J Neurosurg. 1968 Feb;28(2):93-9. doi: 10.3171/jns.1968.28.2.0093
7. Ezzat S, Asa SL, Couldwell WT, Barr CE, Dodge WE, Vance ML, McCutcheon IE. The prevalence of pituitary adenomas: a systematic review. Cancer. 2004 Aug 1;101(3):613-9. doi: 10.1002/cncr.20412
8. Wang EW, Zanation AM, Gardner PA, Schwartz TH, Eloy JA, Adappa ND, Bettag M, Bleier BS, Cappabianca P, Carrau RL, Casiano RR, Cavallo LM, Ebert CS Jr, El-Sayed IH, Evans JJ, Fernandez-Miranda JC, Folbe AJ, Froelich S, Gentili F, Harvey RJ, Hwang PH, Jane JA Jr, Kelly DF, Kennedy D, Knosp E, Lal D, Lee JYK, Liu JK, Lund VJ, Palmer JN, Prevedello DM, Schlosser RJ, Sindwani R, Solares CA, Tabaee A, Teo C, Thirumala PD, Thorp BD, de Arnaldo Silva Vellutini E, Witterick I, Woodworth BA, Wormald PJ, Snyderman CH. ICAR: endoscopic skull-base surgery. Int Forum Allergy Rhinol. 2019 Jul;9(S3):S145-S365. doi: 10.1002/alr.22326
9. Asa SL, Mete O, Perry A, Osamura RY. Overview of the 2022 WHO Classification of Pituitary Tumors. Endocr Pathol.

2022 Mar;33(1):6-26. doi: 10.1007/s12022-022-09703-7
10. Rutkowski MJ, Chang KE, Cardinal T, Du R, Tafreshi AR, Donoho DA, Brunswick A, Micko A, Liu CJ, Shiroishi MS, Carmichael JD, Zada G. Development and clinical validation of a grading system for pituitary adenoma consistency. J Neurosurg. 2020 Jun 5;134(6):1800-1807. doi: 10.3171/2020.4.JNS193288
11. Abouaf L, Vighetto A, Lebas M. Neuro-ophthalmologic exploration in non-functioning pituitary adenoma. Ann Endocrinol (Paris). 2015 Jul;76(3):210-9. doi: 10.1016/j.ando.2015.04.006
12. Sivakumar W, Chamoun R, Nguyen V, Couldwell WT. Incidental pituitary adenomas. Neurosurg Focus. 2011 Dec;31(6):E18. doi: 10.3171/2011.9.FOCUS11217
13. Marigil Sanchez M, Karekezi C, Almeida JP, Kalyvas A, Castro V, Velasquez C, Gentili F. Management of Giant Pituitary Adenomas: Role and Outcome of the Endoscopic Endonasal Surgical Approach. Neurosurg Clin N Am. 2019 Oct;30(4):433-444. doi: 10.1016/j.nec.2019.05.004
14. Westall SJ, Aung ET, Kejem H, Daousi C, Thondam SK. Management of pituitary incidentalomas. Clin Med (Lond). 2023 Mar;23(2):129-134. doi: 10.7861/clinmed.2023-0020
15. Melmed S, Kaiser UB, Lopes MB, Bertherat J, Syro LV, Raverot G, Reincke M, Johannsson G, Beckers A, Fleseriu M, Giustina A, Wass JAH, Ho KKY. Clinical Biology of the Pituitary Adenoma. Endocr Rev. 2022 Nov 25;43(6):1003-1037. doi: 10.1210/endrev/bnac010
16. Yasargil M.G. Microsurgery Applied to Neurosurgery. Stuttgart: Thieme, 1969.
17. Lee JP, Park IW, Chung YS. The volume of tumor mass and visual field defect in patients with pituitary macroadenoma. Korean J Ophthalmol. 2011 Feb;25(1):37-41. doi: 10.3341/kjo.2011.25.1.37
18. Nishimura M, Kurimoto T, Yamagata Y, Ikemoto H, Arita N, Mimura O. Giant pituitary adenoma manifesting as homonymous hemianopia. Jpn J Ophthalmol. 2007 Mar-Apr;51(2):151-3. doi: 10.1007/s10384-006-0419-9
19. Foroozan R. Chiasmal syndromes. Curr Opin Ophthalmol. 2003 Dec;14(6):325-31. doi: 10.1097/00055735-200312000-00002.
20. Glisson CC. Visual loss due to optic chiasm and retrochiasmal visual pathway lesions. Continuum (Minneap Minn). 2014 Aug;20(4 Neuro-ophthalmology):907-21. doi: 10.1212/01.CON.0000453312.37143.d2
21. Gnanalingham KK, Bhattacharjee S, Pennington R, Ng J, Mendoza N. The time course of visual field recovery following transphenoidal surgery for pituitary adenomas: predictive factors for a good outcome. J Neurol Neurosurg Psychiatry. 2005 Mar;76(3):415-9. doi: 10.1136/jnnp.2004.035576
22. Guk MO, Ukrainets OV. Endoscopic endonasal surgical management of giant pituitary adenomas with extension into ventricle system. Ukr Neurosurg J. 2023Dec.26;29(4):13-21. doi: 10.25305/unj.286547

Original article

Ukrainian Neurosurgical Journal. 2025;31(3):30-36
doi: 10.25305/unj.328642

Features of peripheral and intrathecal content of immunological markers of inflammation in combatants with mild TBI depending on the chronicity of its course

Valentina V. Geiko [1], Mykola F. Posokhov [2], Zaza M. Lemondzhava [2]

[1] Laboratory of Neurophysiology, Immunology and Biochemistry, State Institution «P. V. Voloshyn Institute of Neurology, Psychiatry and Narcology of the National Academy of Medical Sciences of Ukraine», Kharkiv, Ukraine
[2] Department of Functional Neurosurgery with a Group of Pathomorphology, State Institution «P. V. Voloshyn Institute of Neurology, Psychiatry and Narcology of the National Academy of Medical Sciences of Ukraine», Kharkiv, Ukraine

Received: 06 May 2025
Accepted: 26 May 2025

Address for correspondence*: Valentina V. Geiko, Laboratory of Neurophysiology, Immunology and Biochemistry, State Institution «P. V. Voloshyn Institute of Neurology, Psychiatry and Narcology of the National Academy of Medical Sciences of Ukraine», 46 Academician Pavlova St., Kharkiv, Ukraine, 61068; e-mail: vvgeiko@gmail.com*

Aim: To investigate the levels of inflammatory mediators of the immune system in blood serum and cerebrospinal fluid (CSF) in combatants with mild traumatic brain injury (mTBI) at different time periods after its acquisition.

Materials and methods: IL-6, TNFα, IL-10 and TGFβ1 concentrations were measured according to the instructions of the «Human ELISA Kit» (Elabscience Bionovation Inc., USA) in 53 paired serum and CSF samples from patients with combat mTBI.

Results: In the general group of patients with mTBI, a significant increase in the peripheral content of IL-6, IL-10, TGFβ1 was found, compared with healthy donors (control). When studying these indicators depending on the duration of the post-traumatic period, a persistent increase in the level of IL-6 was shown in combination with significantly increased TGFβ1 concentration indicators and a tendency to an increased level of IL-10. At the same time, the analysis of the central content of inflammatory biomarkers did not reveal their significant changes at different times after TBI, with the exception of a tendency to a decrease in the presence of IL-6, the presence of which in paired analytes prevailed in CSF along with the prevalence of peripheral finding of TNFα, IL-10, TGFβ1.

Conclusions: Thus, the increased content of circulating pro-inflammatory IL-6 and TNFα in the intermediate and remote periods of the course of TBI and a significantly (approximately 6 times) increased level of pleiotropic TGFβ1 in combination with anti-inflammatory IL-10 indicate the persistent nature of inflammation, which indicates the possibility of induction of neurodegenerative processes in combatants with TBI. Such results confirm the feasibility of comprehensive monitoring of immunological markers of inflammation to identify potential directions for adequate pathogenetic therapy even in the context of significantly distant consequences of TBI.

Keywords: *combat mild TBI; inflammatory markers of the immune system; time periods of TBI*

Introduction

Traumatic brain injuries, which are widespread among young people, are often a factor in the development of long-term neurological deficits, cognitive impairments, and emotional disorders. These consequences pose important medical and socio-economic challenges associated with high mortality and disability of patients, as well as with the triggering value of post-traumatic neuroinflammation in the occurrence of neurodegenerative processes, which subsequently lead to an increased risk of developing Alzheimer's and Parkinson's diseases, chronic traumatic encephalopathy, etc. [1–7]. Currently, TBI is a global health problem worldwide, exacerbated by inadequate monitoring and the lack of effective diagnostic methods and pathogenetic treatment at various stages of the post-traumatic period, which can cause complications of the disease due to the initiation of complex biochemical cascades and immunological processes leading to secondary neuroinflammation [8–12].

Moreover, the issue of TBI-related consequences is becoming increasingly urgent in the context of a full-scale war of aggression in Ukraine with a violation of the world charter of the sovereignty of democratic states due to the Russian invasion. This applies both to direct participants in hostilities using modern destructive weapons, and to the civilian population, which is permanently exposed to stochastic terrorist bombing.

In the overall structure of brain injuries, mine-explosive injuries are detected in 70% of victims, and at least 80% of them are diagnosed as mild injuries [13, 14]. The most common type of mTBI among military personnel is concussion and mild brain contusion, and such injuries, most often caused by an explosion, are considered "signature wounds" of the wars in Iraq and Afghanistan [15–18]. Currently, there are quite limited objective indicators for identifying individuals with a high risk of developing neuropsychiatric disorders and adverse consequences and complications [18], in particular, among military personnel and veterans of

modern wars against the background of the staggering spread of TBI [19].

It is known that TBI is accompanied by an immediate immune system response. Innate immunity helps to reduce the progression of pathogens by activating the healing processes and remodeling of nerve tissue damage while also preparing the body for an adaptive immune response, which is based on the activation of T and B lymphocytes, the excess of which has the ability to stimulate neuroinflammation [11]. Previous studies have documented a reversible increase in the levels of inflammatory cytokines IL-6, TNFα and IL-10 within 24 hours after the explosion during training [20], and as a result of the acute phase reaction in combatants with severe TBI [21]. The cytokines promote the induction of the first phase of inflammation, which is aimed at neuroprotection and restoration of homeostasis and nervous tissue integrity [22, 23].

Accordingly, the study of neuroinflammation and its associated immune biomarkers is of growing importance [23, 24]. Evidence suggests that uncontrolled or insufficiently effective regulation of the balance of pro- and anti-inflammatory activity of mediators of the immunological response may be the cause of the formation of long-term symptoms of CNS damage due to TBI [25–28] with the development of autoimmune processes and the subsequent formation of neurodegenerative pathology.

It is noteworthy that most of the literature on the pathogenesis of neuroinflammation focuses on studying the mechanisms of its development, which are activated in patients with severe TBI in the most acute period (the first hours, days, weeks) [14, 21, 29, 30]. At the same time, studies of immunological markers in the chronic course of combat mTBI are not sufficiently presented.

Taking this into account, the aim of the work was to study the levels of inflammatory mediators of the immune system in the serum and CSF in combatants with mTBI at different time periods after its acquisition.

Materials and methods

Study participants

The study was performed using 53 paired serum and CSF samples obtained from male patients aged 36.03±1.40 years, who were treated in the neurosurgical department of the P. V. Voloshyn Institute of Neurology, Psychiatry and Narcology of the National Academy of Medical Sciences of Ukraine during 2024 years.

Inclusion criteria

Patients who suffered mTBI in the form of concussion and mild brain contusion during active hostilities in Ukraine.

Exclusion criteria

Severe TBI, the presence of multiple trauma and chronic somatic diseases.

Group characteristics

Depending on the duration of the post-traumatic period, the combatants were divided into three groups: I (acute period) – 1.22±0.19 months; II (interim period) – 6.39±0.74 months; III (remote period) – 13.43±1.13 months. The control group, limited to serum samples only for ethical and medical reasons, consisted of 8 practically healthy male donors aged 37.38±2.40 years. All patients with TBI, regardless of the time after its acquisition, were included in the general comparison group – TBI.

Study design

Peripheral blood with a volume of up to 8 ml was obtained by puncture from the cubital vein with subsequent centrifugation (4000 revolutions per minute, within 10 minutes), serum collection (120 μl into separate Eppendorf tubes) and storage at -80°C until quantitative ELISA.

CSF samples were obtained with patient consent during neurosurgical intervention by lumbar puncture with subsequent storage of the required number of its samples (120 μl) at -80°C. The process from serum and CSF sample collection to storage lasted no more than 3 hours. Serum and CSF samples were used with one freeze-thaw cycle.

The concentrations of immune system mediators were measured spectrophotometrically with recording of values on a microplate enzyme immunoassay analyzer GBG Stat Fax 2010 (USA) with a wavelength of 450 nm according to the instructions and protocols of the manufacturer of «Human ELISA Kit» from «Elabscience Bionovation Inc.» (USA), «…which are used for their determination in blood serum and other biological fluids of the body (plasma, CSF, tissue homogenates, supernatants of cell structures, etc.)». The concentrations of pro-inflammatory cytokines IL-6 and TNFα and anti-inflammatory IL-10 and TGFβ1 were determined. The sensitivity of the analyses was: IL-6 – 0.94 pg/ml, IL-10 – 0.94 pg/ml, TNFα – 4.69 pg/ml, TGFβ1 – 18.75 pg/ml; detection range: IL-6 – 1.56–100 pg/ml, IL-10 – 1.56–100 pg/ml, TNFα – 7.81–500 pg/ml, TGFβ1 – 31.25–2000 pg/ml. Since the «Human ELISA Kit» is intended for research purposes only and cannot be used for clinical diagnosis or any other related procedures, reference values for cytokine levels in peripheral blood and CSF are not provided in this test system.

Statistical analysis

Statistical analysis of the results was performed using the Microsoft Office Excel program using Student's t-test to assess differences between comparison groups.

Results

Determination of concentrations of inflammatory mediators of the immune system in the generalized group of patients with combat TBI revealed a significant increase, compared with controls, in the peripheral content of pro-inflammatory IL-6, anti-inflammatory IL-10 and TGFβ1 (***Table 1***). When studying these indicators depending on the duration of the post-traumatic period, it was shown that the increased level of IL-6 production was preserved in combination with significantly increased, relative to healthy donors, serum TGFβ1 concentrations and a tendency to an increased level of IL-10 at all stages of the course of TBI.

This article contains some figures that are displayed in color online but in black and white in the print edition.

At the same time, analysis of the content of inflammatory markers in CSF did not reveal significant differences at different times after TBI, with the exception of a tendency to decrease the concentration of IL-6 depending on the increase in the duration of the post-traumatic period. When comparing the ratio of peripheral and central inflammatory cytokine content in paired biological analytes, it was found that in the process of chronicity of TBI consequences in combatants, only the content of IL-6 prevails in CSF along with the prevalence of peripheral TNFα, IL-10 and TGFβ1 (***Fig. 1***).

The obtained results do not contradict the literature data on the content of immune system mediators in patients with TBI, taking into account the severity and time periods of its course. Thus, when studying the concentrations of IL-6, IL10, TNFα, TGFβ1, their multidirectional correlation was revealed with a particularly significant (28 times) predominance of IL-6 content in CSF compared to serum, which demonstrated its important role in the initiation of the acute phase [21, 30], and in our study, the quantitative features of the representation of inflammatory cytokines in the brain and blood reflect the consequences of chronic neuroinflammation.

Table 1. Levels of pro- and anti-inflammatory cytokines in the serum and CSF in patients with combat mTBI at different periods after its receipt

Cytokines (pg/ml)	Analytes	Groups				
		Control	mTBI	I (acute period, 1.22±0.19 months)	II (interim period, 6.39±0.74 months)	III (remote period, 13.43±1.13 months)
IL-6	serum	0.20±0.03	0.30±0.04**	0.32±0.05**	0.26±0.05	0.32±0.07
	CSF	—	1.06±0.19	1.68±0.54	0.81±0.09#	0.76±0.16#
IL-10	serum	0.04±0.01	0.38±0.14***	0.35±0.26	0.46±0.24*	0.34±0.26
	CSF	—	0.19±0.04	0.27±0.10	0.14±0.05	0.14±0.05
TNFα	serum	15.93±3.54	65.04±31.02*	5.37±3.01**	51.39±26.45#	149.44±94.40
	CSF	—	6.95±0.85	6.00±1.36	5.94±1.00	9.17±1.91
TGFβ1	serum	242.80±81.70	1374.78±230.13*****	1471.90±41.11****	1450.50±447.80***	1179.50±345.80***
	CSF	—	88.31±12.78	82.30±16.10	104.70±30.60	77.60±18.10

Notes. * p ≤ 0.1; ** p ≤ 0.05; *** p ≤ 0.02; **** p ≤ 0.01; ***** p ≤ 0.001: compared to control; # p ≤ 0.1: compared to group I

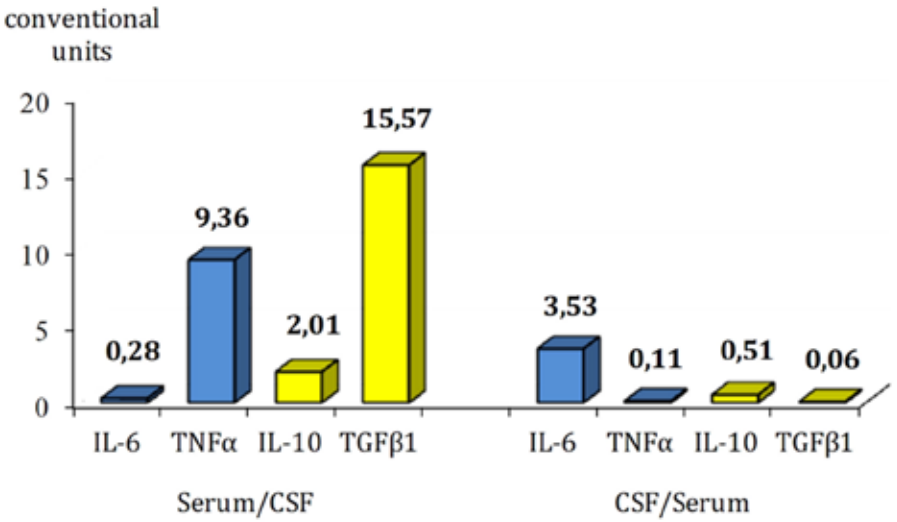

Fig. 1. Relation between peripheral and central inflammatory cytokine levels in the serum and CSF in patients with combat TBI

Conclusion

The moderately elevated serum IL-6 level is consistent with the idea that it can escape from the injured brain into the bloodstream. It is believed that this is the main mechanism for activating peripheral metabolism, endocrine and immune responses, i.e., its production in the periphery is stimulated [31] with simultaneous induction of the synthesis of anti-inflammatory IL-10 and TGFβ1 to provide a regulatory immunosuppressive effect [30]. This likely demonstrates a physiological normalization of the balance of pro- and anti-inflammatory cytokines as a mechanism for restraining the intensity of the secondary phase of neuroinflammation, which in the process of chronic mTBI is aimed at slowing down or preventing complications, which in the case of uncontrolled hyperadaptive immune response leads to "secondary injury", which can contribute to further strengthening of neuropsychiatric symptoms in much later periods.

Given that IL-6 plays a key role in both the acute and chronic phase of the response, and persistent neuroinflammation is associated with a poor prognosis [26, 32], our long-term findings after mTBI suggest the persistence of chronic inflammatory processes with a predominance of their activity in the periphery. This likely reflects the consequences of secondary neuroinflammation with changes in systemic immunity, which may be associated with disruption of the vascular network of the CNS barrier structures, leading to the leakage of detritus (a product of tissue breakdown) and inflammatory mediators with the development of complications such as systemic inflammatory response syndrome (SIRS) [11, 33–35], which in turn may complicate the consequences of the primary injury and local inflammatory reaction. According to the increase in the post-traumatic period, the body compensates for SIRS by increasing the peripheral level of inflammatory mediators, which, along with the activation of anti-inflammatory cytokines, contributes to the normalization of their balance and outlines directions for selective immunomodulatory therapeutic interventions at much later stages of the course of TBI.

In the context of the current study, the results obtained are organically combined with the literature and our previous data on the features of immune reactivity at different times after mTBI in combatants, which indicate chronic inflammation in the remote periods of its course, which is capable of initiating the formation of autoimmune processes with subsequent induction of neurodegenerative pathology. This concerns the increase in serum concentrations of immunoglobulins of the main classes, especially IgG, which reflected the formation and long-term maintenance of the humoral component of adaptive immunity in the remote periods of mTBI, as well as the modulation of the eliminating (detoxification) function of the immune system in the form of an increase in the number of small, most pathogenic, soluble antigen-antibody complexes along with the suppression of the formation of large and medium-sized conglomerates that stimulate the activity of micro- and macrophage systems of nonspecific natural resistance of the organism [36]. In addition, a slight increase in the content of circulating pro-inflammatory cytokines IL-6 and TNFα in the intermediate and long-term observation periods, along with a significantly (approximately 6 times) increased level of pleiotropic TGFβ1 in serum, confirms the persistent character of inflammation, which does not exclude its role in stimulating neurodegenerative processes in patients with mTBI.

It is known that activation of TGFβ1 production can be a consequence of both beneficial and harmful effects of neuroinflammation in order to suppress proinflammatory reactions and enhance tissue repair of reactive astrocytes and microglia [37]. Astrocytes are the main source of endogenous TGFβ1 production in the CNS, providing metabolic and structural support for neurons and participating in the regulation of brain homeostasis, synaptic plasticity and blood-brain barrier (BBB) integrity [38–40]. In addition, astrocytes play a crucial role in responses to the pathological effects of disease and brain injury [38–42]. TGFβ, among other inflammatory cytokines, is a key regulator and signaling factor in the transformation of normal astrocytes into reactive phenotypes [40, 43, 44]. As TGFβ1 is a pleiotropic cytokine, its excess may contribute to neuronal dysfunction and cognitive impairment in TBI [45–47], as well as to the inhibition of microglial proliferation, astrocyte activity, and glial scar formation [41, 43, 48]. Reactive astrogliosis is thought to be a protective mechanism aimed at limiting damage, controlling inflammation, and restoring homeostasis [38, 49, 50]. However, like peripheral inflammation, astrogliosis can become maladaptive and contribute to secondary damage to neural tissues [51]. As a result of studying these aspects of reactivity, neurotoxic (A1) and neuroprotective (A2) astrocytes have been identified [52]. The importance of considering the context-dependent modulation of their reactivity by TGFβ1 signaling is emphasized. It is noteworthy that TGFβ1 promotes the development of macrophages and their polarization into an M-2-like pool, which is associated with neuroprotection, migration, and angiogenesis [53].

Thus, when studying the content of inflammatory mediators of the immune response in patients with combat mTBI, a total increase in their level in the peripheral blood serum was found, which corresponds to the literature data on the important role of the immune system in the course of TBI and the formation of its long-term consequences and complications [26, 29, 33, 54]. Modern scientific studies have obtained numerous data indicating the global role of the immune system both in the mechanisms of acute response and in the chronic course of TBI, which emphasizes the need to modulate neuroinflammation in the process of forming secondary trauma due to its uncontrolled development. At the same time, there is a lack of consensus on the methodology of TBI research in connection with the measurement of inflammatory cytokines in peripheral blood, which does not provide accurate differentiation of the causes of inflammation in patients who suffer multiple trauma during combat operations [32]. In view of this, studies of both peripheral and central content of immune response mediators are of particular importance, which is one of the virtues of this work.

Thus, the results of our study indicate the feasibility of comprehensive monitoring of central and peripheral inflammatory cytokine content to determine potential directions of adequate pathogenetic therapy even in

conditions of significantly distant consequences of mTBI in order to substantiate the possibility of returning servicemen to direct participation in combat operations, which is extremely relevant during war.

Against the background of the high modernity of the actual study, which was carried out using biological materials from participants and veterans of active hostilities in Ukraine, unfortunately, a certain drawback can be noted in the form of a relatively small size of the comparison groups and a limited spectrum of inflammatory cytokines, and the inability of determining neurotrophic factors (BDNF, VEGF, PDGF) in order to study the mechanisms of neuroplasticity in the process of structural and functional recovery of the CNS in patients with TBI. This is objectively related to limited funding for scientific research in a medical institution under the conditions of Russia's full-scale aggressive attack on Ukraine.

In the direction of future research, it seems appropriate to include clinical and immunological comparisons of the course of TBI, taking into account the neurosurgical treatment of comorbid pathology associated with mechanical damage during combat TBI.

Acknowledgments

The authors express their sincere gratitude to laboratory assistant Olha Kyrychenko for her impeccable contribution in the receipt, preparation, and storage of biological analytes, as well as in their systematization according to the research objectives and in the technical support of ELISA analysis, the preparation of the manuscript with constant stimulation and discussion of the work.

Disclosures

Conflicts of interest

The authors declare that they have no conflicts of interest.

Ethical approval

The work was carried out in accordance with the main provisions of the Declaration of Helsinki of the World Medical Association on the ethical principles of conducting scientific research involving human subjects, the Council of Europe Convention on Human Rights and Biomedicine. The study was approved by the Biomedical Ethics Committee of the SI «P. V. Voloshyn Institute of Neurology, Psychiatry and Narcology of the NAMS of Ukraine», which did not reveal any violations of ethical or legal standards during the study (Minutes No.12-a dated 27.12.2024).

Informed consent

Informed consent to participate in the study was obtained from all participants.

Funding

Not applicable.

References

1. Johnson VE, Stewart JE, Begbie FD, Trojanowski JQ, Smith DH, Stewart W. Inflammation and white matter degeneration persist for years after a single traumatic brain injury. Brain. 2013 Jan;136(Pt 1):28-42. doi: 10.1093/brain/aws322
2. Aungst SL, Kabadi SV, Thompson SM, Stoica BA, Faden AI. Repeated mild traumatic brain injury causes chronic neuroinflammation, changes in hippocampal synaptic plasticity, and associated cognitive deficits. J Cereb Blood Flow Metab. 2014 Jul;34(7):1223-32. doi: 10.1038/jcbfm.2014.75
3. Bloom GS. Amyloid-β and tau: the trigger and bullet in Alzheimer disease pathogenesis. JAMA Neurol. 2014 Apr;71(4):505-8. doi: 10.1001/jamaneurol.2013.5847
4. Blennow K, Brody DL, Kochanek PM, Levin H, McKee A, Ribbers GM, Yaffe K, Zetterberg H. Traumatic brain injuries. Nat Rev Dis Primers. 2016 Nov 17;2:16084. doi: 10.1038/nrdp.2016.84
5. Reams N, Eckner JT, Almeida AA, Aagesen AL, Giordani B, Paulson H, Lorincz MT, Kutcher JS. A Clinical Approach to the Diagnosis of Traumatic Encephalopathy Syndrome: A Review. JAMA Neurol. 2016 Jun 1;73(6):743-9. doi: 10.1001/jamaneurol.2015.5015
6. Mendez MF. What is the Relationship of Traumatic Brain Injury to Dementia? J Alzheimers Dis. 2017;57(3):667-681. doi: 10.3233/JAD-161002
7. Raza Z, Hussain SF, Ftouni S, Spitz G, Caplin N, Foster RG, Gomes RSM. Dementia in military and veteran populations: a review of risk factors-traumatic brain injury, post-traumatic stress disorder, deployment, and sleep. Mil Med Res. 2021 Oct 13;8(1):55. doi: 10.1186/s40779-021-00346-z
8. Bramlett HM, Dietrich WD. Long-Term Consequences of Traumatic Brain Injury: Current Status of Potential Mechanisms of Injury and Neurological Outcomes. J Neurotrauma. 2015 Dec 1;32(23):1834-48. doi: 10.1089/neu.2014.3352
9. Anthonymuthu TS, Kenny EM, Bayır H. Therapies targeting lipid peroxidation in traumatic brain injury. Brain Res. 2016 Jun 1;1640(Pt A):57-76. doi: 10.1016/j.brainres.2016.02.006
10. Dorsett CR, McGuire JL, DePasquale EA, Gardner AE, Floyd CL, McCullumsmith RE. Glutamate Neurotransmission in Rodent Models of Traumatic Brain Injury. J Neurotrauma. 2017 Jan 15;34(2):263-272. doi: 10.1089/neu.2015.4373
11. Jassam YN, Izzy S, Whalen M, McGavern DB, El Khoury J. Neuroimmunology of Traumatic Brain Injury: Time for a Paradigm Shift. Neuron. 2017 Sep 13;95(6):1246-1265. doi: 10.1016/j.neuron.2017.07.010
12. Simon DW, McGeachy MJ, Bayır H, Clark RS, Loane DJ, Kochanek PM. The far-reaching scope of neuroinflammation after traumatic brain injury. Nat Rev Neurol. 2017 Mar;13(3):171-191. doi: 10.1038/nrneurol.2017.13. Erratum in: Nat Rev Neurol. 2017 Sep;13(9):572. doi: 10.1038/nrneurol.2017.116
13. Booker J, Sinha S, Choudhari K, Dawson J, Singh R. Predicting functional recovery after mild traumatic brain injury: the SHEFBIT cohort. Brain Inj. 2019;33(9):1158-1164. doi: 10.1080/02699052.2019.1629626
14. Edwards KA, Gill JM, Pattinson CL, Lai C, Brière M, Rogers NJ, Milhorn D, Elliot J, Carr W. Interleukin-6 is associated with acute concussion in military combat personnel. BMC Neurol. 2020 May 25;20(1):209. doi: 10.1186/s12883-020-01760-x
15. Yamamoto EA, Koike S, Luther M, Dennis L, Lim MM, Raskind M, Pagulayan K, Iliff J, Peskind E, Piantino JA. Perivascular Space Burden and Cerebrospinal Fluid Biomarkers in US Veterans With Blast-Related Mild Traumatic Brain Injury. J Neurotrauma. 2024 Jul;41(13-14):1565-1577. doi: 10.1089/neu.2023.0505
16. Wojcik BE, Stein CR, Bagg K, Humphrey RJ, Orosco J. Traumatic brain injury hospitalizations of U.S. army soldiers deployed to Afghanistan and Iraq. Am J Prev Med. 2010 Jan;38(1 Suppl):S108-16. doi: 10.1016/j.amepre.2009.10.006
17. Boyle E, Cancelliere C, Hartvigsen J, Carroll LJ, Holm LW, Cassidy JD. Systematic review of prognosis after mild traumatic brain injury in the military: results of the International Collaboration on Mild Traumatic Brain Injury Prognosis. Arch Phys Med Rehabil. 2014 Mar;95(3 Suppl):S230-7. doi: 10.1016/j.apmr.2013.08.297
18. Kong LZ, Zhang RL, Hu SH, Lai JB. Military traumatic brain injury: a challenge straddling neurology and psychiatry. Mil Med Res. 2022 Jan 6;9(1):2. doi: 10.1186/s40779-021-

00363-y
19. McDonald SJ, O'Brien TJ, Shultz SR. Biomarkers add value to traumatic brain injury prognosis. Lancet Neurol. 2022 Sep;21(9):761-763. doi: 10.1016/S1474-4422(22)00306-4
20. Rodney T, Taylor P, Dunbar K, Perrin N, Lai C, Roy M, Gill J. High IL-6 in military personnel relates to multiple traumatic brain injuries and post-traumatic stress disorder. Behav Brain Res. 2020 Aug 17;392:112715. doi: 10.1016/j.bbr.2020.112715
21. Kossmann T, Hans VH, Imhof HG, Stocker R, Grob P, Trentz O, Morganti-Kossmann C. Intrathecal and serum interleukin-6 and the acute-phase response in patients with severe traumatic brain injuries. Shock. 1995 Nov;4(5):311-7. doi: 10.1097/00024382-199511000-00001
22. Hinson HE, Rowell S, Schreiber M. Clinical evidence of inflammation driving secondary brain injury: a systematic review. J Trauma Acute Care Surg. 2015 Jan;78(1):184-91. doi: 10.1097/TA.0000000000000468
23. Hernandez-Ontiveros DG, Tajiri N, Acosta S, Giunta B, Tan J, Borlongan CV. Microglia activation as a biomarker for traumatic brain injury. Front Neurol. 2013 Mar 26;4:30. doi: 10.3389/fneur.2013.00030
24. McKee CA, Lukens JR. Emerging Roles for the Immune System in Traumatic Brain Injury. Front Immunol. 2016 Dec 5;7:556. doi: 10.3389/fimmu.2016.00556
25. Ramlackhansingh AF, Brooks DJ, Greenwood RJ, Bose SK, Turkheimer FE, Kinnunen KM, Gentleman S, Heckemann RA, Gunanayagam K, Gelosa G, Sharp DJ. Inflammation after trauma: microglial activation and traumatic brain injury. Ann Neurol. 2011 Sep;70(3):374-83. doi: 10.1002/ana.22455
26. Gerber KS, Alvarez G, Alamian A, Behar-Zusman V, Downs CA. Biomarkers of Neuroinflammation in Traumatic Brain Injury. Clin Nurs Res. 2022 Sep;31(7):1203-1218. doi: 10.1177/10547738221107081
27. Puntambekar SS, Saber M, Lamb BT, Kokiko-Cochran ON. Cellular players that shape evolving pathology and neurodegeneration following traumatic brain injury. Brain Behav Immun. 2018 Jul;71:9-17. doi: 10.1016/j.bbi.2018.03.033
28. Needham EJ, Helmy A, Zanier ER, Jones JL, Coles AJ, Menon DK. The immunological response to traumatic brain injury. J Neuroimmunol. 2019 Jul 15;332:112-125. doi: 10.1016/j.jneuroim.2019.04.005
29. Yue JK, Kobeissy FH, Jain S, Sun X, Phelps RRL, Korley FK, Gardner RC, Ferguson AR, Huie JR, Schneider ALC, Yang Z, Xu H, Lynch CE, Deng H, Rabinowitz M, Vassar MJ, Taylor SR, Mukherjee P, Yuh EL, Markowitz AJ, Puccio AM, Okonkwo DO, Diaz-Arrastia R, Manley GT, Wang KKW. Neuroinflammatory Biomarkers for Traumatic Brain Injury Diagnosis and Prognosis: A TRACK-TBI Pilot Study. Neurotrauma Rep. 2023 Mar 24;4(1):171-183. doi: 10.1089/neur.2022.0060
30. Csuka E, Morganti-Kossmann MC, Lenzlinger PM, Joller H, Trentz O, Kossmann T. IL-10 levels in cerebrospinal fluid and serum of patients with severe traumatic brain injury: relationship to IL-6, TNF-alpha, TGF-beta1 and blood-brain barrier function. J Neuroimmunol. 1999 Nov 15;101(2):211-21. doi: 10.1016/s0165-5728(99)00148-4
31. Terreni L, De Simoni MG. Role of the brain in interleukin-6 modulation. Neuroimmunomodulation. 1998 May-Aug;5(3-4):214-9. doi: 10.1159/000026339
32. Malik S, Alnaji O, Malik M, Gambale T, Farrokhyar F, Rathbone MP. Inflammatory cytokines associated with mild traumatic brain injury and clinical outcomes: a systematic review and meta-analysis. Front Neurol. 2023 May 12;14:1123407. doi: 10.3389/fneur.2023.1123407
33. Lu J, Goh SJ, Tng PY, Deng YY, Ling EA, Moochhala S. Systemic inflammatory response following acute traumatic brain injury. Front Biosci (Landmark Ed). 2009 Jan 1;14(10):3795-813. doi: 10.2741/3489
34. Plog BA, Dashnaw ML, Hitomi E, Peng W, Liao Y, Lou N, Deane R, Nedergaard M. Biomarkers of traumatic injury are transported from brain to blood via the glymphatic system. J Neurosci. 2015 Jan 14;35(2):518-26. doi: 10.1523/JNEUROSCI.3742-14.2015
35. Weaver LC, Bao F, Dekaban GA, Hryciw T, Shultz SR, Cain DP, Brown A. CD11d integrin blockade reduces the systemic inflammatory response syndrome after traumatic brain injury in rats. Exp Neurol. 2015 Sep;271:409-22. doi: 10.1016/j.expneurol.2015.07.003
36. Geiko VV, Posokhov MF, Lemondzhava ZM. Features of immunological reactivity of patients with combat traumatic brain injury depending on its type and chronicity. Ukr Bull Psychoneurol. 2025;33,1(122):13-8. doi: 10.36927/2079-0325-V33-is1-2025-2
37. Luo J. TGF-β as a Key Modulator of Astrocyte Reactivity: Disease Relevance and Therapeutic Implications. Biomedicines. 2022 May 23;10(5):1206. doi: 10.3390/biomedicines10051206
38. Sofroniew MV. Astrocyte Reactivity: Subtypes, States, and Functions in CNS Innate Immunity. Trends Immunol. 2020 Sep;41(9):758-770. doi: 10.1016/j.it.2020.07.004
39. Escartin C, Galea E, Lakatos A, O'Callaghan JP, Petzold GC, Serrano-Pozo A, Steinhäuser C, Volterra A, Carmignoto G, Agarwal A, Allen NJ, Araque A, Barbeito L, Barzilai A, Bergles DE, Bonvento G, Butt AM, Chen WT, Cohen-Salmon M, Cunningham C, Deneen B, De Strooper B, Díaz-Castro B, Farina C, Freeman M, Gallo V, Goldman JE, Goldman SA, Götz M, Gutiérrez A, Haydon PG, Heiland DH, Hol EM, Holt MG, Iino M, Kastanenka KV, Kettenmann H, Khakh BS, Koizumi S, Lee CJ, Liddelow SA, MacVicar BA, Magistretti P, Messing A, Mishra A, Molofsky AV, Murai KK, Norris CM, Okada S, Oliet SHR, Oliveira JF, Panatier A, Parpura V, Pekna M, Pekny M, Pellerin L, Perea G, Pérez-Nievas BG, Pfrieger FW, Poskanzer KE, Quintana FJ, Ransohoff RM, Riquelme-Perez M, Robel S, Rose CR, Rothstein JD, Rouach N, Rowitch DH, Semyanov A, Sirko S, Sontheimer H, Swanson RA, Vitorica J, Wanner IB, Wood LB, Wu J, Zheng B, Zimmer ER, Zorec R, Sofroniew MV, Verkhratsky A. Reactive astrocyte nomenclature, definitions, and future directions. Nat Neurosci. 2021 Mar;24(3):312-325. doi: 10.1038/s41593-020-00783-4
40. Lee HG, Wheeler MA, Quintana FJ. Function and therapeutic value of astrocytes in neurological diseases. Nat Rev Drug Discov. 2022 May;21(5):339-358. doi: 10.1038/s41573-022-00390-x
41. Giovannoni F, Quintana FJ. The Role of Astrocytes in CNS Inflammation. Trends Immunol. 2020 Sep;41(9):805-819. doi: 10.1016/j.it.2020.07.007
42. Linnerbauer M, Wheeler MA, Quintana FJ. Astrocyte Crosstalk in CNS Inflammation. Neuron. 2020 Nov 25;108(4):608-622. doi: 10.1016/j.neuron.2020.08.012
43. Colombo E, Farina C. Astrocytes: Key Regulators of Neuroinflammation. Trends Immunol. 2016 Sep;37(9):608-620. doi: 10.1016/j.it.2016.06.006
44. Price BR, Johnson LA, Norris CM. Reactive astrocytes: The nexus of pathological and clinical hallmarks of Alzheimer's disease. Ageing Res Rev. 2021 Jul;68:101335. doi: 10.1016/j.arr.2021.101335
45. Patel RK, Prasad N, Kuwar R, Haldar D, Muneer PMA. Transforming growth factor-beta 1 signaling regulates neuroinflammation and apoptosis in mild traumatic brain injury. Brain Behav Immun. 2017 Aug;64:244-258. doi: 10.1016/j.bbi.2017.04.012
46. Diniz LP, Matias I, Siqueira M, Stipursky J, Gomes FCA. Astrocytes and the TGF-β1 Pathway in the Healthy and Diseased Brain: a Double-Edged Sword. Mol Neurobiol. 2019 Jul;56(7):4653-4679. doi: 10.1007/s12035-018-1396-y
47. Kandasamy M, Anusuyadevi M, Aigner KM, Unger MS, Kniewallner KM, de Sousa DMB, Altendorfer B, Mrowetz H, Bogdahn U, Aigner L. TGF-β Signaling: A Therapeutic Target to Reinstate Regenerative Plasticity in Vascular Dementia? Aging Dis. 2020 Jul 23;11(4):828-850. doi: 10.14336/AD.2020.0222
48. Koyama Y. Signaling molecules regulating phenotypic conversions of astrocytes and glial scar formation in damaged nerve tissues. Neurochem Int. 2014 Dec;78:35-42. doi: 10.1016/j.neuint.2014.08.005
49. Arranz AM, De Strooper B. The role of astroglia in Alzheimer's disease: pathophysiology and clinical

implications. Lancet Neurol. 2019 Apr;18(4):406-414. doi: 10.1016/S1474-4422(18)30490-3
50. Pekny M, Pekna M. Astrocyte reactivity and reactive astrogliosis: costs and benefits. Physiol Rev. 2014 Oct;94(4):1077-98. doi: 10.1152/physrev.00041.2013
51. McConnell HL, Li Z, Woltjer RL, Mishra A. Astrocyte dysfunction and neurovascular impairment in neurological disorders: Correlation or causation? Neurochem Int. 2019 Sep;128:70-84. doi: 10.1016/j.neuint.2019.04.005
52. Liddelow SA, Guttenplan KA, Clarke LE, Bennett FC, Bohlen CJ, Schirmer L, Bennett ML, Münch AE, Chung WS, Peterson TC, Wilton DK, Frouin A, Napier BA, Panicker N, Kumar M, Buckwalter MS, Rowitch DH, Dawson VL, Dawson TM, Stevens B, Barres BA. Neurotoxic reactive astrocytes are induced by activated microglia. Nature. 2017 Jan 26;541(7638):481-487. doi: 10.1038/nature21029
53. Li Z, Xiao J, Xu X, Li W, Zhong R, Qi L, Chen J, Cui G, Wang S, Zheng Y, Qiu Y, Li S, Zhou X, Lu Y, Lyu J, Zhou B, Zhou J, Jing N, Wei B, Hu J, Wang H. M-CSF, IL-6, and TGF-β promote generation of a new subset of tissue repair macrophage for traumatic brain injury recovery. Sci Adv. 2021 Mar 12;7(11):eabb6260. doi: 10.1126/sciadv.abb6260
54. Bouras M, Asehnoune K, Roquilly A. Immune modulation after traumatic brain injury. Front Med (Lausanne). 2022 Dec 1;9:995044. doi: 10.3389/fmed.2022.995044

Original article

Ukrainian Neurosurgical Journal. 2025;31(3):37-44
doi: 10.25305/unj.330933

Invasive monitoring of arterial blood pressure in cerebral arteries during thrombectomy

Andrii M. Netliukh [1,2], Andrian A. Sukhanov [1,2]

[1] Department of Neurology and Neurosurgery, Faculty of Postgraduate Education, Danylo Halytsky Lviv National Medical University, Lviv, Ukraine
[2] Department of Neurology and Vascular Neurosurgery, Municipal Non-Profit Enterprise "First Territorial Medical Association of Lviv", Lviv, Ukraine

Received: 26 May 2025
Accepted: 21 June 2025

Address for correspondence*: Andrian A. Sukhanov, Department of Neurology and Vascular Neurosurgery, Municipal Non-Profit Enterprise "First Territorial Medical Association of Lviv", 9 Ivan Mykolaychuk St., Lviv, 79000, Ukraine, email: sukhanov.andrian@gmail.com*

Objective: to assess the arterial blood pressure measured invasively in the internal carotid artery and distal to the site of thrombotic occlusion (in the middle cerebral artery) during mechanical thrombectomy in patients with acute ischemic stroke.

Materials and methods: In 2024, a total of 90 patients with acute cerebrovascular occlusion who underwent thrombectomy were examined. Data from 23 patients in whom intraoperative arterial pressure (AP) was measured invasively were analyzed. Patient age ranged from 44 to 81 years, with a mean age of 66.3±10.4 years. The majority of patients were male (61%). Stroke severity was assessed using the National Institutes of Health Stroke Scale (NIHSS), and functional outcomes were evaluated using the modified Rankin Scale (mRS) at discharge (0–3 points – favorable outcome, 4–6 points – unfavorable outcome). Ischemic changes were graded according to the Alberta Stroke Program Early CT Score (ASPECTS), with ≤7 points indicating extensive changes and ≥8 points indicating moderate changes.

Results: No statistically significant differences were found in AP levels in the internal carotid artery before and after thrombectomy depending on the degree of neurological deficit, volume of ischemic changes, or functional outcome ($p>0.1$). The mean AP measured distal to the site of occlusion was significantly higher in patients with NIHSS scores ≤15 compared to those with NIHSS scores>15 ((59.7±4.7) vs. (51.0±10.9) mm Hg, $p=0.02$), in patients with moderate ischemic changes ((58.5±5.4) vs. (44.3±11.9) mm Hg, $p=0.03$), and in those with a favorable functional outcome ((59.2±5.5) vs. (49.0±11.1) mm Hg, $p=0.02$). The mean AP in the internal carotid artery after thrombectomy was significantly higher in patients with hemorrhagic transformation ((114.4±9.0) vs. (100.4±13.4) mm Hg, $p=0.01$).

Conclusions: A correlation was found between the mean AP levels, measured invasively in intracranial arteries at various stages of mechanical thrombectomy for acute ischemic stroke, and stroke severity, infarct volume, development of hemorrhagic transformation, and functional outcome. These findings highlight the importance of investigating local hemodynamics to predict treatment outcomes in acute ischemic stroke and to explore personalized AP management strategies during thrombectomy and in the early postoperative period.

Keywords: *acute ischemic stroke; mechanical thrombectomy; cerebral perfusion pressure monitoring; hemorrhagic transformation; cerebral edema*

Stroke is often a leading cause of disability and remains one of the primary causes of mortality worldwide [1]. Over the past decade, a number of large clinical trials have confirmed the efficacy of mechanical thrombectomy (MT) compared to standard medical therapy, particularly intravenous thrombolysis using tissue plasminogen activator (tPA). The effectiveness of MT has been demonstrated in patients with acute ischemic stroke (AIS) caused by large vessel occlusion in the anterior circulation [2]. Despite similar clinical and radiological manifestations, MT outcomes may vary significantly among different patient groups [3]. Elevations in systolic or diastolic AP are observed in up to 80% of patients following AIS, even among those without a prior history of hypertension. This may reflect a stress response or a compensatory mechanism to maintain cerebral perfusion [4].

Contemporary studies have identified AP and collateral circulation as key factors in maintaining cerebral blood flow and influencing clinical outcomes [5]. Collaterals play a critical role in sustaining perfusion to brain regions distal to the arterial occlusion. They are particularly important in the acute phase of ischemic stroke prior to recanalization therapy [6].

The literature presents conflicting data on the relationship between baseline AP, collateral status, and the efficacy of endovascular treatment of ischemic stroke. While some researchers suggest a compensatory

benefit of elevated AP [7], others report a detrimental effect [8]. Most studies have focused on systemic AP measurements, whereas the hemodynamic state of cerebral vessels distal to the thrombus remains underexplored [9]. This local pressure may be vital to understanding the pathophysiological processes in the ischemic zone and could help predict the success of endovascular interventions and patients' functional recovery [10]. Invasive intra-arterial AP monitoring is standard practice in intensive care units abroad and is also frequently utilized during surgery to obtain beat-to-beat AP readings. For critically ill patients, intra-arterial monitoring facilitates frequent blood sampling and assists in the differential diagnosis of certain pathological conditions. It is an additional tool that experienced clinicians can use to improve patient management [11].

Special attention has been given to the role of AP in the development of hemorrhagic transformation (HT) following reperfusion therapy. According to the literature, both excessive hypertension and rapid AP reduction after reperfusion are associated with an increased risk of intracerebral hemorrhage [12]. Data from E.A. Mistry et al. (2019) indicate that systolic AP>180 mmHg within the first 24 hours after MT is associated with a higher risk of symptomatic HT and poorer functional outcomes [13]. Other studies emphasize that not only absolute AP values but also AP variability are important: increased variability may disrupt the blood–brain barrier and contribute to secondary brain injury [14].

Establishing correlations between hemodynamic parameters and clinical as well as radiological indicators (infarct volume, severity of neurological deficit, collateral status, and presence of HT may, in our view, provide a better understanding of the mechanisms of cerebral autoregulation, collateral blood flow, and changes in blood–brain barrier permeability during ischemic injury. The obtained data may contribute to the individualization of AP management strategies during the in-hospital stage, taking into account local cerebral perfusion pressure, the degree of neurological deficit, and the risk of HT.

Objective: to assess the level of arterial pressure measured invasively in the internal carotid artery and distal to the site of thrombotic occlusion (in the middle cerebral artery) during mechanical thrombectomy in patients with acute ischemic stroke.

Materials and methods

Study participants

In 2024, a total of 90 patients with acute cerebrovascular occlusion who underwent mechanical thrombectomy were examined. Data from 23 patients, in whom intraoperative invasive AP monitoring was performed, were analyzed. Patient age ranged from 44 to 81 years, with a mean age of 66.3±10.4 years. The majority of participants were male (61%).

Informed and voluntary written consent for participation in the study and publication of the data was obtained from all patients or their legal representatives. The study was approved by the Ethics Committee of the Municipal Non-Profit Enterprise "First territorial medical association of Lviv" (Minutes No. 13, dated 08.09.2022). The research complies with the principles of the Declaration of Helsinki.

Inclusion Criteria

The study included patients with AIS confirmed by computed tomography data (Alberta Stroke Program Early CT Score [ASPECTS] ≥ 6 points), who underwent MT, and in whom invasive AP monitoring in the internal carotid artery (ICA) and distal to the occlusion site was technically feasible.

Group Characteristics

The severity of patients' condition at admission was assessed using the National Institutes of Health Stroke Scale (NIHSS). Based on NIHSS scores, patients were divided into groups with moderately severe (NIHSS ≤15 points, 10 patients) and severe (NIHSS>15 points, 13 patients) neurological deficits. A score<4 points on the NIHSS is considered a minor stroke, 5–15 points indicate a moderate stroke, 16–20 points a severe stroke, and ≥21 points a very severe stroke.

To diagnose ischemic stroke, all patients underwent non-contrast brain CT using a Philips Ingenuity CT 2019 scanner (Philips Healthcare [Suzhou] Co., Ltd., Suzhou, China). Early ischemic changes were assessed using the Alberta Stroke Program Early CT Score (ASPECTS), where a score of 10 indicates the absence of ischemic changes, and 0 indicates diffuse ischemia throughout the entire middle cerebral artery (MCA) territory. The site of arterial occlusion was also determined. Based on CT findings, patients were stratified into groups with pronounced (ASPECTS ≤7, 6 patients) and moderate (ASPECTS ≥8, 17 patients) ischemic changes.

Following thrombectomy, the degree of reperfusion was assessed using the expanded Thrombolysis in Cerebral Infarction (eTICI) scale: 0 – no reperfusion; 3 – complete reperfusion with filling of all distal branches.

Functional outcomes were evaluated prior to hospital discharge using the mRS, classified as favorable (scores 0–3, 13 patients) or unfavorable (scores 4–6, 10 patients). The mRS is a simplified universal tool for assessing patient independence and disability during medical rehabilitation and at 90–115 days post-stroke. A score of 0 indicates no symptoms; a score of 5 indicates severe disability; and 6 indicates death.

The presence of HT was determined by control CT, performed in all patients 24 hours after the procedure or earlier in cases of clinical deterioration by ≥4 NIHSS points.

Invasive mean arterial pressure (MAP) values were analyzed in patient groups stratified by clinical severity, functional outcome, infarct size, and presence of HT.

Study design

In all cases, direct intraoperative AP measurements were performed in the C_1-segment of the internal carotid artery (ICA) proximal to the site of occlusion, both before and after thrombectomy (ICA-pre and ICA-post, respectively), and in the M_1-segment of the MCA at the occlusion site prior to MT (MCA-pre) (***Fig. 1***).

This article contains some figures that are displayed in color online but in black and white in the print edition.

Invasive AP monitoring was performed under fluoroscopic guidance in the extracranial segment of the main artery (C1 segment of the ICA) using a standard aspiration catheter (length – 132 cm; inner diameter – 1.80 mm) and in the MCA distal to the thrombus using a standard microcatheter (length – 153 cm; inner diameter – 0.81 mm) prior to the deployment of a stent retriever. The results were recorded using an HP Engage Flex Pro portable computer (HP Inc., USA) connected to a compatible pressure transducer (part of the Philips Azurion 7 angiographic hemodynamic monitoring system; Philips Medical Systems Nederland B.V., Best, Netherlands). After calibration, the transducer was connected via a fluid-filled line to the catheter cannula. Calibration of the sensor was performed before each measurement (***Fig. 2***).

A **B** **C**

Fig. 1. Catheter positioning during invasive AP measurement: A – in the internal carotid artery (ICA) before thrombectomy (via aspiration catheter); B – in the middle cerebral artery (MCA) distal to the thrombus (via microcatheter); C – in the ICA after thrombectomy. Arrows indicate the location of the distal catheter markers

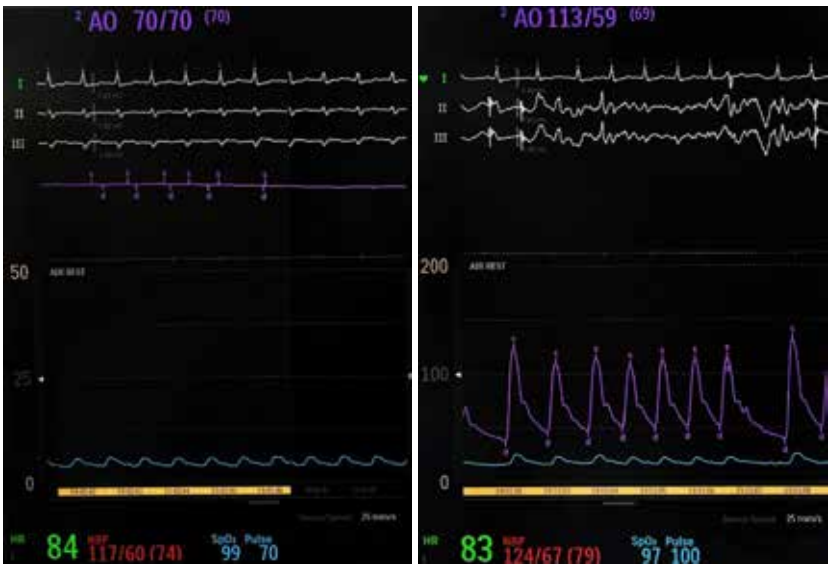

A **B**

Fig. 2. Invasive AP waveform recording: A – distal to the thrombus in the middle cerebral artery (MCA); B – proximal to the thrombus in the internal carotid artery (ICA)

Statistical analysis

Statistical analysis of the obtained data was performed using the software package "Statistica 7.0" (StatSoft Inc., USA). Descriptive statistics were presented as means (M) and standard deviations (SD) or 95% confidence intervals (95% CI) for quantitative variables. Prior to group comparisons, the normality of data distribution was assessed using the Shapiro–Wilk test. All distributions demonstrated no statistically significant deviation from normality ($p>0.05$), allowing the use of parametric methods. Welch's t-test was applied to compare means between two independent groups, as it accounts for unequal variances and sample sizes. Paired t-tests (Student's t-test for dependent samples) were used to compare pre- and post-intervention values within the same subjects. A p-value of <0.05 was considered statistically significant.

Results

Invasive blood pressure monitoring (***Table 1***) revealed that the MAP in the ICA prior to achieving reperfusion during thrombectomy was 113.9±16.5 mmHg, while after reperfusion it decreased to 103.6±13.7 mmHg. A paired t-test showed a statistically significant difference between these values (t=2.31, p=0.03), indicating a reduction in MAP following the procedure. Additionally, the MAP at the occlusion site (MCA-pre) was 54.8±9.7 mmHg. Comparison of MAP between the ICA and the occlusion site demonstrated a significantly lower pressure in the occluded segment both before and after reperfusion ($p<0.001$) (***Fig. 3***).

Table 1. Invasive blood pressure measurements, mmHg (M±SD)

Group	Systolic AP	Diastolic AP	MAP
ICA-pre	147,2 ± 18,0	97,2 ± 23,1	113,9 ± 16,5
ICA-post	140,8 ± 29,4	85,0 ± 13,9	103,6 ± 13,7
MCA-pre	66,0 ± 14,8	49,0 ± 12,2	54,8 ± 9,7

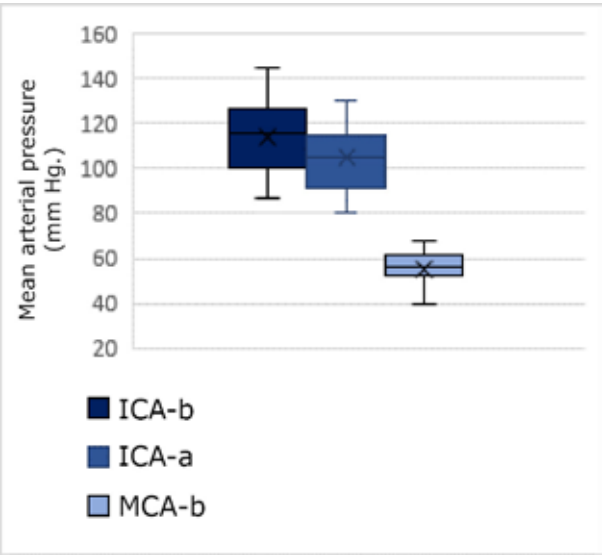

Fig. 3. Comparison of invasive arterial pressure values by measurement site

The MAP in the ICA prior to reperfusion in the group of patients with moderately severe neurological deficit (NIHSS ≤15 points, n=10) was 119.5±16.7 mmHg (95% CI: 108.7–130.3 mmHg), whereas in the group with severe neurological deficit (NIHSS>15 points, n=13), it was 109.2±14.1 mmHg (95% CI: 100.8–117.7 mmHg). The difference between the groups was not statistically significant (t=1.60, p=0.13).

Following reperfusion, MAP in the ICA for the NIHSS ≤15 group was 107.8±11.7 mmHg (95% CI: 99.9–115.7 mmHg), while for the NIHSS>15 group it was 101.6±14.1 mmHg (95% CI: 94.1–109.1 mmHg). According to Welch's unequal variance t-test, the difference was not statistically significant (t=1.06, p=0.3).

The mean AP at the occlusion site in the group with NIHSS ≤15 was 59.7±4.7 mmHg (95% CI: 56.3–63.1 mmHg), whereas in the NIHSS>15 group it was 51.0±10.9 mmHg (95% CI: 44.8–57.2 mmHg). This difference was statistically significant (t=2.57, $p \approx 0.02$), with a mean difference of 8.62 mmHg (95% CI: 1.48–15.77 mmHg), suggesting a probable association between local perfusion pressure and the degree of neurological impairment (***Fig. 4***).

When comparing patients with pronounced ischemic changes (ASPECTS ≤7 points, n=6) and those with moderate changes (ASPECTS ≥8 points, n=17), no statistically significant differences in MAP values were observed in the ICA prior to thrombectomy (107.5±15.6 mmHg; 95% CI: 92.0–123.1 mmHg vs. 117.0±16.5 mmHg; 95% CI: 108.5–125.5 mmHg; t=–1.30, p=0.22) or after thrombectomy (101.2±15.3 mmHg; 95% CI: 85.6–116.8 mmHg vs. 106.4±13.4 mmHg; 95% CI: 99.4–113.4 mmHg; t=–0.68, p=0.51).

Analysis of MAP distal to the occlusion site revealed a statistically significant difference: in the group with pronounced ischemic changes, AP was lower (44.3±11.9 mmHg; 95% CI: 32.6–56.0 mmHg) compared to the group with moderate changes (58.5±5.4 mmHg; 95% CI: 55.6–61.4 mmHg; t=–2.82, p=0.03), with a mean difference of 14.1 mmHg (95% CI: 1.73–26.54 mmHg). This may indicate the influence of altered local hemodynamics distal to the occlusion site on the development of ischemic changes, and suggest that more severe flow impairment contributes to greater ischemic injury (***Fig. 5***).

It was also found that the MAP in the ICA prior to reperfusion during thrombectomy was slightly higher in patients with a favorable functional outcome (mRS 0–3 points, n=13) — 118.3±15.9 mmHg (95% CI: 108.9–127.7 mmHg), compared to 110.7±13.3 mmHg (95% CI: 101.3–120.1 mmHg) in patients with an unfavorable outcome (mRS 4–6 points, n=10); however, the difference was not statistically significant (t=–1.34, p=0.19).

After reperfusion, MAP in the ICA did not differ significantly between groups — 107.5±13.1 mmHg (95% CI: 100.0–115.1 mmHg) in the mRS 0–3 group and 101.7±13.4 mmHg (95% CI: 92.6–110.8 mmHg) in the mRS 4–6 group (t=–1.09, p=0.28); the difference did not reach statistical significance.

In contrast, MAP distal to the occlusion site was significantly higher in patients with a favorable outcome — 59.2±5.5 mmHg (95% CI: 55.6–62.8 mmHg), compared to 49.0±11.1 mmHg (95% CI: 40.9–57.1 mmHg) in those with an unfavorable outcome. This difference was statistically significant (t=–2.67, p=0.02),

with a mean difference of 10.2 mmHg (95% CI: 1.92–18.54 mmHg), indicating a potential association between local perfusion pressure prior to reperfusion and patients' final functional status (***Fig. 6***).

It was found that prior to reperfusion during thrombectomy, MAP did not significantly differ between patients who developed HT (n=7) and those who did not (n=16). In the HT group, MAP was 119.3±11.9 mmHg (95% CI: 106.86–131.72 mmHg), compared to 112.7±20.1 mmHg (95% CI: 102.23–123.14 mmHg) in the non-HT group (t=0.86, p=0.41), indicating no significant differences in hemodynamic parameters prior to thrombectomy.

After thrombectomy, a statistically significant difference was observed: patients with HT had substantially higher MAP — 114.4±9.0 mmHg (95% CI: 104.53–124.33 mmHg), compared to 100.4±13.4 mmHg (95% CI: 91.04–109.84 mmHg) in the non-HT group (t=2.93, p=0.01). The mean difference was 13.99 mmHg (95% CI: 3.97–23.99 mmHg), suggesting that elevated AP in the ICA after thrombectomy was associated with an increased risk of HT.

Analysis of MAP distal to the occlusion site revealed no statistically significant differences between groups: 52.0±7.4 mmHg (95% CI: 44.59–59.41 mmHg) in the HT group vs. 55.1±10.4 mmHg (95% CI: 49.24–60.87 mmHg) in the non-HT group (t=–0.78, p=0.45). This may indicate that the critical factor is the post-intervention AP in the ICA, which reflects the impact of reperfusion on the blood–brain barrier (***Fig. 7***).

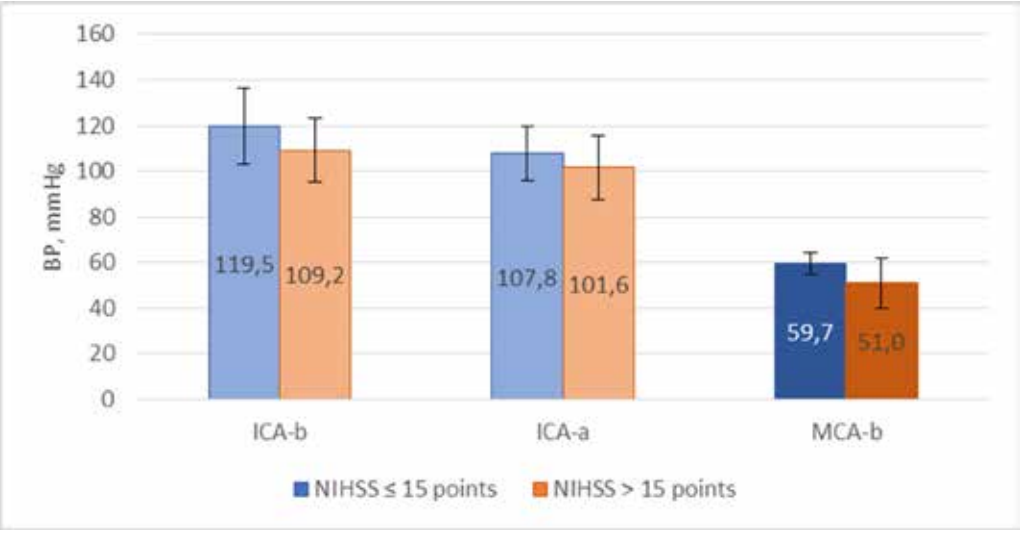

Fig. 4. Invasive MAP measurements in the proximal segments of the ICA before and after reperfusion (ICA-pre and ICA-post, respectively), and in the MCA distal to the occlusion site (MCA-pre), in groups with moderately severe (NIHSS ≤15 points) and severe (NIHSS>15 points) neurological deficit

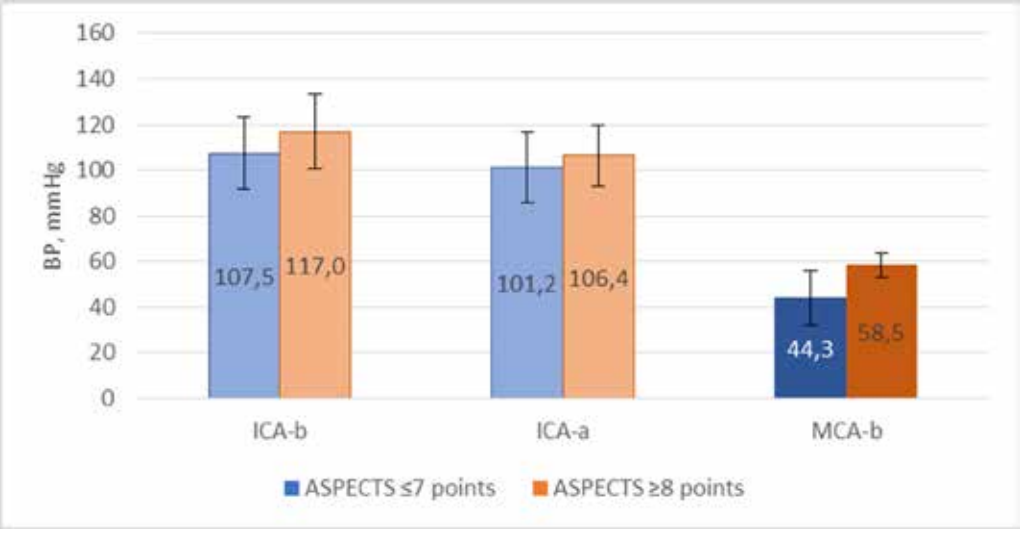

Fig. 5. Invasive MAP measurements in the proximal segments of the ICA before and after thrombectomy (ICA-pre and ICA-post, respectively), and in the middle cerebral artery distal to the occlusion site (MCA-pre), in groups with pronounced (ASPECTS ≤7 points) and moderate (ASPECTS ≥8 points) ischemic changes

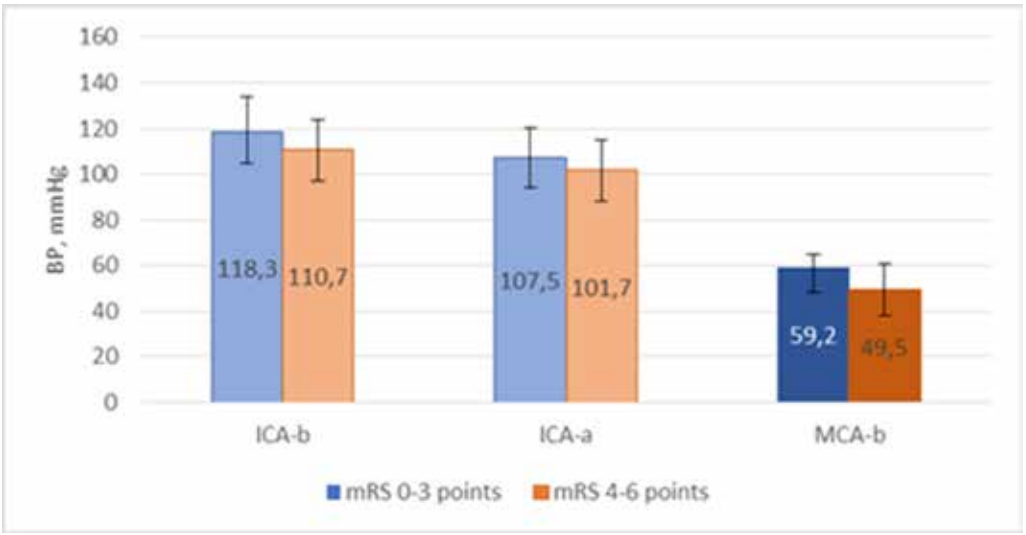

Fig. 6. Invasive MAP measurements in the proximal segments of the internal carotid artery before and after thrombectomy (ICA-pre and ICA-post, respectively), and in the MCA at the occlusion site (MCA-pre), in groups with favorable (mRS 0–3 points) and unfavorable (mRS 4–6 points) functional outcomes

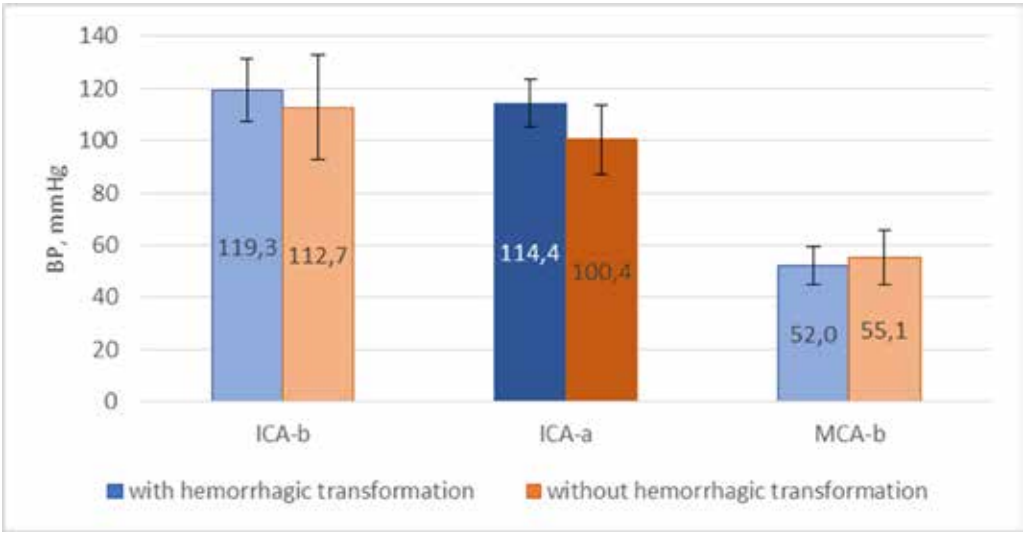

Fig. 7. Invasive MAP measurements in the proximal segments of the ICA before and after thrombectomy (ICA-pre and ICA-post, respectively) and in the MCA at the site of occlusion (MCA-pre) in patients with and without hemorrhagic transformation

Discussion

Despite significant advances in the treatment of AIS using MT, the role of local hemodynamics in the region of distal hypoperfusion remains insufficiently studied. Most studies are limited to systemic non-invasive AP measurements, which may not accurately reflect the true perfusion pressure in the penumbra area near the site of occlusion [15]. Invasive MAP measurements and the assessment of hemodynamic parameters obtained from different segments of intra- and extracranial arteries provide additional objective information about cerebral perfusion pressure during endovascular neuroradiological interventions [16].

Recent experimental studies have demonstrated that AP measurements in vessels distal to the occlusion more accurately reflect local perfusion and may reveal significant pressure gradients that remain hidden during systemic measurements [9]. This is of particular importance, as adequate perfusion pressure in the at-risk area can delay infarct progression and preserve neuronal viability in the penumbra [17]. Furthermore, impaired cerebral autoregulation during AIS may lead to discrepancies between local AP and values obtained through non-invasive techniques.

Cerebral blood flow autoregulation, which typically maintains stable cerebral perfusion within a MAP range of 50–150 mmHg, becomes ineffective during acute ischemia, especially in the presence of marked systemic hypotension or hypertension [18]. The status of collateral circulation is a critical modifier of hemodynamics at the

level of thrombosis. Well-developed collateral pathways can sustain higher perfusion pressure in distal vessels and thereby reduce infarct core volume, as supported by observations showing that patients with better collateral status had smaller infarcts and more favorable functional outcomes [19]. However, direct invasive measurements at the site of occlusion remain limited due to technical challenges and the risks associated with additional manipulations during MT. Initial clinical series have demonstrated that this technique is both feasible and safe, provided appropriate equipment and experienced teams are available, and may offer valuable insights for tailoring individualized AP management strategies during and after the procedure [20].

The AP distal to the occlusion site may be influenced not only by the efficiency of collateral circulation but also by thrombus permeability—such as residual lumen or porosity. In our study, perfusion through the thrombus was not assessed using CT perfusion imaging or contrast angiography. Therefore, the recorded values should be interpreted as the cumulative result of collateral blood flow and potential residual blood flow through the thrombus. This constitutes a limitation of our study and necessitates further investigation in larger cohorts.

According to the classical Cushing triad, pronounced ischemia and elevated intracranial pressure are expected to trigger a compensatory increase in systemic AP. However, in our study, patients with marked ischemic changes or unfavorable functional outcomes exhibited lower MAP in the distal hypoperfusion zone. This discrepancy may be attributed to the fact that MAP at the site of occlusion is determined not only by the level of systemic hypertension but primarily by the status of collateral circulation and thrombus permeability. Inadequate collateral supply during massive ischemia leads to a significant reduction in distal perfusion pressure, even in the presence of elevated systemic AP. Moreover, the Cushing triad typically manifests during later stages of severe cerebral edema and may not be evident in the acute phase of ischemic stroke.

High AP in the post-reperfusion period may be associated with an increased risk of HT. An elevation in systolic AP, particularly within the first 24 hours following endovascular intervention, can lead to hyperperfusion states, wherein disruption of the blood–brain barrier results in hemorrhage into previously ischemic tissue. Some authors emphasize that not only absolute AP values, but also AP variability, play a significant role in the pathogenesis of HT [12]. Post-reperfusion BP elevation may serve either as a compensatory mechanism to maintain perfusion of the ischemic penumbra or as a marker of severe underlying pathology, including impaired cerebral autoregulation. In some cases, abrupt AP fluctuations or sustained hypertension can cause mechanical damage to the vascular wall and reduce the adhesive properties of endothelial cells, thereby increasing the risk of HT [21]. Individual patient characteristics, such as a history of hypertension or reduced vascular elasticity, may influence the extent to which post-thrombectomy AP contributes to HT. Recurrent AP elevations can lead to structural remodeling of the vascular system, reducing the vessels' ability to adapt to reperfusion and making them more vulnerable to damage under hyperperfusion conditions [22].

Thus, elevated AP levels and significant variability in the post-reperfusion period are likely important risk factors for the development of HT, as confirmed by our study ($p<0.05$). Although Welch's t-test—appropriate for groups with unequal sizes and variances—was used for comparisons, interpretation of the results must be approached with caution due to the relatively small number of patients in the subgroup with ASPECTS ≤7 (n=6), which may limit the statistical power of the analysis. A similar limitation applies to the subgroup of patients who developed HT (n=7), where the small sample size may affect the reliability of the conclusions.

Of particular interest is the observed pattern: higher AP at the site of occlusion was associated with favorable functional outcomes, whereas excessive AP elevation in the ICA after reperfusion was linked to the occurrence of HT. This dual role of AP underscores the complex pathophysiology: moderately elevated local pressure before reperfusion supports collateral circulation and preserves penumbral viability, while excessive systemic pressure following restoration of flow may lead to hyperperfusion, blood–brain barrier disruption, and secondary hemorrhage. Therefore, a balanced approach to AP control during and after thrombectomy is essential, taking into account individual collateral reserve and the condition of brain parenchyma [23].

Although elevated AP is a common finding in AIS, its prognostic significance remains insufficiently studied. It remains unclear whether AP elevation is a direct cause of HT or merely a marker of severe ischemic injury and impaired autoregulation. This uncertainty highlights the need for further studies evaluating AP dynamics during and after thrombectomy and their relationship to HT. While modern techniques have shifted the paradigm of acute stroke treatment and are now considered standard care, optimal hemodynamic management strategies in patients with AIS remain unresolved [24]. Progress in this area may facilitate personalized BP control in interventional neurosurgery, reduce complication rates, and improve functional outcomes for patients with AIS.

Conclusions

1. Associations were identified between mean arterial pressure, measured invasively in intracranial arteries at different stages of mechanical thrombectomy for acute ischemic stroke, and stroke severity and volume, the occurrence of hemorrhagic transformation, and functional outcomes.

2. Our findings underscore the importance of investigating local hemodynamics to predict treatment outcomes in acute ischemic stroke and to develop personalized blood pressure management strategies during thrombectomy and in the early postoperative period.

Disclosure

Conflict of interest

The authors declare no conflicts of interest.

Ethical standards

All procedures performed on patients in the course of this study were conducted in accordance with the ethical standards of the institutional and national research ethics committees, the 1964 Helsinki Declaration and its later amendments, or comparable ethical standards.

Informed consent

Informed consent was obtained from each individual participant.

Funding

This research received no external funding or sponsorship.

References

1. Licher S, Darweesh SKL, Wolters FJ, Fani L, Heshmatollah A, Mutlu U, et al. Lifetime risk of common neurological diseases in the elderly population. J Neurol Neurosurg Psy-chiatry. 2019 Feb;90(2):148-156. doi: 10.1136/jnnp-2018-318650
2. Li H, Ye SS, Wu YL, et al. Predicting mortality in acute ischaemic stroke treated with mechanical thrombectomy: analysis of a multicentre prospective registry. BMJ Open. 2021 Apr 1;11(4):e043415. doi: 10.1136/bmjopen-2020-043415
3. Nogueira RG, Jadhav AP, Haussen DC, et al. Thrombectomy 6 to 24 Hours after Stroke with a Mismatch between Deficit and Infarct. N Engl J Med. 2018 Jan 4;378(1):11-21. doi: 10.1056/NEJMoa1706442
4. Kvistad CE, Oygarden H, Logallo N, Thomassen L, Waje-Andreassen U, Moen G, Naess H. A stress-related explanation to the increased blood pressure and its course following ischemic stroke. Vasc Health Risk Manag. 2016 Nov 11;12:435-442. doi: 10.2147/VHRM.S109032
5. Liebeskind DS, Saber H, Xiang B, et al. Collateral Circulation in Thrombectomy for Stroke After 6 to 24 Hours in the DAWN Trial. Stroke. 2022 Mar;53(3):742-748. doi: 10.1161/STROKEAHA.121.034471
6. Chatterjee D, Nagarajan K, Narayan SK, Narasimhan RL. Regional leptomeningeal collateral score by computed tomographic angiography correlates with 3-month clinical outcome in acute ischemic stroke. Brain Circ. 2020 Jun 26;6(2):107-115. doi: 10.4103/bc.bc_55_19
7. Kaloss AM, Theus MH. Leptomeningeal anastomoses: Mechanisms of pial collateral remodeling in ischemic stroke. WIREs Mech Dis. 2022 Jul;14(4):e1553. doi: 10.1002/wsbm.1553
8. Malhotra K, Goyal N, Katsanos AH, et al. Association of Blood Pressure With Outcomes in Acute Stroke Thrombectomy. Hypertension. 2020 Mar;75(3):730-739. doi: 10.1161/HYPERTENSIONAHA.119.14230
9. Spence JD. Blood Pressure Gradients in the Brain: Their Importance to Understanding Pathogenesis of Cerebral Small Vessel Disease. Brain Sci. 2019 Jan 23;9(2):21. doi: 10.3390/brainsci9020021
10. Albers GW, Marks MP, Kemp S, et al. Thrombectomy for Stroke at 6 to 16 Hours with Selection by Perfusion Imaging. N Engl J Med. 2018 Feb 22;378(8):708-718. doi: 10.1056/NEJMoa1713973
11. Shevaga VM, Netliukh AM, Kobyletskyi OYa, Salo VM. Invasive blood pressure monitoring during endovascular embolization of intracranial arterial aneurysms. Ukr Neurosurg J. 2015;(1):59–63. doi: 10.25305/unj.42709
12. Kim TJ, Park HK, Kim JM, et al. Blood pressure variability and hemorrhagic transformation in patients with successful recanalization after endovascular recanalization therapy: A retrospective observational study. Ann Neurol. 2019 Apr;85(4):574-581. doi: 10.1002/ana.25434
13. Mistry EA, Sucharew H, Mistry AM, et al. Blood Pressure after Endovascular Therapy for Ischemic Stroke (BEST): A Multicenter Prospective Cohort Study. Stroke. 2019 Dec;50(12):3449-3455. doi: 10.1161/STROKEAHA.119.026889
14. Maïer B, Delvoye F, Labreuche J, et al. Impact of Blood Pressure After Successful Endovascular Therapy for Anterior Acute Ischemic Stroke: A Systematic Review. Front Neurol. 2020 Oct 29;11:573382. doi: 10.3389/fneur.2020.573382
15. Jansen IG, Mulder MJ, Goldhoorn RB, et al. Impact of single phase CT angiography collateral status on functional outcome over time: results from the MR CLEAN Registry. J Neurointerv Surg. 2019 Sep;11(9):866-873. doi: 10.1136/neurintsurg-2018-014619
16. Shevaga VM, Netlyukh AM, Paienok AV, Kobyletskyi OYa, Salo VM, Matolinets NV. Monitoring of pressure in different segments of cerebral arteries as a method of cerebral perfusion control in surgery of intracranial arterial aneurysms. Ukr Interv Neuroradiol Surg. 2016;(2(16)):43–50.
17. Liebeskind DS, Tomsick TA, Foster LD, et al. Collaterals at angiography and outcomes in the Interventional Management of Stroke (IMS) III trial. Stroke. 2014 Mar;45(3):759-64. doi: 10.1161/STROKEAHA.113.004072
18. Nogueira RC, Beishon L, Bor-Seng-Shu E, Panerai RB, Robinson TG. Cerebral Autoregulation in Ischemic Stroke: From Pathophysiology to Clinical Concepts. Brain Sci. 2021 Apr 16;11(4):511. doi: 10.3390/brainsci11040511
19. Anadani M, Finitsis S, Clarençon F, et al. Collateral status reperfusion and outcomes after endovascular therapy: insight from the Endovascular Treatment in Ischemic Stroke (ETIS) Registry. J Neurointerv Surg. 2022 Jun;14(6):551-557. doi: 10.1136/neurintsurg-2021-017553
20. Varela LB, Díaz Menai S, Escobar Liquitay CM, Burgos MA, Ivaldi D, Garegnani L. Blood pressure management in reperfused ischemic stroke. Cochrane Database Syst Rev. 2025 Mar 4;3(3):CD016085. doi: 10.1002/14651858.CD016085
21. Li X, Simo L, Zhao Q, Kim EG, Ding Y, Geng X. Endothelial Cells and the Blood-Brain Barrier: Critical Determinants of Ineffective Reperfusion in Stroke. Eur J Neurosci. 2025 Feb;61(3):e16663. doi: 10.1111/ejn.16663
22. De Georgia M, Bowen T, Duncan KR, Chebl AB. Blood pressure management in ischemic stroke patients undergoing mechanical thrombectomy. Neurol Res Pract. 2023 Mar 30;5(1):12. doi: 10.1186/s42466-023-00238-8
23. Cherenko TM, Heletiuk YL. Functional recovery in patients with acute ischemic stroke and its dependence on the blood pressure variability. Ukr Sci Med Youth J. 2018;105(1):11–16. doi: 10.32345/USMYJ.1(105).2018.11-16
24. Lylyk P, Netliukh A, Kobyletskyi O, Holub O, Sukhanov A. The influence of vessel curvature and thrombus composition on the effectiveness and outcomes of thrombectomy in the case of acute ischemic stroke. Proc Shevchenko Sci Soc Med Sci. 2023 Dec.22;72(2). doi: 10.25040/ntsh2023.02.12

Original article

Ukrainian Neurosurgical Journal. 2025;31(3):45-57
doi: 10.25305/unj.330291

Long-term implant-related complications following anterior-only stabilization of thoracolumbar junction injuries: a radiological and clinical analysis

Oleksii S. Nekhlopochyn [1], Muhammad Jehanzeb [2], Vadim V. Verbov [3]

[1] Spine Surgery Department, Romodanov Neurosurgery Institute, Kyiv, Ukraine
[2] Department of Neurosurgery, Punjab Institute of Neurosciences, Lahore, Pakistan
[3] Restorative Neurosurgery Department, Romodanov Neurosurgery Institute, Kyiv, Ukraine

Received: 19 May 2025
Accepted: 22 June 2025

Address for correspondence*:*
Oleksii S. Nekhlopochyn, Spine Surgery Department, Romodanov Neurosurgery Institute, 32 Platona Maiborody st., Kyiv, 04050, Ukraine, e-mail: AlexeyNS@gmail.com

Objective: To evaluate the long-term implant-related complications following anterior-only stabilization of traumatic thoracolumbar injuries and to identify structural and radiological patterns associated with construct failure.

Materials and methods: A retrospective multicenter study was conducted at two neurosurgical institutions (Kyiv, Ukraine; Lahore, Pakistan) between 2000 and 2023. Sixteen patients who underwent anterior stabilization at T11–L2 and developed mechanical complications ≥5 years postoperatively were included. Radiographic analysis (CT, X-ray) assessed signs of construct instability, segmental kyphosis (modified Cobb method), global sagittal balance (SVA), and bone mineral density (Hounsfield units, HU). Neurological status was graded using the ASIA scale; pain was assessed via VAS. A complication severity score was developed based on the type of implant failure. Statistical analysis was performed using R version 4.0.5.

Results: The most frequent complications were screw-related failures (87.5%), plate migration (68.8%), and cage subsidence/displacement (31.3%). A direct correlation was observed between the severity of structural failure and kyphotic deformity: the median Cobb angles for high-severity cases reached 57°. Global sagittal imbalance (SVA>50 mm) was present in 31.3% of patients, primarily among those with the most severe failures. Neurological decline occurred in 25% of cases, exclusively in the presence of marked kyphosis or implant migration. A bone density < 135 HU was associated with a higher risk of earlier complication onset (HR = 2.83; p = 0.068). Pain intensity showed only a weak correlation with structural deformity.

Conclusions: Anterior-only stabilization at the thoracolumbar junction provides effective decompression and anterior column support but carries a risk of delayed mechanical complications, particularly in the absence of posterior reinforcement. The cantilever effect remains a key biomechanical vulnerability. Patients with HU < 135 should be considered at an elevated risk. A tailored surgical strategy, meticulous implant positioning, and long-term radiological surveillance are critical. In cases with poor bone quality or suspected PLC injury, posterior stabilization may offer superior long-term outcomes.

Keywords: *thoracolumbar junction; anterior stabilization; implant-related complications; cage subsidence; segmental kyphosis; bone mineral density; cantilever effect*

Introduction

Surgical treatment of thoracolumbar junction injuries is influenced by a broad spectrum of factors, including fracture morphology, neurological status, patient-specific anatomical conditions, and surgeon preference [1, 2]. The primary objective in managing such injuries is to achieve effective decompression of neural elements while restoring or maintaining spinal stability and alignment, ideally with the minimal number of segments involved in fixation [3].

Advancements in surgical techniques and implant technology have enabled the reliable use of short-segment stabilization using either anterior or posterior approaches. Single-stage procedures through either approach are now widely considered viable strategies, offering a compromise between stability, invasiveness, and decompression efficacy [4].

The thoracolumbar junction is considered a biomechanically vulnerable region due to transitional loading characteristics, making it a frequent site of traumatic injury [5]. The optimal choice of surgical approach in this region remains debated, primarily centered on two competing principles of spinal trauma surgery [6].

The first advocates for decompression from the side of the injury—typically via an anterior approach—allowing direct removal of bone fragments and reconstruction of anterior column integrity through

partial corpectomy, interbody cage placement, and anterior plating [7]. The second favors posterior approaches, which offer biomechanical advantages, safer access, and the potential for indirect decompression with lower complication rates [8, 9]. Posterior transpedicular instrumentation is widely accepted and broadly utilized due to its reproducibility and favorable risk profile [10].

As with any spinal instrumentation procedure, thoracolumbar stabilization carries the risk of complications. These may be influenced by injury characteristics, implant selection, surgical technique, and patient factors. While posterior fixation techniques and their long-term outcomes especially regarding construct failure, hardware fatigue, pseudarthrosis, and alignment loss have been extensively studied, data on implant-related complications following anterior-only stabilization remain scarce [11].

Given the increasing use of anterior-only constructs in select cases, understanding the nature and long-term risks of this approach is critical. Delayed mechanical failure, although less frequent than early complications, may be more challenging to manage and often requires greater surgical expertise than primary fixation [12].

The aim of this study was to evaluate the long-term implant-related complications following anterior-only stabilization of traumatic thoracolumbar injuries and to identify structural and radiological patterns associated with construct failure.

Materials and Methods

Study design and setting

This was a multicenter retrospective observational study conducted between 2000 and 2023. Clinical and radiological data were obtained from two centers: the State Institution "Romodanov Institute of Neurosurgery, National Academy of Medical Sciences of Ukraine" (Kyiv, Ukraine) and the Punjab Institute of Neurosciences (Lahore, Pakistan). The study focused on long-term mechanical complications following anterior-only stabilization of thoracolumbar junction trauma. All patients provided informed consent for the processing of their data in compliance with institutional and ethical requirements.

Eligibility criteria

Inclusion criteria

- History of thoracolumbar junction trauma (T11–L2) surgically treated via a ventrolateral approach with anterior-only stabilization;
- Availability of adequate clinical and surgical records to assess injury characteristics and treatment parameters;
- Age ≥18 years at the time of surgery;
- Minimum interval of 5 years between the index surgery and the documented complication;
- Presence of follow-up imaging (radiographs and/or CT) sufficient to assess mechanical construct failure.

While preoperative and early postoperative imaging were desirable for comparative assessment, they were not a strict requirement to preserve the inclusion of cases with long-term follow-up.

Exclusion criteria

- Documented infectious or inflammatory complications in the postoperative period;
- Any reoperation or revision at the index level prior to the complication being analyzed;
- Presence of malignant disease or any severe decompensated systemic pathology;
- Severe osteoporosis (HU < 80);
- Cognitive, psychiatric, or behavioral disorders precluding clinical follow-up or valid data interpretation.

Endpoints

The primary endpoint was the identification and classification of long-term implant-related complications following anterior-only stabilization of thoracolumbar junction injuries. Secondary endpoints included the evaluation of associated deformities (sagittal and coronal), changes in neurological status, and subjective pain intensity.

Imaging protocol and measurement techniques

All imaging data were evaluated using RadiAnt DICOM Viewer (Medixant, Poland; version 2025.1, license no. 193060A6).

Segmental deformity

Segmental sagittal kyphosis was assessed using a modified Cobb method, measured between the superior endplate of the vertebra above and the inferior endplate of the vertebra below the instrumented segment [13]. Deformity severity was graded as follows: ≤10° – normal/compensated; 11–20° – mild; 21–30° – moderate; 31–40° – severe; 40° > marked [14].

Global sagittal alignment

The sagittal vertical axis (SVA) was measured as the horizontal distance between a vertical line dropped from the center of the C7 vertebral body and the posterosuperior corner of the S1 body. An SVA ≤50 mm was defined as normal; values >50 mm were interpreted as sagittal imbalance [15].

Bone density assessment

Trabecular bone mineral density was estimated using HU values from native CT scans. An elliptical (region of interest) ROI was placed in the anterior two-thirds of the trabecular part of the L3 vertebral body, avoiding cortical bone. Classification was based on Pickhardt et al. (2011): HU >135 – normal bone density; HU 110–135 – osteopenia; HU <110 – osteoporosis [16].

Patients with HU <80 were excluded due to the high risk of confounding biomechanical instability [17].

Functional and clinical parameters

Neurological function was assessed using the ASIA Impairment Scale [18]. Fractures were classified using the AOSpine Thoracolumbar Injury Classification System [19]. Pain intensity was recorded using a standard 10-point Visual Analog Scale (VAS) [20].

Statistical analysis

All statistical computations were performed using R version 4.0.5 (R Core Team, 2021) in RStudio version 1.4.1106 (Posit Team, 2025). Continuous variables were summarized as medians with interquartile ranges (IQR). Categorical variables were presented as frequencies and percentages. Between-group comparisons were conducted using the Mann–Whitney U test or Fisher's

This article contains some figures that are displayed in color online but in black and white in the print edition.

exact test, as appropriate. Time-to-failure analysis was performed using the Kaplan–Meier method, with the log-rank test applied for group comparisons. Cox proportional hazards regression was used to estimate hazard ratios (HR) and 95% confidence intervals (CI) for complication-free survival in relation to bone density.

Results

Patient characteristics

Following initial screening, 27 cases met the search criteria. Of these, 11 were excluded from further analysis due to factors that precluded objective long-term evaluation. Specifically, reasons for exclusion included: improper implant positioning and/or revision surgery prior to the identified complication (n = 3), postoperative infection (n = 2), confirmed oncological pathology (n = 1), decompensated systemic conditions including diabetes mellitus (n = 2), and severe osteoporosis (n = 3).

As a result, 16 patients were included in the final analysis. The mean age at the time of complication diagnosis was 44.6 years (95% CI: 39.7–49.6), and the male-to-female ratio was 1.7:1. A detailed breakdown of the cohort's demographic and clinical characteristics is provided in ***Table 1***.

To better illustrate the clinical and radiological profiles of the complications described below, selected representative clinical cases are presented.

Table 1. Baseline characteristics of the study population (n = 16)

Parameter	Value (95% CI / range)
Sex	
– Male	62.5% (35.4–84.8%)
– Female	37.5% (15.2–64.6%)
Age at complication diagnosis (yrs)	45.5 (95% CI: 39–49); range 27–62
Age at injury (yrs)	37.5 (95% CI: 29–41); range 19–47
Interval to complication (yrs)	9.45 (95% CI: 6.8–11); range 5.2–19.4
Mechanism of injury	
– Fall	50% (24.7–75.3%)
– Road traffic accident	37.5% (15.2–64.6%)
– Sports-related	12.5% (1.6–38.3%)
Fracture level	
– T11	12.5% (1.6–38.3%)
– T12	31.2% (11.0–58.7%)
– L1	37.5% (15.2–64.6%)
– L2	18.8% (4.0–45.6%)
Fracture type (AOSpine)	
– A4	68.8% (41.3–89.0%)
– B2	12.5% (1.6–38.3%)
– C	18.8% (4.0–45.6%)
Neurological status (ASIA)	
– C	6.2% (0.2–30.2%)
– D	37.5% (15.2–64.6%)
– E	56.2% (29.9–80.2%)
Bone mineral density (HU)	
– HU ≥ 135 (median HU)	56.2%; 172 HU (95% CI: 141–184)
– HU < 135 (median HU)	43.8%; 121 HU (95% CI: 114–123)

Clinical case 1

Patient K., a 19-year-old female, sustained a thoracolumbar injury in a motor vehicle accident. Computed tomography (CT) imaging confirmed a burst fracture of the L1 vertebral body with minor retropulsion of bone fragments into the spinal canal. The patient exhibited no neurological deficit (ASIA grade E). Surgical management consisted of partial corpectomy via a ventrolateral approach, placement of a titanium mesh cage for anterior column support, and stabilization using an anterior plate fixed to the T12 and L2 vertebral bodies with screws.

Following rehabilitation, the patient returned to full physical activity. Five years postoperatively, she began to report intermittent low back pain following physical exertion, which did not require analgesic therapy. At 7.3 years postoperatively, she developed new-onset epigastric pain. After excluding visceral causes, CT of the thoracic and lumbar spine was performed.

CT imaging revealed complete loosening and extraction of all fixation screws, along with dislocation of the anterior plate (***Fig. 1 A, B, D***). The migrated screws were found in direct proximity to the abdominal aorta, with one causing localized indentation of the vessel wall (***Fig. 1E***). A pronounced segmental kyphotic deformity at the instrumented level was noted, with a bisegmental Cobb angle between T12 and L2 measuring 39.8°. However, overall sagittal alignment was preserved, presumably due to compensatory lumbar hyperlordosis. No segmental or global coronal deformity was observed (***Fig. 1B, C***). Bone mineral density (BMD) was measured at 192.26 HU (SD 43.82). On clinical examination, the patient remained neurologically intact. Pain intensity was 3 out of 10 on the visual analog scale (VAS).

Revision surgery was planned, including removal of the anterior implant and screws, followed by posterior transpedicular stabilization. Due to the high risk of intraoperative complications, particularly related to screw proximity to the aorta, vascular surgical backup was scheduled. However, the patient deferred the procedure indefinitely due to family circumstances.

Clinical case 2

Patient H. underwent anterior stabilization of a thoracolumbar fracture at the age of 16 in 2009. Eleven years after the initial surgery, she presented with progressive spinal deformity and chronic lower back pain.

Radiographic and CT assessment revealed implant failure, anterior construct loosening, and severe kyphotic deformity. The measured Cobb angle was 69°, accompanied by global sagittal imbalance (increased SVA) and segmental instability (***Fig. 2***).

The patient underwent revision surgery via a posterior-only approach. The procedure involved posterior instrumentation with pedicle screws, vertebral body resection, cage placement, and posterior column osteotomy for correction of the deformity. Anterior implants were not revised. Postoperative imaging confirmed restoration of sagittal alignment and segmental stability (***Fig. 3***).

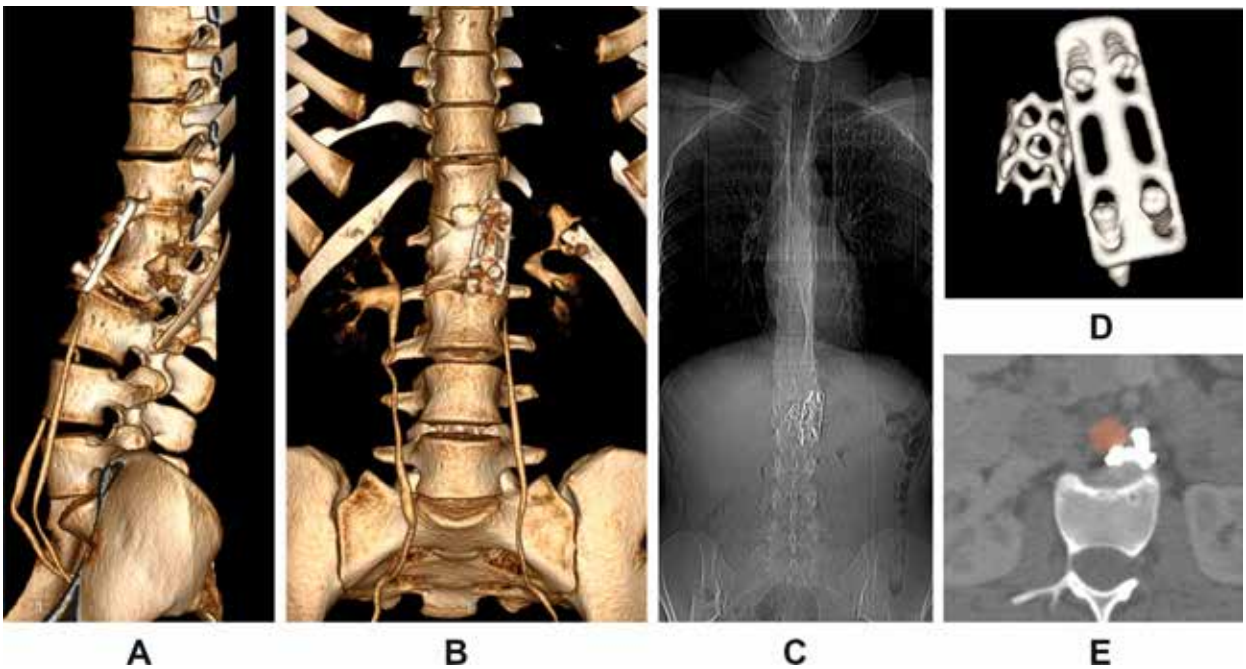

Fig. 1. Multiplanar CT reconstructions in Patient K.
A: 3D posterior oblique view of the thoracolumbar junction;
B: anterior 3D reconstruction;
C: anteroposterior scout view;
D: isolated 3D view of the displaced instrumentation;
E: axial view showing displaced screws in close contact with the abdominal aorta (highlighted in red)

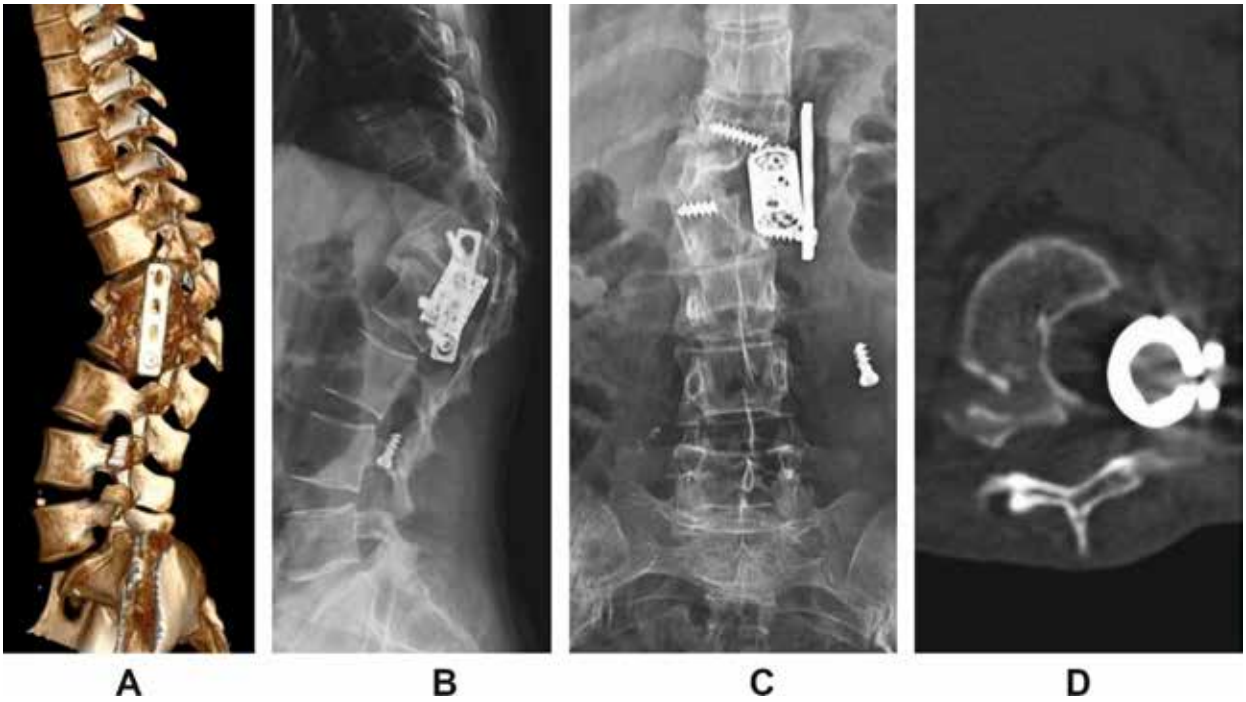

Fig. 2. Imaging findings in Patient H. prior to revision surgery.
A: 3D lateral reconstruction;
B: lateral scout view;
C: anteroposterior scout view;
D: axial view showing cage subsidence and anterior column failure.

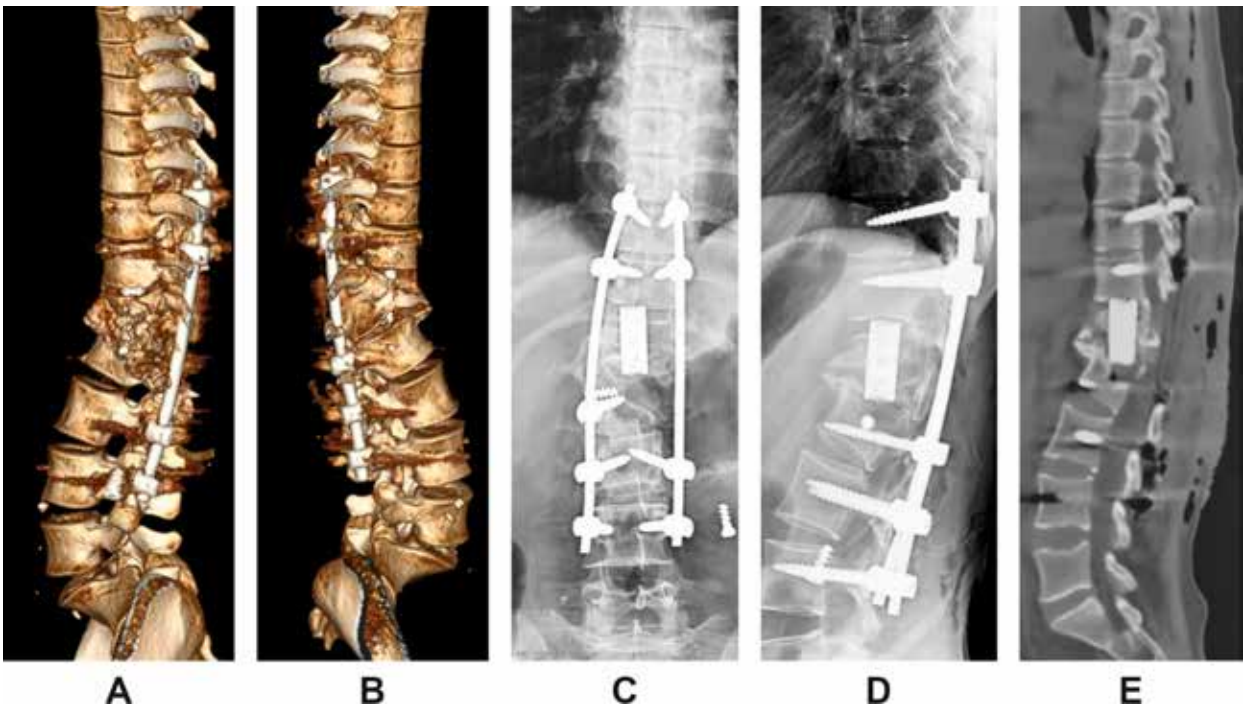

Fig. 3. Postoperative imaging following posterior revision in Patient H.
A and B: 3D lateral reconstructions from left and right sides;
C and D: scout views (anteroposterior and lateral);
E: midsagittal CT reconstruction demonstrating correction of segmental alignment.

Complication analysis and classification

To facilitate a detailed assessment of complication patterns and potential causative factors, all confirmed implant-related abnormalities were categorized into the following groups:

- structural complications involving the implanted construct;
- local and global spinal alignment disturbances, with a focus on the operated segment;
- neurological deterioration and pain-related clinical manifestations.

Statistical analysis of the recorded complications revealed the following findings.

Screw-related failures represented the most prevalent complication group, occurring in 87.5% of cases. Among these, **screw fragmentation** was documented in 6 patients (37.5%), while **extraction of visually intact screws** was observed in 9 patients (56.3%). Notably, screw fragmentation was accompanied by **screw migration** in 83.3% of cases. Only one patient demonstrated an intracorporeal screw fracture without displacement. A combined failure pattern was observed in a single patient, where two screws were fragmented and the remaining two were displaced without structural failure.

Plate-related complications were also present: **structural failure (fracture)** of the anterior plate was identified in 18.8% of cases, and **plate migration** in 68.8% (11 patients). In 12.5% of cases (n = 2), a specific failure mode was observed, where the anterior plate had lost its stabilizing function due to screw failure. Still, it remained in its anatomical position, maintaining contact along the vertebral bodies, without frank migration.

Cage migration, representing the most severe form of anterior construct failure, was identified in 31.3% of cases. In the remaining patients (n = 11), the cage remained within the vertebral body but **progressive endplate subsidence and segmental kyphosis** were noted. These findings suggest structural weakening of the anterior support zone without gross implant displacement. The frequency and overlap of all implant-related failure types are presented in ***Fig. 4***.

Severity scoring of implant-related complications

To provide a standardized framework for evaluating the clinical relevance of implant-related complications, a custom complication severity score was developed. This scale was based on a combination of radiographically confirmed indicators of construct instability. Each complication type was assigned a weighted score reflecting its presumed clinical impact and potential for functional deterioration. These scores were used for subgroup comparisons and correlation analysis with bone mineral density, neurological status, and pain intensity.

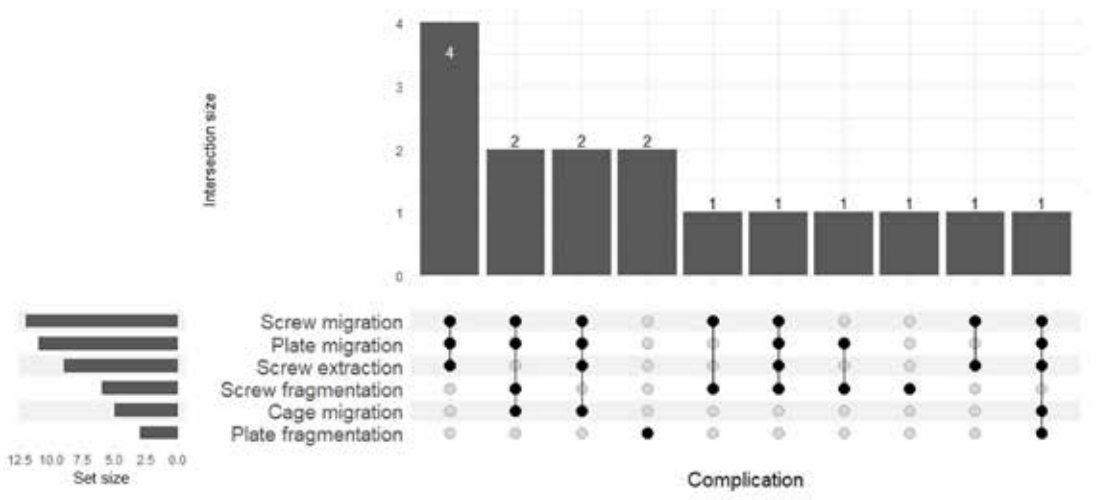

Fig. 4. Overlap and frequency of implant-associated failure modes (UpSet plot)

Table 2. Scoring matrix for implant-related complication severity based on combinations of structural failure

Primary complication ↓ / In combination with →	Cage migration	Plate migration	Screw migration	Plate fragmentation	Screw fragmentation	Score
Cage migration	✔	✔	✔	–	–	5
Plate migration	✘	✔	✔	–	–	4
Screw migration	✘	✘	✔	–	–	3
Plate fragmentation	✘	✘	✘	✔	–	2
Screw fragmentation	✘	✘	✘	✘	✔	1

Notes. ✔ – feature present; ✘ – feature absent; — – presence does not affect score

Segmental sagittal deformity and structural failure

The second group of complications analyzed in this study included secondary deformities within the previously operated spinal segment. The most common manifestation was segmental sagittal kyphosis, observed in 12 patients (75%). Given the biomechanical characteristics of the thoracolumbar junction, all cases were classified as kyphotic deformities.

When analyzing the relationship between implant failure patterns and segmental deformity, the following trends were noted:

- Cage migration (score 5) was associated with sagittal deformity in 100% of cases;
- Anterior plate migration (score 4) led to kyphotic deformity in 83.3% of cases;
- Lower-grade structural failures (scores 3, 2, and 1) demonstrated segmental kyphosis in 50%, 50%, and 0% of cases, respectively.

Due to methodological constraints, it was not feasible to precisely compare the degree of kyphotic deformity with early postoperative alignment. Nonetheless, the available data allowed for a descriptive assessment of actual segmental deformity and its relationship to implant failure characteristics.

Quantitative analysis of the bisegmental Cobb angle revealed a linear increase in deformity severity in relation to complication score. The most pronounced deformities were recorded in patients with scores of 4 and 5, with median angles of 34° (IQR: 32–40°) and 57° (IQR: 48–69°), respectively. In contrast, an isolated intracorporeal screw fracture without displacement (score 1) did not result in significant sagittal collapse — the angle measured 8°, corresponding to a compensated or minimal deformity.

These findings suggest a direct relationship between the structural severity of implant-related failure and the degree of posttraumatic segmental kyphosis. The association is visualized in ***Fig. 5***.

Global sagittal balance and its association with implant failure severity

The influence of implant-related complications on global sagittal alignment was of particular clinical interest. Despite the presence of substantial local segmental kyphotic deformity in the majority of patients, analysis showed that signs of global sagittal imbalance, as defined by the sagittal vertical axis (SVA), were present in only 31.3% of cases.

Importantly, sagittal imbalance was found almost exclusively in patients with the most severe implant-related failures—those assigned a complication severity score of 5. Only one case of sagittal imbalance occurred in a patient with a score of 4. No signs of global malalignment were observed in patients with lower complication scores.

Several factors may explain this observation:

- First, the most extreme angular deformities were documented in patients with 5-point complications, potentially exceeding the spine's capacity for sagittal compensation.
- Second, the nature and progression of the deformity appear to differ based on the type of structural failure. For example, cage migration may lead to rapid loss of anterior support and more abrupt segmental kyphosis. In contrast, plate migration—in cases where interbody support remains intact—may result in slower progression, allowing more time for the development of compensatory mechanisms such as lumbar hyperlordosis or pelvic retroversion.

Two representative cases provide support for this hypothesis. In one, a patient with a bisegmental angle of 48° and a complication score of 5 exhibited a marked increase in SVA, consistent with decompensated sagittal balance. In contrast, another patient with a Cobb angle of 54° and a score of 4 demonstrated preserved sagittal alignment, suggesting successful compensation.

Segmental coronal deformity

In contrast to sagittal deformity—which, in most cases, represented the primary radiographic manifestation of construct failure—segmental coronal deformity was observed far less frequently, being documented in only 25% of cases.

Notably, there was no consistent correlation between the presence or severity of coronal deformity and the overall complication severity score. Specifically, coronal malalignment was identified in two patients with a score of 3 and in two others with a score of 5 (see ***Fig. 2***). In the remaining cases, even in the presence of significant sagittal kyphosis, the coronal profile of the operated segment remained essentially preserved (see ***Fig. 1***).

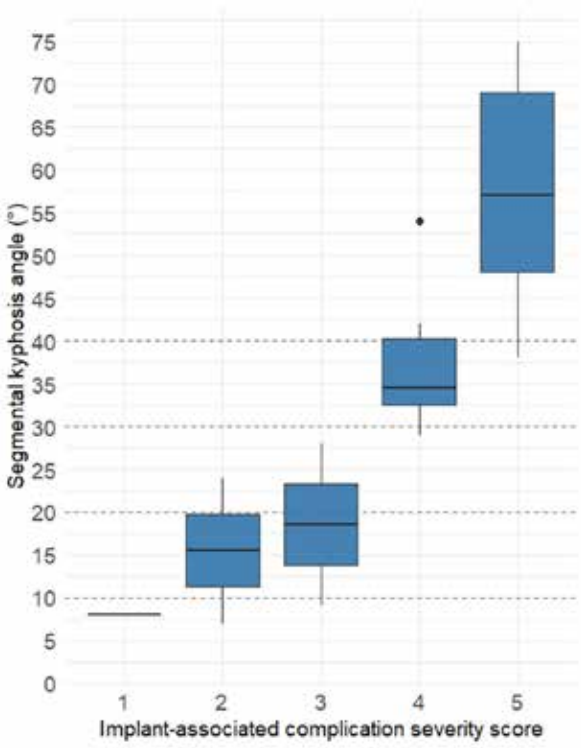

Fig. 5. Segmental kyphosis angle (in degrees) relative to implant-related complication severity. *Notes*. Boxplots represent median values and interquartile ranges of the bisegmental Cobb angle in each severity group. Dashed lines indicate threshold values for clinical grading of kyphotic deformity.

The likely mechanism underlying the development of coronal deformity in these patients was presumed to be asymmetric loss of structural support, possibly due to unilateral screw failure or cage subsidence. This assumption is supported by detailed radiographic analysis of individual cases, in which isolated implant loosening on one side appeared to precede the onset of coronal angulation.

Neurological decline associated with implant failure

The third group of complications addressed in this study involved neurological deterioration as a potential clinical manifestation of long-term anterior construct failure. A decline in neurological status was documented in 4 of 16 patients (25%).

In three cases, the ASIA grade worsened from E to D, and in one case from D to C, reflecting the development of new or progressive neurological deficits during long-term follow-up.

Analysis of complication severity in these patients revealed the following distribution:

- Two patients with neurological decline had complications classified as score 5;
- One patient had a score of 4;
- One patient had a score 3, primarily due to screw migration.
- It is notable that all patients with neurological deterioration exhibited relatively high segmental kyphotic angles:
- In the two score 5 cases, kyphosis measured 75° and 69°, respectively;
- In the score 4 case, the angle was 42°;
- In the score 3 case, although the sagittal deformity was moderate (28°), a concurrent coronal deformity of 34° was present, which may have contributed to neural compromise.

Despite these findings, meaningful statistical analysis of neurological outcomes was limited by the small sample size, which precluded definitive conclusions regarding causality or predictive risk.

Pain intensity and its clinical correlation

Among all the parameters assessed, pain intensity proved to be the most variable and least correlated with the structural manifestations of complications categorized into the first two groups. Analysis of VAS scores demonstrated that 56.2% of patients reported mild pain, 31.2% reported moderate pain, and only 12.5% experienced severe pain.

Attempts to identify a statistically significant relationship between pain severity and structural parameters of implant failure were unsuccessful (***Fig. 6A***). Moreover, it is worth noting that in one case, where the only radiographically confirmed sign of implant instability was an intracorporeal screw fracture (assigned complication score = 1), the progressive onset of pain was the primary reason for performing follow-up CT imaging, which was conducted 6.5 years after the initial surgery.

Similarly, segmental sagittal deformity exhibited only a weak correlation with the severity of pain symptoms. Statistical analysis using Spearman's rank correlation coefficient showed no significant association ($\rho = 0.23$; $p = 0.38$). While an overall trend toward increasing VAS scores with greater deformity angles was observed, the severity of pain was not consistently proportional to the anatomical degree of kyphosis.

This variability may be attributed to the influence of several additional factors, including individual differences in pain threshold, the presence of concurrent degenerative changes in adjacent structures, and variations in compensatory mechanisms such as postural adaptation or segmental stiffening. These factors must be considered when interpreting the clinical significance of pain in the context of long-term implant-related failure.

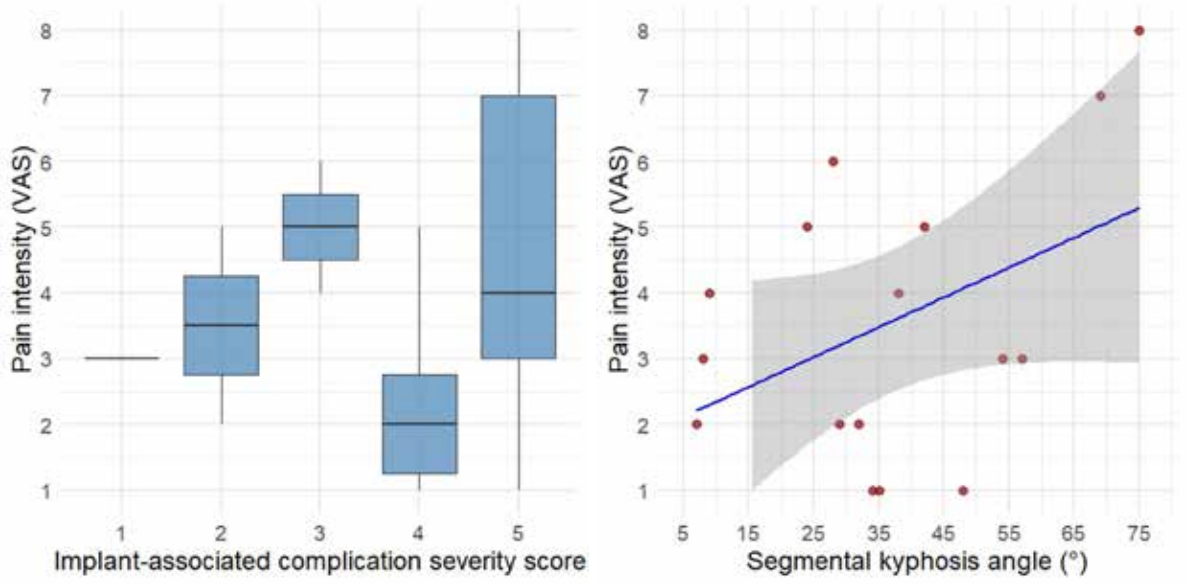

Fig. 6. A - Distribution of pain intensity (VAS) by complication severity score. B - Correlation between segmental kyphotic angle and pain intensity (VAS).

Bone quality and its association with long-term construct failure

As a potential factor influencing both the timing and nature of implant failure in the long-term postoperative period, we investigated BMD using CT-based HU analysis. This hypothesis was driven by the observation that, in cases of technically improper implant placement, complications tend to become clinically apparent much earlier.

In contrast, even when anterior instrumentation is placed correctly, the long-term mechanical integrity of the bone–implant interface may be substantially influenced by the quality of local cancellous bone. Progressive trabecular rarefaction, combined with continuous micro-motion at the implant interface, may ultimately lead to critical stress concentrations at points of contact between the implant and the vertebral body. This biomechanical vulnerability can lead to progressive failure of fixation, even in the absence of any technical errors during the initial surgery.

Therefore, bone mineral density should be considered a potentially modifiable risk factor for delayed mechanical failure following anterior spinal stabilization. Our findings provide preliminary support for this hypothesis (***Fig. 7***).

According to the results of Cox proportional hazards regression analysis, a HU value < 135 was associated with a trend toward increased risk of earlier complication onset. The calculated hazard ratio (HR) was 2.83 (95% CI: 0.93–8.67; p = 0.068), suggesting an approximately threefold increase in risk among patients with lower bone density. Although statistical significance was not reached, the direction and magnitude of the observed effect point to a clinically meaningful association between reduced BMD and construct failure.

Discussion

The results of this retrospective analysis of the long-term postoperative period highlight several key aspects related to the use of isolated anterior approaches for stabilization in thoracolumbar junction injuries. Despite the theoretical advantages of this strategy—such as direct decompression of the spinal canal, restoration of the anterior load-bearing column, and minimization of the number of instrumented segments—the identified complications point to the presence of specific, including delayed, risks that must be carefully considered when selecting the surgical approach and planning postoperative monitoring.

Mechanical stability of the construct and its failure mechanisms

One of the most significant findings in our cohort was the high incidence of mechanical complications related to fixation elements—primarily screw loosening and plate migration. These results are consistent with previously published data. Early generations of anterior fixation systems (e.g., AO-ATL-P) were characterized by limited rigidity of the screw–plate interface, which often led to loosening and implant migration within several years postoperatively, occurring in nearly one out of five cases [21]. Improvements in implant design (e.g., ATLP, Synthes) have led to more favorable outcomes: in the series by Wilson J. A. et al., screw breakage occurred in only 3.2% of cases, with no reported instances of pseudarthrosis [22].

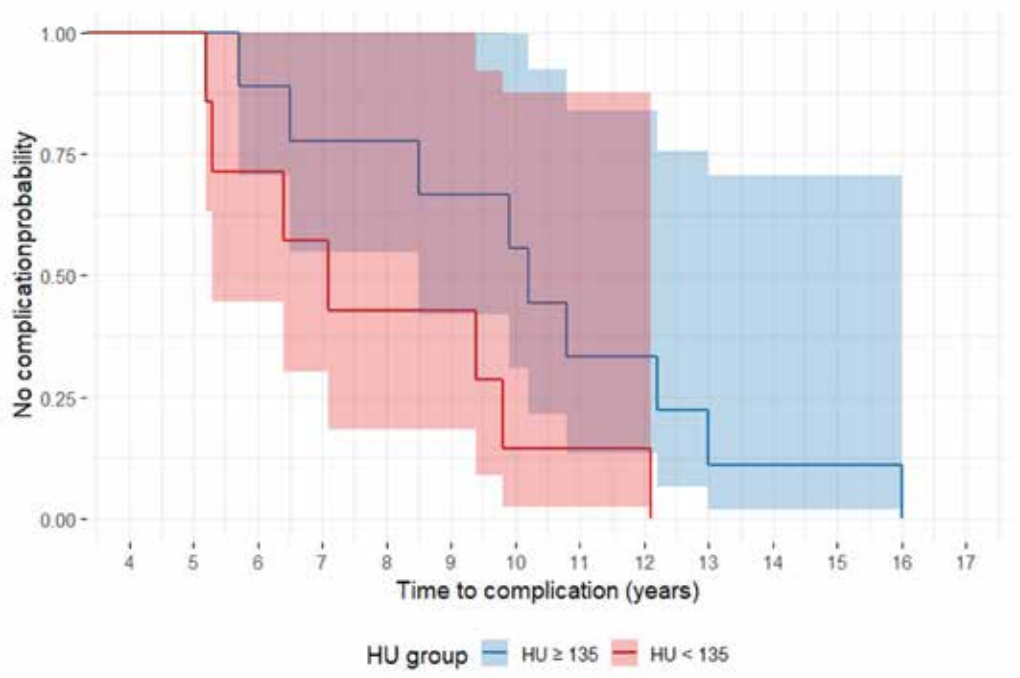

Fig. 7. Kaplan–Meier curves showing the time to implant-related complications in relation to bone mineral density (Hounsfield units, HU)

A large meta-analysis involving over 700 patients demonstrated that revision surgery due to mechanical failure was required in 10.8% of patients following isolated anterior fixation, compared to 4.7% after isolated posterior fixation. The overall complication rate was 30% and 14%, respectively [23]. This disparity is commonly attributed to the fact that although anterior constructs offer excellent axial support, they are less resistant to shear and rotational forces, particularly in cases of poor bone quality or suboptimal preparation of the vertebral endplates. Excessive loading on the anterior implant without supplemental posterior support may lead to micromotion at the screw–bone interface, resulting in osteolysis and, ultimately, clinically significant implant migration. The timely and solid formation of an interbody fusion plays a critical role. As the graft consolidates, axial loads are gradually transferred from the hardware to the bone, thereby reducing the risk of implant fatigue and failure [24].

While advances in implant design aim to reduce the incidence of implant-related complications, outcomes for isolated anterolateral corpectomy remain inconclusive [25]. Locking plates can reduce the frequency of screw migration but do not prevent periscrew osteolysis and eventual load redistribution, which may lead to intravertebral fragmentation of fixation elements. Similarly, telescoping vertebral body replacement systems—introduced to replace traditional cylindrical mesh cages—facilitate implantation and allow for controlled correction of sagittal alignment. However, their lack of dedicated cavities for bone grafting essentially eliminates the potential for forming a stable fusion mass [26]. As a result, complications may not decrease in frequency but instead shift in character, often presenting with delayed onset after a prolonged asymptomatic period.

A critical factor in the biomechanical reliability of anterior-only spinal stabilization—especially following corpectomy—is the cantilever effect. In classical mechanics, a cantilever is a beam anchored at one end and loaded at the other. Similarly, in spinal surgery, an anterior fixation system (e.g., a plate and interbody cage) functions as a cantilevered beam, transmitting significant compressive and bending forces in the absence of posterior support. Under physiological loading—especially during trunk flexion—the entire upper body weight is transmitted through the anterior construct, while posterior elements remain unsupported. This generates a pronounced bending moment in the sagittal plane, concentrated at the cage–endplate interface. Without posterior stabilization, the anterior implant behaves as a fixed lever arm, significantly increasing the risk of cage subsidence, implant migration, progressive segmental kyphosis, and ultimately, loss of global sagittal alignment [27].

As demonstrated by multiple biomechanical and clinical studies, effective load transfer from the patient to the implant system requires minimizing the moment arm and establishing a compressive force across the construct. This configuration enables the interbody cage to participate in vertical load sharing, thereby enhancing overall construct stability [28]. This means that when properly applied, the plate and screws should generate targeted axial compression across the cage, enabling it to participate in vertical load sharing. However, such a configuration is technically demanding and depends on precise implant positioning and meticulous endplate preparation. Moreover, even under ideal conditions, the absence of posterior tension-band support remains a biomechanical limitation: compression can mitigate the cantilever effect to some extent, but cannot fully neutralize it [29].

Kyphotic Deformity and Sagittal Imbalance

Progressive segmental kyphosis emerged as one of the most clinically relevant consequences of mechanical construct instability. In our cohort, kyphotic angles exceeding 40° were strongly associated with combined mechanical failures, including cage dislocation and plate migration. This finding aligns with previously published studies, which emphasize that even minor implant migration can significantly alter sagittal spinal alignment.

While anterior corpectomy with interbody fusion effectively restores anterior column height and corrects local kyphosis in the immediate postoperative period, subsequent failure of secondary interbody fusion or inadequate fixation may result in gradual subsidence of the graft or implant protrusion, leading to progressive kyphotic collapse [25]. The WFNS Spine Committee recommends maintaining the residual kyphotic angle below 20°, underscoring the importance of assessing not only the local angle but also global sagittal alignment parameters, such as sagittal vertical axis (SVA) and pelvic incidence–lumbar lordosis (PI–LL) mismatch [14, 30].

A prospective study by Avanzi et al. demonstrated that even in patients with segmental kyphosis >30°, quality-of-life outcomes may remain satisfactory as long as pelvic alignment and lumbar lordosis are preserved [31]. This is attributed to compensatory mechanisms such as pelvic retroversion and lumbar hyperlordosis, which maintain the center of gravity over the femoral heads and reduce the load on paraspinal musculature. However, in younger patients with high functional demands or in those with baseline hyperlordosis, these compensatory capacities are limited [32]. In such cases, even moderate increases in kyphotic angulation may result in chronic back pain, muscle fatigue, and gait disturbances [33].

For these patients, early detection of correction loss (typically ≥5° compared to early postoperative radiographs) is recommended, along with consideration of posterior augmentation. Furthermore, kyphotic deformity at the segmental level has been shown to increase mechanical stress on both fixation elements and bone–implant interfaces exponentially. This creates a positive feedback loop: the more pronounced the deformity, the higher the mechanical load, and the greater the risk of further implant-related or structural failure [34].

Neurological and Functional Outcomes

Spinal canal decompression achieved via anterior corpectomy is typically radical and durable. In the series by Wilson et al., none of the 31 patients experienced neurological deterioration during long-term follow-up [22]. However, isolated reports in the literature describe late complications such as cage or screw migration into the spinal canal, leading to compression

of the dural sac [30]. Delayed neurological decline is usually associated with either significant cage collapse in the setting of severe osteoporosis, or posterior (less commonly lateral) displacement of a long cortical screw inserted at an excessive craniocaudal divergence angle [35]. These events highlight the importance of early postoperative imaging control and meticulous implant placement. Specifically, screws should be positioned within the cortical ring of the vertebral body, and cage endplates should be closely apposed to the adjacent vertebral endplates to minimize the risk of subsidence.

In our series, the incidence of neurological worsening was low. All such cases were associated with major mechanical failures—marked segmental kyphosis (>60°), cage collapse, or spinal canal stenosis due to implant migration. These findings suggest the potential for delayed neural compromise due to either secondary compression or vascular insufficiency related to spinal canal deformation. Biomechanical modeling by Farley et al. [3] demonstrated that segmental kyphosis exceeding 50° may result in excessive spinal cord tension and impaired perfusion [36].

Interestingly, the severity of pain did not always correlate with the degree of mechanical degradation. Some patients with pronounced structural instability reported minimal pain, whereas others experienced significant discomfort in the context of isolated screw migration. Similar observations have been reported in the literature, highlighting the complex and multifactorial nature of post-fixation pain syndromes [37, 38].

Bone Mineral Density and Prognostic Value

Assessment of BMD using HU measurements revealed a significant correlation between lower HU values and increased risk of early implant failure. A prospective analysis by Su et al. demonstrated that patients with HU < 135 had an almost threefold higher risk of screw loosening or cage subsidence [39]. The HU values observed in our cohort are consistent with these findings.

A growing body of evidence suggests that thresholds of <110 HU are critical for predicting posterior fixation failure, while values <135 HU carry similar implications for anterior constructs [40]. This indicates that CT-based HU analysis may serve not only as a tool for assessing fusion status but also as a reliable method for stratifying patients according to their individual risk of mechanical failure.

Limitations

This study has several significant limitations that must be acknowledged. First, the relatively small sample size (n = 16) limits the statistical power and generalizability of the findings. Although this reflects the low frequency of anterior-only stabilization in thoracolumbar trauma and the rarity of long-term follow-up beyond 5 years, it nonetheless restricts subgroup comparisons and predictive modeling.

Second, the retrospective design of the study introduces an inherent risk of selection and information bias. Incomplete early postoperative imaging in some cases limited our ability to quantify deformity progression over time. While efforts were made to include only cases with sufficient radiological and clinical documentation, variability in imaging quality and follow-up intervals may have influenced the results.

Third, some outcome parameters—particularly pain intensity—are inherently subjective and may have been affected by patient-specific psychological and physiological factors not captured in this dataset.

Finally, the study cohort was limited to two institutions, which may influence surgical technique consistency, rehabilitation protocols, and implant selection. Multicenter prospective validation in larger cohorts is warranted to confirm these findings and further refine risk stratification based on bone quality and implant design.

Conclusion

Anterior-only stabilization for thoracolumbar junction injuries remains an acceptable option in carefully selected clinical scenarios, providing effective spinal canal decompression and restoration of anterior column support while minimizing the number of instrumented segments. However, long-term follow-up demonstrates the presence of specific risks of mechanical failure, particularly in the absence of supplemental posterior support. The most frequently encountered complications included screw loosening, anterior plate migration, and cage subsidence—often accompanied by segmental kyphotic deformity and, in more severe cases, global sagittal imbalance and delayed neurological deterioration.

The cantilever effect constitutes a key biomechanical vulnerability of anterior constructs. Despite ongoing advancements in fixation technologies, the risk of delayed structural failure cannot be entirely eliminated. A Hounsfield Unit value <135 may serve as a prognostically unfavorable marker and should be considered for incorporation into preoperative risk stratification.

Given the multifactorial nature of these complications and their clinical significance, an individualized approach is essential in selecting the stabilization strategy. This includes strict adherence to technical principles of implant placement and long-term radiological surveillance. In cases of low predicted bone quality, suspected or confirmed disruption of the posterior ligamentous complex, or in patients with high functional demands, isolated posterior stabilization appears to be a more favorable option.

This study clearly demonstrates that even technically successful surgical correction of thoracolumbar trauma via an anterior-only approach does not guarantee the absence of long-term complications. In contrast to isolated posterior fixation, where complications tend to be more predictable, easier to identify, and technically simpler to revise, patients treated with anterior corpectomy and stabilization require closer long-term monitoring. These observations raise doubts about the routine use of anterior-only constructs in a broad patient population.

To validate these findings and refine the risk stratification approach, prospective multicenter studies with larger sample sizes are warranted. Additionally, the proposed implant-related complication severity scoring system should be further standardized, verified, and—if necessary—refined or modified, to support the development of evidence-based clinical guidelines

for selecting the optimal stabilization method in thoracolumbar junction trauma.

Disclosure

Conflict of interest

The authors declare that they have no conflicts of interest.

Funding

The study was not sponsored.

References

1. Costa F, Sharif S, Bajamal AH, Shaikh Y, Anania CD, Zileli M. Clinical and Radiological Factors Affecting Thoracolumbar Fractures Outcome: WFNS Spine Committee Recommendations. Neurospine. 2021;18(4):693-703. doi: 10.14245/ns.2142518.259
2. Zhao QM, Gu XF, Yang HL, Liu ZT. Surgical outcome of posterior fixation, including fractured vertebra, for thoracolumbar fractures. Neurosciences (Riyadh, Saudi Arabia). 2015;20(4):362-367. doi: 10.17712/nsj.2015.4.20150318
3. Xu J, Yin Z, Li Y, Xie Y, Hou J. Clinic choice of long or short segment pedicle screw-rod fixation in the treatment of thoracolumbar burst fracture: From scan data to numerical study. Int J Numer Method Biomed Eng. 2023;39(9):e3756. doi: 10.1002/cnm.3756
4. Rajasekaran S, Kanna RM, Shetty AP. Management of thoracolumbar spine trauma: An overview. Indian J Orthop. 2015;49(1):72-82. doi: 10.4103/0019-5413.143914
5. Bruno AG, Burkhart K, Allaire B, Anderson DE, Bouxsein ML. Spinal Loading Patterns From Biomechanical Modeling Explain the High Incidence of Vertebral Fractures in the Thoracolumbar Region. Journal of bone and mineral research : the official journal of the American Society for Bone and Mineral Research. 2017;32(6):1282-1290. doi: 10.1002/jbmr.3113
6. Ren EH, Deng YJ, Xie QQ, Li WZ, Shi WD, Ma JL, et al. [Anterior versus posterior decompression for the treatment of thoracolumbar fractures with spinal cord injury:a Meta-analysis]. Zhongguo Gu Shang. 2019;32(3):269-277. doi: 10.3969/j.issn.1003-0034.2019.03.015
7. Mittal S, Rana A, Ahuja K, Ifthekar S, Yadav G, Sudhakar PV, et al. Outcomes of Anterior Decompression and Anterior Instrumentation in Thoracolumbar Burst Fractures-A Prospective Observational Study With Mid-Term Follow-up. J Orthop Trauma. 2022;36(4):136-141. doi: 10.1097/BOT.0000000000002261
8. Kim WS, Jeong TS, Kim WK. Three-column reconstruction through the posterior approach alone for the treatment of a severe lumbar burst fracture in Korea: a case report. J Trauma Inj. 2023;36(3):290-294. doi: 10.20408/jti.2022.0075
9. Shokouhi G, Iranmehr A, Ghoilpour P, Fattahi MR, Mousavi ST, Bitaraf MA, Sarpoolaki MK. Indirect Spinal Canal Decompression Using Ligamentotaxis Compared With Direct Posterior Canal Decompression in Thoracolumbar Burst Fractures: A Prospective Randomized Study. Med J Islam Repub Iran. 2023;37:59. doi: 10.47176/mjiri.37.59
10. Moreira CHT, Krause W, Meves R. Thoracolombar Burst Fractures: Short Fixation, without Arthrodesis and without Removal of the Implant. Acta Ortop Bras. 2023;31(spe1):e253655. doi: 10.1590/1413-785220233101e253655
11. Vilela A, Couto B, Ferreira D, Cruz A, Azevedo J, Pereira J, et al. Risk factors for failure in short segment pedicle instrumentation in thoracolumbar fractures. Brain Spine. 2025;5:104266. doi: 10.1016/j.bas.2025.104266
12. Hu X, Barber SM, Ji Y, Kou H, Cai W, Cheng M, et al. Implant failure and revision strategies after total spondylectomy for spinal tumors. J Bone Oncol. 2023;42:100497. doi: 10.1016/j.jbo.2023.100497
13. Cobb's Method For Quantitative Evaluation Of Spinal Curvature: A Review. Journal of Pharmaceutical Negative Results. 2023:4153-4159. doi: 10.47750/pnr.2022.13.S06.550
14. Yaman O, Zileli M, Senturk S, Paksoy K, Sharif S. Kyphosis After Thoracolumbar Spine Fractures: WFNS Spine Committee Recommendations. Neurospine. 2021;18(4):681-692. doi: 10.14245/ns.2142340.170
15. Glassman SD, Berven S, Bridwell K, Horton W, Dimar JR. Correlation of radiographic parameters and clinical symptoms in adult scoliosis. Spine (Phila Pa 1976). 2005;30(6):682-688. doi: 10.1097/01.brs.0000155425.04536.f7
16. Pickhardt PJ, Lee LJ, del Rio AM, Lauder T, Bruce RJ, Summers RM, et al. Simultaneous screening for osteoporosis at CT colonography: bone mineral density assessment using MDCT attenuation techniques compared with the DXA reference standard. Journal of bone and mineral research : the official journal of the American Society for Bone and Mineral Research. 2011;26(9):2194-2203. doi: 10.1002/jbmr.428
17. Shu L, Wang X, Li L, Aili A, Zhang R, Liu W, Muheremu A. Computed Tomography-Based Prediction of Lumbar Pedicle Screw Loosening. BioMed research international. 2023;2023:8084597. doi: 10.1155/2023/8084597
18. Rupp R, Biering-Sorensen F, Burns SP, Graves DE, Guest J, Jones L, et al. International Standards for Neurological Classification of Spinal Cord Injury: Revised 2019. Top Spinal Cord Inj Rehabil. 2021;27(2):1-22. doi: 10.46292/sci2702-1
19. Vaccaro AR, Oner C, Kepler CK, Dvorak M, Schnake K, Bellabarba C, et al. AOSpine thoracolumbar spine injury classification system: fracture description, neurological status, and key modifiers. Spine (Phila Pa 1976). 2013;38(23):2028-2037. doi: 10.1097/BRS.0b013e3182a8a381
20. Astrom M, Thet Lwin ZM, Teni FS, Burstrom K, Berg J. Use of the visual analogue scale for health state valuation: a scoping review. Qual Life Res. 2023;32(10):2719-2729. doi: 10.1007/s11136-023-03411-3
21. Thalgott JS, Kabins MB, Timlin M, Fritts K, Giuffre JM. Four year experience with the AO Anterior Thoracolumbar Locking Plate. Spinal Cord. 1997;35(5):286-291. doi: 10.1038/sj.sc.3100399
22. Wilson JA, Bowen S, Branch CL, Jr., Meredith JW. Review of 31 cases of anterior thoracolumbar fixation with the anterior thoracolumbar locking plate system. Neurosurg Focus. 1999;7(1):e1. doi: 10.3171/foc.1999.7.1.3
23. P PO, Tuinebreijer WE, Patka P, den Hartog D. Combined anterior-posterior surgery versus posterior surgery for thoracolumbar burst fractures: a systematic review of the literature. Open Orthop J. 2010;4:93-100. doi: 10.2174/1874325001004010093
24. Cheers GM, Weimer LP, Neuerburg C, Arnholdt J, Gilbert F, Thorwachter C, et al. Advances in implants and bone graft types for lumbar spinal fusion surgery. Biomater Sci. 2024;12(19):4875-4902. doi: 10.1039/d4bm00848k
25. Ortiz Torres MJ, Ravipati K, Smith CJ, Norby K, Pleitez J, Galicich W, et al. Outcomes for standalone anterolateral corpectomy for thoracolumbar burst fractures. Neurosurg Rev. 2024;47(1):816. doi: 10.1007/s10143-024-03049-w
26. Bhat AL, Lowery GL, Sei A. The use of titanium surgical mesh-bone graft composite in the anterior thoracic or lumbar spine after complete or partial corpectomy. Eur Spine J. 1999;8(4):304-309. doi: 10.1007/s005860050178
27. Kallemeier PM, Beaubien BP, Buttermann GR, Polga DJ, Wood KB. In vitro analysis of anterior and posterior fixation in an experimental unstable burst fracture model. J Spinal Disord Tech. 2008;21(3):216-224. doi: 10.1097/BSD.0b013e31807a2f61
28. Li Z, Liu H, Yang M, Zhang W. A biomechanical analysis of four anterior cervical techniques to treating multilevel cervical spondylotic myelopathy: a finite element study. BMC Musculoskelet Disord. 2021;22(1):278. doi: 10.1186/s12891-021-04150-7
29. Calek AK, Cornaz F, Suter M, Fasser MR, Baumgartner S, Sager P, et al. Load distribution on intervertebral cages with and without posterior instrumentation. Spine J. 2024;24(5):889-898. doi: 10.1016/j.spinee.2023.10.017
30. Sharif S, Shaikh Y, Yaman O, Zileli M. Surgical Techniques for Thoracolumbar Spine Fractures: WFNS Spine Committee Recommendations. Neurospine. 2021;18(4):667-680. doi: 10.14245/ns.2142206.253
31. Avanzi O, Meves R, Silber Caffaro MF, Buarque de Hollanda JP, Queiroz M. Thoracolumbar Burst Fractures: Correlation

between Kyphosis and Function Post Non-Operative Treatment. Rev Bras Ortop. 2009;44(5):408-414. doi: 10.1016/S2255-4971(15)30271-8
32. Le Huec JC, Thompson W, Mohsinaly Y, Barrey C, Faundez A. Sagittal balance of the spine. Eur Spine J. 2019;28(9):1889-1905. doi: 10.1007/s00586-019-06083-1
33. Hira K, Nagata K, Hashizume H, Asai Y, Oka H, Tsutsui S, et al. Relationship of sagittal spinal alignment with low back pain and physical performance in the general population. Sci Rep. 2021;11(1):20604. doi: 10.1038/s41598-021-00116-w
34. McLain RF. The biomechanics of long versus short fixation for thoracolumbar spine fractures. Spine (Phila Pa 1976). 2006;31(11 Suppl):S70-79; discussion S104. doi: 10.1097/01.brs.0000218221.47230.dd
35. Iwata S, Kotani T, Sakuma T, Iijima Y, Okuwaki S, Ohyama S, et al. Risk Factors for Cage Subsidence in Minimally Invasive Lateral Corpectomy for Osteoporotic Vertebral Fractures. Spine surgery and related research. 2023;7(4):356-362. doi: 10.22603/ssrr.2022-0215
36. Farley CW, Curt BA, Pettigrew DB, Holtz JR, Dollin N, Kuntz Ct. Spinal cord intramedullary pressure in thoracic kyphotic deformity: a cadaveric study. Spine (Phila Pa 1976). 2012;37(4):E224-230. doi: 10.1097/BRS.0b013e31822dd69b
37. Sanderson PL, Fraser RD, Hall DJ, Cain CM, Osti OL, Potter GR. Short segment fixation of thoracolumbar burst fractures without fusion. Eur Spine J. 1999;8(6):495-500. doi: 10.1007/s005860050212
38. Tisot RA, Vieira JdS, Santos RTd, Badotti AA, Collares DdS, Stumm LD, et al. Burst fracture of the thoracolumbar spine: correlation between kyphosis and clinical result of the treatment. Coluna/Columna. 2015;14(2):129-133. doi: 10.1590/s1808-185120151402146349
39. Su YF, Tsai TH, Lieu AS, Lin CL, Chang CH, Tsai CY, Su HY. Bone-Mounted Robotic System in Minimally Invasive Spinal Surgery for Osteoporosis Patients: Clinical and Radiological Outcomes. Clin Interv Aging. 2022;17:589-599. doi: 10.2147/CIA.S359538
40. Orosz LD, Schuler KA, Allen BJ, Lerebo WT, Yamout T, Roy RT, et al. Performance comparison between Hounsfield units and DXA in predicting lumbar cage subsidence in the degenerative population. Spine J. 2025. doi: 10.1016/j.spinee.2025.03.028

Case Report

Ukrainian Neurosurgical Journal. 2025;31(3):58-62
doi: 10.25305/unj.325815

Transparsinterarticularis approach for resection of a malignant melanotic nerve sheath tumour of the dorsal spine: A case report

Tamajyoti Ghosh [1], Dhruv Agarwal [1], Pranjal Kalita [2], Biswajit Dey [2], Binoy K Singh [3]

[1] Department of Neurosurgery, NEIGRIHMS, Shillong, India
[2] Department of Pathology, NEIGRIHMS, Shillong, India
[3] Department of Neurosurgery, AIIMS Raipur, India

Received: 30 March 2025
Accepted: 21 May 2025

Address for correspondence*:*
Tamajyoti Ghosh, Assistant Professor, Department of Neurosurgery, NEIGRIHMS, Shillong, 793018, India, e-mail:tamajyoti@gmail.com

Introduction: Malignant melanotic nerve sheath tumours are extremely rare central nervous system neoplasms. Initially termed as Melanotic schwannoma the nomenclature was revised in 2020 WHO classification to malignant melanotic nerve sheath tumour (MMNST). They are rare aggressive peripheral nerve sheath tumours. In spine, they more commonly occur in the lumbosacral region (47.2%), followed by the thoracic (30.5%) and cervical (22.2%) segments. Most common age group affected is between 20-50 years. MMNSTs often tend to metastasize early and have poor prognosis. Surgical excision is the mainstay of treatment followed by radiotherapy and/or chemotherapy.

Case report: Here we present the case of a 54-year- old male who presented with gradually progressive lower limb weakness and hypertonia with bowel and bladder involvement. Magnetic resonance study of the spine suggested an intradural extramedullary melanoma at D4 level of spine. The rest of the physical examination and metastatic workup were unremarkable. The patient subsequently underwent tumour excision via trans-parsinterarticularis approach. Histopathological examination was suggestive of malignant melanotic nerve sheath tumour. Following surgery the patient's lower limb weakness improved significantly. At six-month follow-up patient did not show any signs of recurrence.

Conclusion: Malignant melanotic nerve sheath tumours (MMNSTs) are extremely rare highly aggressive lesions that are often misdiagnosed on neuroimaging. When a spinal tumour arising from a nerve root demonstrating the characteristic of T1 hyperintensity and T2 hypointensity, MMNST should always be included in differential diagnosis and metastatic workup, Clinical and radiological evaluation should be done to rule out other associated syndromes. Complete surgical excision followed by vigilant follow-up for early detection of recurrence is recommended.

Keywords: *spinal tumour; malignant melanotic nerve sheath tumour; immunohistochemistry; spine surgery*

Introduction

Malignant melanotic nerve sheath tumours (MMNSTs) are extremely rare tumours of the central nervous system [1]. Initially termed as melanotic schwannoma the nomenclature was revised in 2020 WHO classification to malignant melanotic nerve sheath tumour (MMNST) [2]. These tumours are rare aggressive peripheral nerve sheath neoplasms [3]. In the spine they most commonly occur in the lumbrosacral region (47.2%), followed by thoracic (30.5%) and cervical (22.2%) regions [4]. Most common age group affected is between 20-50 years. MMNSTs often tend to metastasize early and have poor prognosis [5]. Surgical excision is the mainstay of treatment followed by radiotherapy and chemotherapy [6]. Through this case report we aim to highlight the presentation and management of a thoracic MMNST.

Case Report

Here we present a 54-year-old male with two-month history of gradually progressive weakness and tightness in both lower limbs. On examination the power of both lower limbs was assessed as grade 2/5 according to Medical research council (MRC). Hypertonia of grade 3 was noted bilaterally in the lower limbs, and sensory hypoaesthesia was present in approximately 80% of the area below the nipple line.

He had bladder and bowel incontinence. The remainder of his physical examination was within normal limits. Magnetic resonance imaging (MRI) of his spine revealed a T1 hyperintense and T2 hypointense lesion at the level of D4 vertebra. (***Figures 1A, 1B, 2A*** and ***2B***). The lesion was homogeneously enhancing on contrast and was located intradurally and extramedullary on the left side. A differential diagnosis of metastatic lesion was made and thorough metastatic workup done, which however failed to show any primary tumour elsewhere.

The patient underwent left transparsinterarticularis approach under general anesthesia and tumour was identified. Grossly, the tumour was blackish in colour, highly vascular and adherent to adjacent structures and the dura arising from the exiting dorsal nerve root

(***Fig.3***). The tumour was meticulously dissected from the dura and surrounding tissues; the involved dorsal nerve root was sacrificed (***Fig. 4***). The lateral portion of the tumour was found adherent to pleura and was excised (***Fig. 5***). The total duration of surgery was 120 minutes, with an estimated blood loss of approximately 150 ml.

The patient was mobilized with support the very next day of surgery, followed by aggressive passive and active lower limb physiotherapy. Postoperatively, patient's lower limb power improved to MRC grade 4/5 and sensory hypoaesthesia reduced by 50%. The patient was able to walk with support. Histopathological examination revealed the tumour as malignant melanotic nerve sheath tumour (***Fig. 6A*** and ***6B***). IHC panel showed HMB45, S100, SOX10 positive, Ki67 index was 3%. GFAF, BRAF and V600E were negative (***Fig.7A*** and ***7B***).

The patient was followed up after 6 months demonstrating substantial improvement in neurological status and no evidence of recurrence. In the absence of recurrence at thesix-month months follow-up, no adjuvant therapy was recommended on multidisciplinary team meeting.

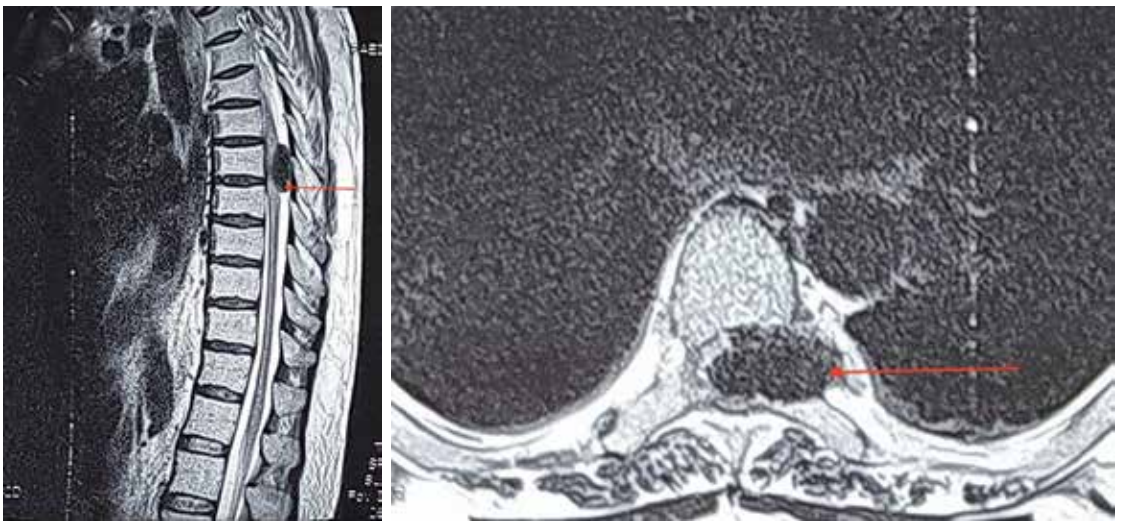

A **B**

Fig. 1A. Saggital T2-weighted MRI showing a hypointense lesion compressing the spinal cord at D4 level (red arrow)
Fig. 1B. Axial T2-weighted image showing a hypointense dumbbell-shaped lesion on left side with significant cord compression extending transforaminally (red arrow)

A **B**

Fig. 2A. Contrast-enhancing lesion at D4 (red arrow)
Fig. 2B. Coronal section image showing spinal lesion extending to the thorax (red arrow)

This article contains some figures that are displayed in color online but in black and white in the print edition.

Fig. 3. Melanotic lesion observed lateral to thecal sac extending transforaminally (white arrow)

Fig.4. Complete excision of the lesion

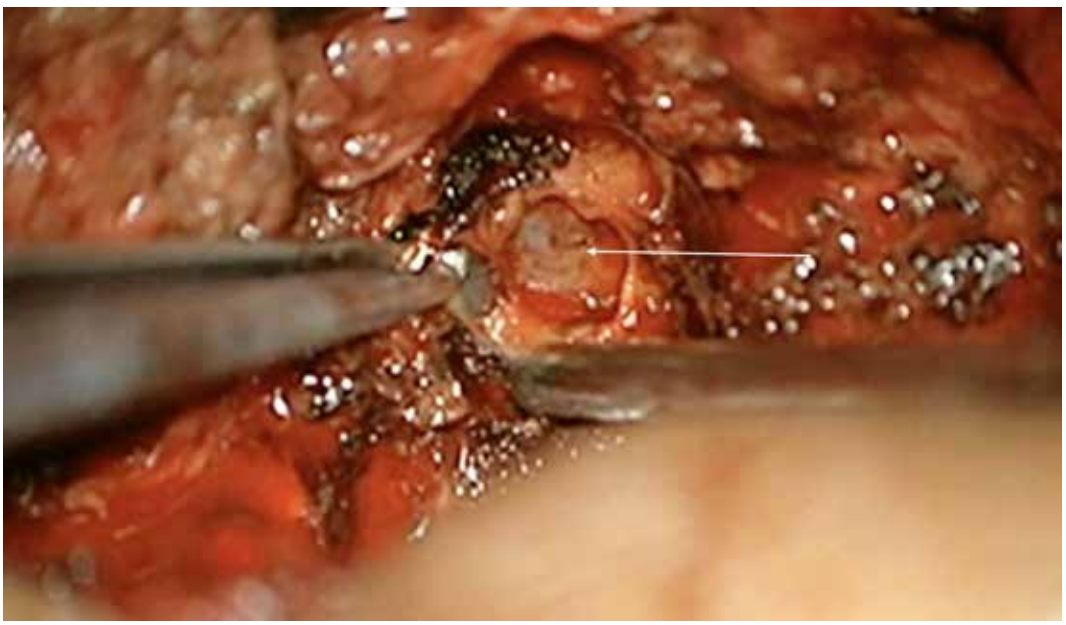

Fig.5. Careful dissection of the lateral portion of the tumour from the parietal pleura (white arrow)

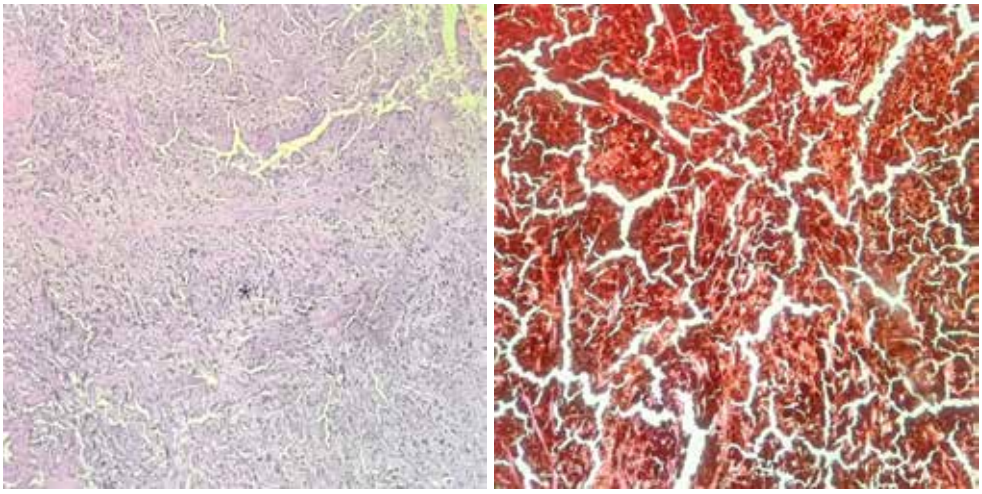

A B

Fig. 6A. Tumour composed of plump spindle cells arranged in interlacing fascicles. (H&E, 100X), marked with asterisks
Fig. 6B. Tumour cells obscured by melanin pigment (H&E, 100X)

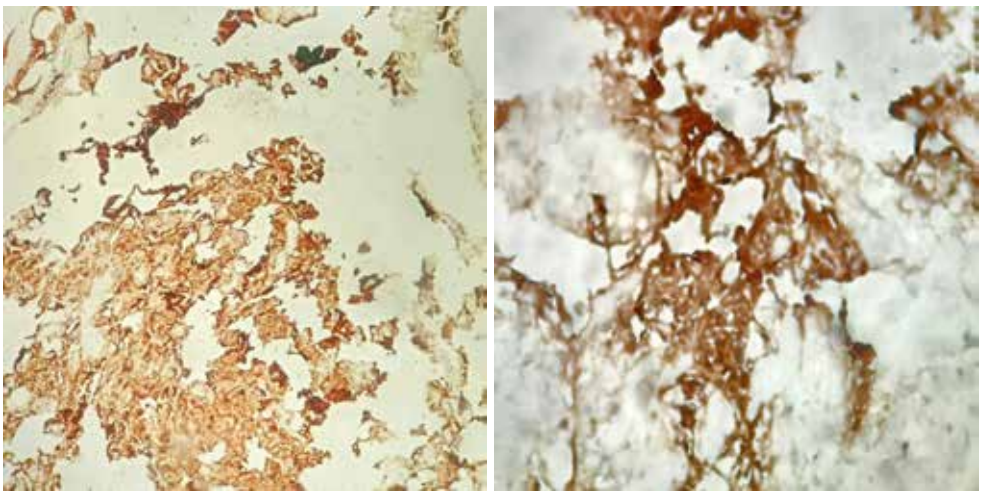

A B

Fig. 7A. Tumour cells positive for HMB45 (IHC, 400X)
Fig. 7B. Tumour cells positive for S100 (IHC 400X)

Discussion

Malignant melanotic nerve sheath tumour (MMNST) occurs due to melanogenesis of Schwann cells [7]. The most common syndromic association is Carney complex in 50% of cases [5]. Carney complex includes autosomal dominant disorder comprising of myxomas such as cardiac, cutaneous and mammary, spotty pigmentation and endocrine overactivity like Cushing's syndrome and acromegaly [8]. Our case had none of the above features in preoperative clinical and radiological evaluation. Extramedullary spinal melanotic schwannomas typically present in the 30-40 years age group [9]. However, in our case the age of the patient was 54 years old. According to the literature, about 50% of MMNST cases has local recurrence or distant metastasis at the time of detection [9]. Metastatic workup of our case did not reveal any metastasis. MRI findings includes T1 hyperintensity and T2 hypointensity in a dumbell shaped tumour arising from nerve root [10, 11] which was consistent with our case. However, signal intensity may vary depending upon the concentration of melanin [12]. Patients undergoing surgery for MMNST should be subjected to rigorous follow-up. The differential diagnosis of MMNST includes leptomeningeal melanocytoma, ancient schwannoma, pigmented neurofibroma, biphasic sarcoma, neurilemmoma and melanoma [5].

Conclusion

Malignant melanotic nerve sheath tumours (MMNSTs) are extremely rare and highly aggressive neoplasms that are often misdiagnosed in neuroimaging. Tumours arising from nerve root having characteristic of T1 hyperintensity and T2 hypointensity, MMNST should always be included in differential diagnosis. Metastatic

workup along with clinical and radiological evaluation should be done to rule out other associated syndromes. Surgical excision followed by vigilant follow-up for early detection of recurrence is recommended.

Disclosure

Conflict of Interest

The authors declare no conflict of interest.

Informed consent

Informed consent for data disclosure was obtained from the patient.

References

1. Alexiev BA, Chou PM, Jennings LJ. Pathology of Melanotic Schwannoma. Arch Pathol Lab Med. 2018 Dec;142(12):1517-1523. doi: 10.5858/arpa.2017-0162-RA
2. Choi JH, Ro JY. The 2020 WHO Classification of Tumors of Soft Tissue: Selected Changes and New Entities. Adv Anat Pathol. 2021 Jan;28(1):44-58. doi: 10.1097/PAP.0000000000000284
3. Folpe AL, Hameed M. Malignant melanotic nerve sheath tumour. In: WHO Classification of Tumours. 5th Editio. Volume 3.Soft Tissue and Bone Tumours. Lyon: IARC Press; 2020: 258-260.
4. Keskin E, Ekmekci S, Oztekin O, Diniz G. Melanotic Schwannomas Are Rarely Seen Pigmented Tumors with Unpredictable Prognosis and Challenging Diagnosis. Case Rep Pathol. 2017;2017:1807879. doi: 10.1155/2017/1807879
5. Carney JA. Psammomatous melanotic schwannoma. A distinctive, heritable tumor with special associations, including cardiac myxoma and the Cushing syndrome. Am J Surg Pathol. 1990 Mar;14(3):206-22.doi: 10.1097/00000478-199003000-00002
6. Bonomo G, Gans A, Mazzapicchi E, Rubiu E, Alimonti P, Eoli M, Paterra R, Pollo B, Iess G, Restelli F, Falco J, Acerbi F, Schiariti MP, Ferroli P, Broggi M. Sporadic spinal psammomatous malignant melanotic nerve sheath tumor: A case report and literature review. Front Oncol. 2023 Feb 24;13:1100532. doi: 10.3389/fonc.2023.1100532
7. Bird CC, Willis RA. The histogenesis of pigmented neurofibromas. J Pathol. 1969 Apr;97(4):631-7. doi: 10.1002/path.1710970407
8. Carney JA, Gordon H, Carpenter PC, Shenoy BV, Go VL. The complex of myxomas, spotty pigmentation, and endocrine overactivity. Medicine (Baltimore). 1985 Jul;64(4):270-83. doi: 10.1097/00005792-198507000-00007
9. Solomou G, Dulanka Silva AH, Wong A, Pohl U, Tzerakis N. Extramedullary malignant melanotic schwannoma of the spine: Case report and an up to date systematic review of the literature. Ann Med Surg (Lond). 2020 Oct 7;59:217-223. doi: 10.1016/j.amsu.2020.10.003
10. Marton E, Feletti A, Orvieto E, Longatti P. Dumbbell-shaped C-2 psammomatous melanotic malignant schwannoma. Case report and review of the literature. J Neurosurg Spine. 2007 Jun;6(6):591-9. doi: 10.3171/spi.2007.6.6.14
11. Benson JC, Marais MD, Flanigan PM, Bydon M, Giannini C, Spinner RJ, Folpe AL. Malignant Melanotic Nerve Sheath Tumor. AJNR Am J Neuroradiol. 2022 Dec;43(12):1696-1699. doi: 10.3174/ajnr.A7691
12. Liessi G, Barbazza R, Sartori F, Sabbadin P, Scapinello A. CT and MR imaging of melanocytic schwannomas; report of three cases. Eur J Radiol. 1990 Sep-Oct;11(2):138-42. doi: 10.1016/0720-048x(90)90163-6

Case report

Ukrainian Neurosurgical Journal. 2025;31(3):63-67
doi: 10.25305/unj.328774

Intracranial mesenchymal tumor with FET::CREB fusion: diagnostic and therapeutic challenges in an adult patient: A case report

Nazar Imam, Krushi Soladhra, Dharmikkumar Velani, Renish Padshala, Varshesh Shah

Department of Neurosurgery, Smt. NHL Municipal Medical College, Ahmedabad, Gujarat, India

Received: 05 May 2025
Accepted: 26 May 2025

Address for correspondence:
Nazar Imam, MD, Department of Neurosurgery, Smt. NHL Municipal Medical College, 2H9C+2FR, Pritan Rai Cross Road, Ellise Bridge, Paldi, Ahmedabad, Gujarat 380006, India, e-mail: mohd.nazar002@gmail.com

Aims: To highlight the diagnostic and therapeutic challenges of intracranial mesenchymal tumors with FET::CREB fusion, emphasizing the role of molecular diagnostics and immunohistochemistry in accurate identification.

Case report: A 44-year-old male presented with seizures and chronic headaches. Brain MRI revealed a well-defined, enhancing lesion in the left frontal lobe with significant perilesional edema. Gross total resection was performed. Histopathological analysis showed round to oval, spindle, and epithelioid cells within a mucoid stroma, along with lymphoplasmacytic infiltration and prominent vasculature. Immunohistochemistry revealed positivity for EMA, CD99, and Desmin, while molecular testing confirmed the presence of EWSR1::CREB fusion. Adjuvant chemotherapy with temozolomide and irinotecan was administered.

Discussion: FET::CREB fusion-positive tumors, a molecular variant of angiomatoid fibrous histiocytoma, exhibit diverse morphological features resembling meningiomas or schwannomas. Accurate diagnosis relies on advanced molecular tools. Treatment primarily involves surgical resection, with adjuvant therapies tailored to the tumor's molecular profile.

Conclusion: Early and precise diagnosis using molecular studies is critical for guiding treatment decisions. Further research is needed to refine therapeutic strategies and explore targeted therapies for these rare tumors.

Keywords: *intracranial mesenchymal tumor; FET::CREB fusion; angiomatoid fibrous histiocytoma; EWSR1::CREB; CNS tumor; molecular diagnostics*

Introduction

Intracranial mesenchymal tumor, FET::CREB fusion-positive, is a recently recognized provisional entity in the 2021 WHO Classification of Tumors of the Central Nervous System [1]. These tumors are mesenchymal, non-meningothelial in nature, exhibiting a wide morphological spectrum. Mitotic activity is typically low (<5 mitoses/mm²), and the tumor architecture may range from syncytial or sheet-like to reticular or cord-like structures. The stroma is generally collagenous or myxoid. The defining diagnostic feature of these tumors is the fusion between a member of the FET RNA-binding protein family (EWSR1 or FUS) and a member of the CREB family of transcription factors (ATF1, CREB, or CREM). EWSR1::CREB fusion has been identified in angiomatoid fibrous histiocytoma and clear cell sarcoma [2,3]. Prior diagnostic terms such as "intracranial myxoid variant of angiomatoid fibrous histiocytoma" or "intracranial myxoid mesenchymal tumor with EWSR1::CREB family gene fusions" are no longer recommended. This report presents a case of an intracranial mesenchymal tumor, FET::CREB fusion-positive, located in the left frontal lobe of an adult patient.

Case report

A 44-year-old male patient presented with a history of one episode of seizure and chronic persistence headache for the past 10 years. Brain MRI with contrast showed a well-defined, lobulated lesion in the left frontal lobe, extending from the superior to the middle frontal gyrus, with intense enhancement and hyperperfusion. Significant perilesional edema was observed in the left frontal lobe, particularly in the perisylvian region, as well as in the genu and body of the corpus callosum. There was also a mass effect on the bilateral lateral ventricles (***Fig. 1***). The patient was started on oral steroids (dexamethasone) and antiepileptic medication (levetiracetam), resulting in significant improvement in the headache. Neurological examination was unremarkable.

The patient underwent a left frontal craniotomy, and gross total resection of the tumor was achieved.

The tumor was well delineated, with firm and rubbery consistency, consistent with the MRI findings (***Fig. 2***).

Postoperative imaging confirmed that a gross total resection had been achieved (***Fig. 3***).

Histopathological Findings

Microscopic examination of Hematoxylin and Eosin (H&E) - stained tissue sections revealed that the tumor was composed of round to oval, spindle, and epithelioid cells embedded in mucoid stroma. The tumor periphery showed a lymphoplasmacytic infiltrate. Amianthoid fibers-like collagen were observed at the tumor's

edge, along with microcystic changes and prominent vasculature. No marked cytological atypia, necrosis, atypical mitotic figures, or whorling patterns were noted (***Fig. 4***). Immunohistochemical staining revealed that the tumor cells were positive for EMA, CD99, and Desmin. However, they were negative for GFAP, Synaptophysin, S-100, CD-34, TTF-1, PR, and Pan-cytokeratin. These findings were consistent with an intracranial myxoid mesenchymal tumor.

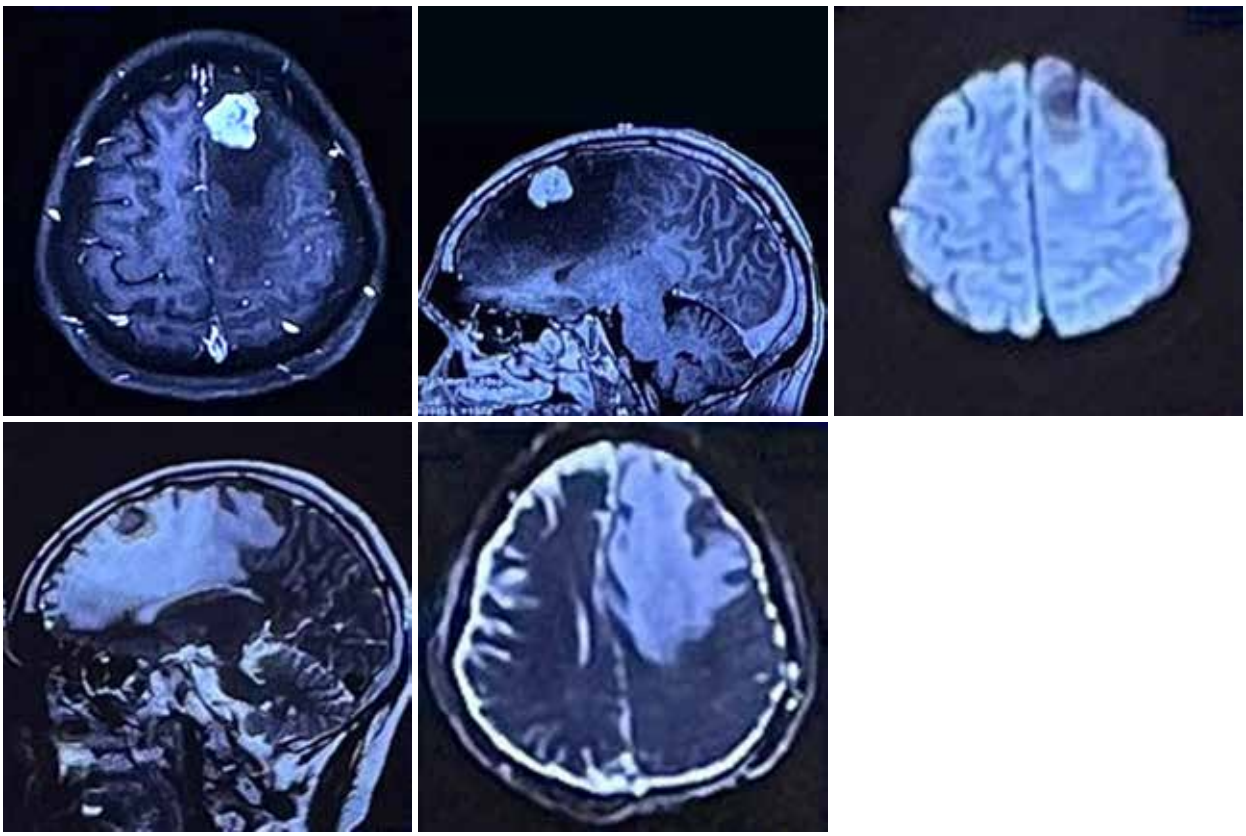

Fig. 1. MRI images show a well-defined, intensely enhancing lesion in the left frontal lobe (superior frontal gyrus and extending into the middle frontal gyrus) with hyperperfusion

Fig. 2. Gross specimen of the excised tumor

This article contains some figures that are displayed in color online but in black and white in the print edition.

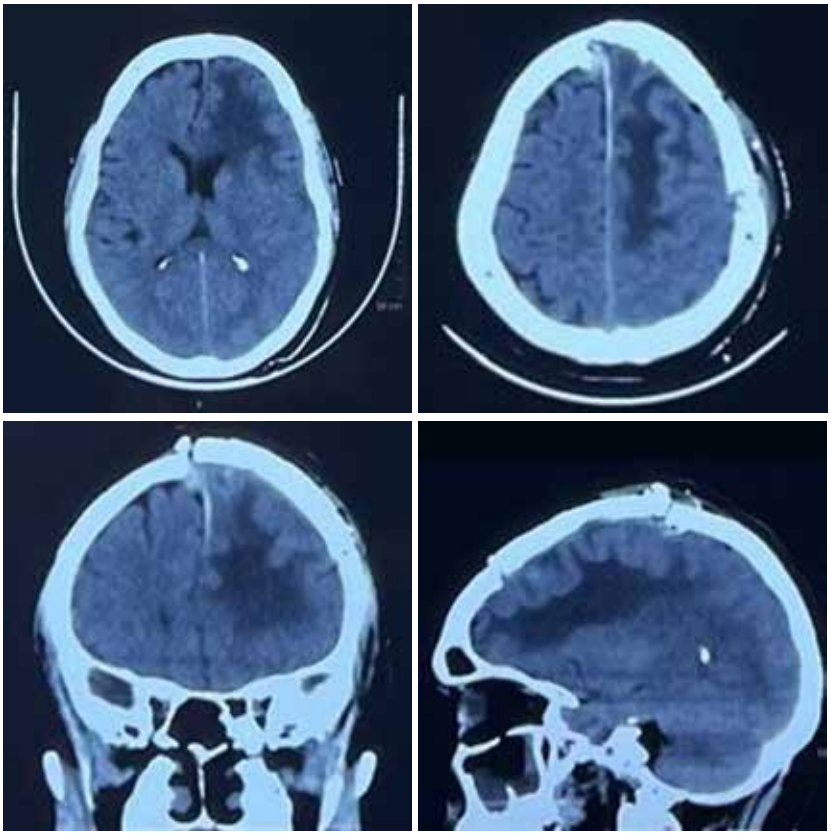

Fig. 3. Postoperative imaging

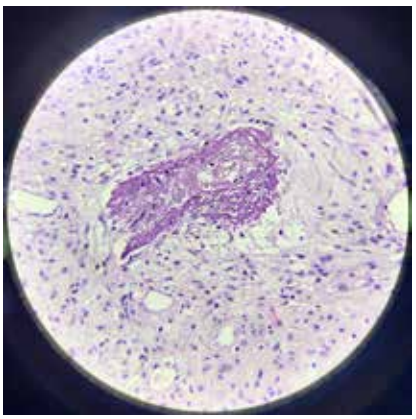

Fig. 4. Microscopic images of tumor sections showing round to oval and spindle to epithelioid cells embedded in mucoid stroma, with lymphoplasmacytic infiltrate, amianthoid fibers, microcystic changes, and prominent vasculature

Discussion

In 1979, Enzinger described angiomatoid fibrous histiocytoma (AFH) as a distinct fibrohistiocytic tumor, primarily affecting children and young adults, and resembling a vascular neoplasm [4]. AFH was included in the 2021 WHO CNS classification as an intracranial mesenchymal tumor [1]. Intracranial AFH is a rare primary CNS tumor, with the longest reported patient outcomes of up to five years and a median progression-free survival of 28 months 8 [3]. Patients with subtotal resections tend to experience local recurrence within 12 months [5].

Histologically, AFH is characterized by a multinodular proliferation of spindle-shaped or round cells with syncytial growth, forming bundles surrounded by a fibrous pseudocapsule, pericapsular lymphoplasmacytic cuffing, and pseudovascular spaces filled with blood. Desmin is often expressed, but myogenin or MyoD,

EMA, and CD68 are negative. Diagnosing AFH remains challenging due to its overlapping histological features with other tumors [2, 5].

Intracranial mesenchymal tumors with FET::CREB fusion represent a molecular variant of AFH. These tumors are often characterized by a collagenous stroma and dense intracellular matrix, which may resemble myofibroblastic tumors, poorly differentiated carcinomas, or meningiomas. Radiologically, these tumors typically show hypointense T1 signals and hyperintense T2 signals, with strong enhancement following gadolinium administration. Differential diagnoses include meningiomas and schwannomas, as these tumors may mimic extra-axial lesions with homogeneous contrast enhancement and a small dural tail on T1 fluid-attenuated inversion recovery (FLAIR) [2, 6].

Tauziède-Espariat et al. described 11 cases of CNS mesenchymal tumors with FET::CREB fusion. Of these, six were clustered with DNA methylation patterns, while the remaining five were similar to extra-CNS tumors such as angiomatoid fibrous histiocytomas, clear cell sarcomas, or solitary fibrous tumors [3]. These findings suggest that FET::CREB-fused intracranial tumors do not represent a single molecular entity, but rather a family of related tumors.

Treatment for intracranial mesenchymal tumors is primarily surgical, with complete resection being the goal. However, adjuvant therapies, including radiotherapy and chemotherapy (often sarcoma-based regimens), have been used in some cases [2, 7]. In our patient, the initial diagnosis was challenging, but following a comprehensive immunohistochemical panel and molecular analysis, the correct diagnosis of intracranial mesenchymal tumor, FET::CREB fusion-positive, was established. The patient subsequently received systemic chemotherapy, including temozolomide and irinotecan, tailored to sarcoma protocols, with good tolerability. The patient exhibited a favorable initial response to the sarcoma-based chemotherapy regimen, with good tolerability and no significant adverse effects noted during treatment. Follow-up MRI at 1 year postoperatively showed no evidence of tumor recurrence (***Fig. 5***).

Conclusion

This case highlights the importance of molecular studies and an extensive immunohistochemical workup in diagnosing rare CNS tumors, such as FET::CREB fusion-positive intracranial mesenchymal tumors. Early and accurate diagnosis is critical to guide treatment decisions, and personalized therapies based on molecular profiles may improve patient outcomes. Further studies and case reports will help refine treatment strategies and explore novel therapeutic options for these rare and complex tumors.

Disclosure

Consent

All authors declare that 'written informed consent was obtained from the patient (or other approved parties) for the publication of this case report and accompanying images. A copy of the written consent is available for review by the Editorial office/Chief Editor/Editorial Board members of this journal.

Ethical approval

All authors hereby declare that all experiments have been examined and approved by the appropriate ethics committee and have therefore been performed in accordance with the ethical standards laid down in the 1964 Declaration of Helsinki.

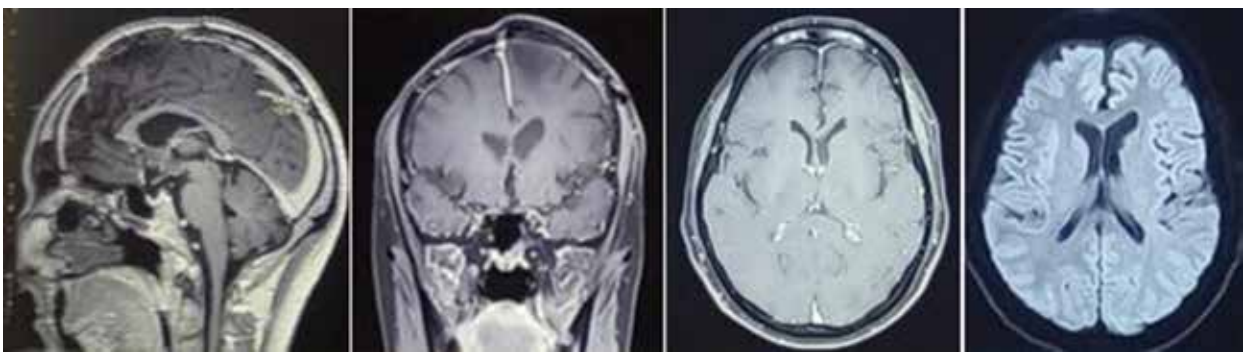

Fig. 5. One-year follow-up brain MRI showing no residual or recurrent lesion in the left frontal region following gross total resection of intracranial mesenchymal tumor with FET::CREB fusion

References

1. Louis DN, Perry A, Wesseling P, Brat DJ, Cree IA, Figarella-Branger D, Hawkins C, Ng HK, Pfister SM, Reifenberger G, Soffietti R, von Deimling A, Ellison DW. The 2021 WHO Classification of Tumors of the Central Nervous System: a summary. Neuro Oncol. 2021 Aug 2;23(8):1231-1251. doi: 10.1093/neuonc/noab106
2. Antonescu CR, Dal Cin P, Nafa K, Teot LA, Surti U, Fletcher CD, Ladanyi M. EWSR1-CREB1 is the predominant gene fusion in angiomatoid fibrous histiocytoma. Genes Chromosomes Cancer. 2007 Dec;46(12):1051-60. doi: 10.1002/gcc.20491
3. Sloan EA, Chiang J, Villanueva-Meyer JE, Alexandrescu S, Eschbacher JM, Wang W, Mafra M, Ud Din N, Carr-Boyd E, Watson M, Punsoni M, Oviedo A, Gilani A, Kleinschmidt-DeMasters BK, Coss DJ, Lopes MB, Raffel C, Berger MS, Chang SM, Reddy A, Ramani B, Ferris SP, Lee JC, Hofmann JW, Cho SJ, Horvai AE, Pekmezci M, Tihan T, Bollen AW, Rodriguez FJ, Ellison DW, Perry A, Solomon DA. Intracranial mesenchymal tumor with FET-CREB fusion-A unifying diagnosis for the spectrum of intracranial myxoid mesenchymal tumors and angiomatoid fibrous histiocytoma-like neoplasms. Brain Pathol. 2021 Jul;31(4):e12918. doi: 10.1111/bpa.12918
4. Enzinger FM. Angiomatoid malignant fibrous histiocytoma: a distinct fibrohistiocytic tumor of children and young adults simulating a vascular neoplasm. Cancer. 1979 Dec;44(6):2147-57. doi: 10.1002/1097-0142(197912)44:6<2147::aid-cncr2820440627>3.0.co;2-8
5. Choi JH, Ro JY. The 2020 WHO Classification of Tumors of Soft Tissue: Selected Changes and New Entities. Adv Anat Pathol. 2021 Jan;28(1):44-58. doi: 10.1097/PAP.0000000000000284
6. Liu C, Liu Y, Zhao Y, Wei J, Ma Y, Liu Y, Huang J. Primary Intracranial Mesenchymal Tumor with EWSR1-CREM Gene Fusion: A Case Report and Literature Review. World Neurosurg. 2020 Oct;142:318-324. doi: 10.1016/j.wneu.2020.07.015
7. Garnier L, Fenouil T, Pissaloux D, Ameli R, Ducray F, Meyronet D, Honnorat J. Intracranial non-myxoid angiomatoid fibrous histiocytoma with EWSR1-CREB1 transcript fusion treated with doxorubicin: A case report. Mol Clin Oncol. 2021 Jul;15(1):131. doi: 10.3892/mco.2021.2293